ORNL/TM-5879

Cy. 97

LOCKHEED MARTIN ENERGY RESEARCH LIBRARIES

3 4456 0509784 6

LMFBR Fuel Reprocessing Program Progress Report for Period January 1 to March 31, 1977

[redacted]

OAK RIDGE NATIONAL LABORATORY
CENTRAL RESEARCH LIBRARY
DOCUMENT COLLECTION
LIBRARY LOAN COPY
DO NOT TRANSFER TO ANOTHER PERSON
If you wish someone else to see this document, send in name with document and the library will arrange a loan.
UCN-7969
(3 3-67)

OAK RIDGE NATIONAL LABORATORY
OPERATED BY UNION CARBIDE CORPORATION FOR THE ENERGY RESEARCH AND DEVELOPMENT ADMINISTRATION

Printed in the United States of America. Available from
the Energy Research and Development Administration,
Technical Information Center
P. O. Box 62, Oak Ridge, Tennessee 37830
Price: Printed Copy $6.00; Microfiche $3.00

This report was prepared as an account of work sponsored by the United States Government. Neither the United States nor the Energy Research and Development Administration/United States Nuclear Regulatory Commission, nor any of their employees, nor any of their contractors, subcontractors, or their employees, makes any warranty, express or implied, or assumes any legal liability or responsibility for the accuracy, completeness or usefulness of any information, apparatus, product or process disclosed, or represents that its use would not infringe privately owned rights.

ORNL/TM-5879
Dist. Category UC-79c

Contract No. W-7405-eng-26

LMFBR FUEL REPROCESSING PROGRAM PROGRESS REPORT

FOR PERIOD JANUARY 1 TO MARCH 31, 1977

W. D. Burch, Program Director

M. J. Feldman
Manager, Engineering Systems

W. S. Groenier
Manager, Engineering Research

B. L. Vondra
Manager, Process Research and Development

Report compiled by
W. E. Unger
Technical Assistant to the Program Director

Date Published: May 1977

NOTICE: This document contains information of a preliminary nature. It is subject to revision or correction and therefore does not represent a final report.

LOCKHEED MARTIN ENERGY RESEARCH LIBRARIES
3 4456 0509784 6

OAK RIDGE NATIONAL LABORATORY
Oak Ridge, Tennessee 37830
operated by
UNION CARBIDE CORPORATION
for the
ENERGY RESEARCH AND DEVELOPMENT AMINISTRATION

CONTENTS

	Page
ABSTRACT	v
1. HIGHLIGHTS	1-1
1.1 Hot-Pilot-Plant (HPP) Conceptual Design	1-1
1.2 Laboratory and Hot-Cell Studies	1-1
1.3 Engineering Research	1-2
1.4 Component Development	1-3
1.5 Integrated Prototype Equipment Test (IPET) Facility and Building Engineering	1-4
REFERENCES FOR SECTION 1	1-4
2. HOT-PILOT-PLANT (HPP) CONCEPTUAL DESIGN	2-1
2.1 HPP Process Design	2-1
2.2 HPP Facilities Design	2-2
2.2.1 Siting and support buildings	2-2
2.2.2 Process building	2-2
3. PROCESS RESEARCH AND DEVELOPMENT	3-1
3.1 Hot-Cell Operations	3-1
3.1.1 Development of in-cell equipment	3-1
3.1.2 Dissolution studies	3-2
3.2 Laboratory Studies	3-9
3.2.1 Plutonium dioxide dissolution studies	3-9
3.2.2 Hydroxylamine and hydrazine chemistry in Purex processing	3-11
3.2.3 Solvent chemistry studies	3-20
3.2.4 Reduction of Pu^{6+} using NO_x	3-26
3.3 Product Conversion	3-28
3.3.1 Uranium conversion process	3-28
3.3.2 Plutonium conversion process	3-29
REFERENCES FOR SECTION 3	3-30
4. ENGINEERING RESEARCH	4-1
4.1 Voloxidation	4-1
4.2 Dissolution	4-2
4.2.1 Four-foot-diameter dissolver prototype	4-2
4.2.2 Operational testing of ferrofluidic seals	4-4
4.3 Feed Preparation	4-5
4.3.1 Nitrogen oxide scrubbing	4-5
4.3.2 Iodine evolution	4-6
4.4 Fluorocarbon Absorption Studies	4-6
4.4.1 Pilot-plant operation	4-7
4.4.2 Process application	4-14
4.4.3 Chemical studies of contaminants in LWR off-gas processing	4-14
4.5 Iodox Process	4-16
4.6 Instrumentation and Control Systems	4-20
4.6.1 Nondestructive assay of spent fuel	4-20
4.6.2 Process sensors and control	4-22

Page

4.7 Solvent Extraction 4-30
REFERENCES FOR SECTION 4 4-32

5. COMPONENT DEVELOPMENT 5-1
5.1 Disassembly and Fuel Cutting — Contracted Work 5-1
5.1.1 Machining 5-1
5.1.2 Disassembly 5-2
5.1.3 Shearing 5-3
5.1.4 Subassembly cutting 5-3
5.2 Disassembly and Fuel Cutting — ORNL Program 5-3
5.2.1 Shear 5-5
5.2.2 Subassembly cutting 5-8
5.2.3 Prototype fuel 5-8
5.2.4 Instrumentation and controls 5-10
5.3 Voloxidation 5-11
5.4 Dissolution 5-11
5.4.1 Prototypical rotary dissolver 5-12
5.4.2 Dissolver support system and process equipment 5-14
5.4.3 Instrumentation and controls 5-16
5.5 Receiving and Storage 5-17
5.5.1 Systems integration 5-18
5.5.2 Sodium-removal system and fuel transporter 5-19
5.5.3 Fuel identification system 5-20
5.5.4 Corrosion program 5-20
5.6 Remote Maintenance 5-28
5.6.1 Electromechanical systems 5-31
5.6.2 Remote viewing 5-32
5.6.3 Connectors and jumpers 5-33
REFERENCE FOR SECTION 5 5-35

6. INTEGRATED PROTOTYPE EQUIPMENT TEST FACILITY (IPET) 6-1
6.1 LMFBR Facility Engineering 6-3
REFERENCE FOR SECTION 6 6-6

ABSTRACT

This quarterly progress report on the Fuel Recycle Program covers the ongoing development program aimed at providing the technology on which to base the design of productive-scale fast-breeder spent fuels. The continuing basic laboratory and hot-cell studies, engineering research, and component equipment development activities are in support of a cold integrated prototype equipment test scheduled for 1981 and a current conceptual design of a hot pilot plant scheduled for operation in 1986.

1. HIGHLIGHTS

1.1 Hot-Pilot-Plant (HPP) Conceptual Design

A major program-study document entitled *LMFBR Spent Fuel Reprocessing: A Study of an Industrial-Scale Facility* was published during this report period.[1] The document presents concepts and analyzes design directions for the HPP. An evaluation of experience with these design directions in the HPP will serve as a forerunner for establishing future major reprocessing facility design criteria.

A second program study concerning the HPP expansion option was transmitted to ERDA, and this concept (design at 0.5-metric ton/day capacity with an ability to expand to 1 metric ton/day) has been reviewed and accepted. The essence of this study and the review comments on the *Conceptual Design Criteria for the LMFBR Hot Pilot Plant* has been transmitted for approval.

The reference program process flowsheet, as it will be applied to the conceptual design phase, is being internally reviewed and will be published during the next quarter. Studies to establish the functional areas of the HPP cell complex have been completed. Cell configuration studies are proceeding and will result in an initial cell configuration proposal during the next quarter.

1.2 Laboratory and Hot-Cell Studies

The distribution of hydrazoic acid between nitric acid and tributyl phosphate (TBP)–normal dodecane (NDD) solutions was measured; hydrazoic acid will be extracted into the solvent and carried to the solvent-cleanup system.

Butylauryl phosphate (a known secondary degradation product) was shown to remain in the solvent after carbonate scrubbing and to strongly complex zirconium.

The plutonium(VI) species are reduced rapidly by nitric oxide (NO), and the amount of NO required to accomplish this reduction is less than twice the stoichiometric requirement. Nitrogen dioxide is also effective for reducing Pu^{6+} to Pu^{4+}, but the rate is much slower.

Hot cells 2 and 3, Building 4507, were committed to hot operation. The first LMFBR tests were initiated using highly irradiated, mechanically blended $(U,Pu)O_2$.

1.3 Engineering Research

Liquid backmixing studies in the 4-ft-diam rotary dissolver (now completed) indicate that the carryover of liquid with solids is less than 6% of the total liquid flow. Particle-rinsing studies have been initiated.

An experiment to study iodine evolution from a dissolver digestion tank has been designed. The experiment will feature steam stripping of iodine in a packed column using a system that is a factor of 10 larger than the previous laboratory apparatus and incorporates most of the features of the pilot-plant conceptual design.

A combination absorber–fractionator column has been identified as a feasible concept that will provide enhanced reliability and economy for the fluorocarbon absorption process. Recent tests have quantified decontamination factors for krypton and xenon at the operating conditions necessary for the combined column. Chemistry studies have resulted in a determination of CO_2 distribution coefficients in R-12 and have verified that TBP is completely miscible in R-12.

Iodox experiment IXC-9 with elemental iodine resulted in the highest decontamination factors observed to date (average 8.2 per plate) despite the presence of NO_2 and water vapor in the feed-gas. The key to the performance apparently was the very high acid concentration (22.5 to 22.8 *M* HNO_3) maintained throughout the column.

The calibration of proton-recoil and helium-3 detectors for the nondestructive assay experiment for spent-fuel assemblies has been completed using low-intensity ^{232}U + Be and ^{232}U + D_2O sources. The study of fission-type detectors and the design of other experimental components are progressing in a satisfactory manner.

Vibration signatures on the rotary dissolver have been analyzed in some detail for each of the modes of operation. We tentatively conclude that the transfer of solids results in high-frequency vibrations, whereas

mixing of solids produces low-frequency vibrations. Variations in the measured patterns and intensities will be studied to identify a method of detecting an increase in solids holdup.

An effort has begun at Argonne National Laboratory to emphasize the development of a critically safe, centrifugal, solvent-extraction contactor for LMFBR fuel reprocessing.

1.4 Component Development

The five areas of investigation under way in Component Development have been modified with reference to the five reported previously.[2] Work on receiving and storage, disassembly and cutting, dissolution, and remote maintenance has continued. Near the end of this quarter, work in the waste-handling task was initiated and will be reported in succeeding quarters.

Seven specific subtasks have been defined in the receiving and storage task, and progress is reported in five of these. The major continuing effort is the corrosion study on sodium-exposed stainless steel coupons. Several of the type 304 stainless steel coupons have failed during simulated water storage; however, none of the type 316 stainless steel coupons have failed. New coupons are being prepared for the second phase of the program.

In the disassembly and cutting task, the detail design of the disassembly machine is proceeding; fabrication estimates have been completed. The testing program with new shear tooling for the ORNL shear has been delayed approximately two months due to fit-up problems. Most of the necessary modifications to the tooling and shear have now been completed.

In the dissolution task, the fabrication of the dissolver has continued. With the exception of the feeder, the design of all auxiliary equipment has been completed, and most orders for fabrication have been placed. Work has been initiated on an installation package for the system. Installation is scheduled to begin early in the fourth quarter of FY 1977.

The primary effort in the remote maintenance task has been directed toward (1) studies to improve electromechanical systems in the areas of signal and power transmission and in position indication and (2) the preparation of a bid package for the development of a new and more radiation-resistant, remotely operated line connector.

1.5 Integrated Prototype Equipment Test (IPET) Facility and Building Engineering

Pre-Title I design planning for the IPET project was completed in January 1977. Title I engineering is now under way with Construction Planning and Design funds which become available this quarter. The major efforts in the IPET project are concerned with upgrading engineering estimates, preparation of project control documentation, and correlating the conceptual design data on IPET with the directions becoming apparent in the HPP conceptual design. Close alignment of these projects (IPET and HPP) is required.

Progress on program facilities in Buildings 7601, 7602, and 7603 has been made this quarter in the vessel off-gas system, the demineralized water system, the electrical power supply, the required office additions, and the process and building waste-handling system.

REFERENCES FOR SECTION 1

1. A. R. Irvine, *LMFBR Spent Fuel Reporcessing: A Study of an Industrial-Scale Facility*, ORNL/TM-5723 (in press).
2. W. D. Burch et al., *LMFBR Fuel Reprocessing Program Progress Report for Period October 1 to December 31, 1976*, ORNL/TM-5768 (February 1977).

2. HOT-PILOT-PLANT (HPP) CONCEPTUAL DESIGN

O. O. Yarbro

The conceptual design of the HPP facility and process equipment is continuing as scheduled; the status of specific items and procedures, either completed or in progress, is summarized in the following sections. Recommendations made during the past quarter in the HPP expandability option study to provide for future capacity expansion capability to 1 ton/day were accepted by ERDA. This modification, along with other specific comments by ERDA, was incorporated into a revision of the *Conceptual Design Criteria for the LMFBR Fuel Processing Hot Pilot Plant*; the revised criteria was transmitted to ERDA for review and approval. A Form 44 Construction Project Data Sheet was prepared and submitted requesting FY 1979 line-item funding to provide for initiating Titles I and II designs and to procure a limited quantity of long-lead materials and equipment.

2.1 HPP Process Design

E. D. North

Preliminary process flow diagrams have been completed for all HPP process systems. The 34 flow diagrams show schematically major pieces of equipment and process streams required to accomplish the HPP reprocessing function from receipt of fuel elements to delivery of solid plutonium and uranium products. All wastes leave as solid products, or as gases or vapors that have been extensively processed to remove radioactive contamination prior to release from the plant stack.

The basic design chosen for the HPP reprocessing function is the chop-leach Purex process, which includes voloxidation and continuous dissolution.

The process flow diagrams are now being converted to process-material-balance flow diagrams by detailed material-balance calculations to determine the major process parameters such as flow rates, concentrations of uranium, plutonium, and major process reagents, temperatures, and pressures. This effort is 50% complete.

2.2 HPP Facilities Design

J. R. White

2.2.1 Siting and support buildings

Preliminary core drilling has begun at the selected HPP site on the west end of Bethel Valley Road near ORNL. Design criteria documents for the site utilities are being prepared.

2.2.2 Process building

An effort is currently under way to develop the conceptual design of the process building, which includes all building areas surrounding the cell complex and all out-of-cell service systems. Bechtel has begun preparing design criteria for the building areas and for conventional building systems. UCC-ND Engineering is preparing design criteria for other systems, including cell cooling, ventilation and purification systems, building heating, ventilation, and air-conditioning systems, and radiation-monitoring and alarm systems.

Cell complex. Figure 2.1 is a schematic of the HPP cell complex selected as the basis for the concept design study. The complex consists of five separate operating cells, two water storage pools, cell(s) for remote decontamination and maintenance of in-cell equipment, and contained area(s) for contact maintenance. All cells, with the possible exception of the uranium product cell, will be remotely maintained. All in-cell equipment that may require maintenance or replacement over the lifetime of the facility will be remotely replaceable without requiring personnel entry.

Design criteria for the overall cell complex have been prepared, and all cell-equipment assignments have been made. An effort is being made to determine the optimum arrangement of process equipment within each cell and the optimum arrangement of the cells relative to each other. The schedule for establishing these optimum arrangements is early May 1977.

ORNL DWG 77-7645

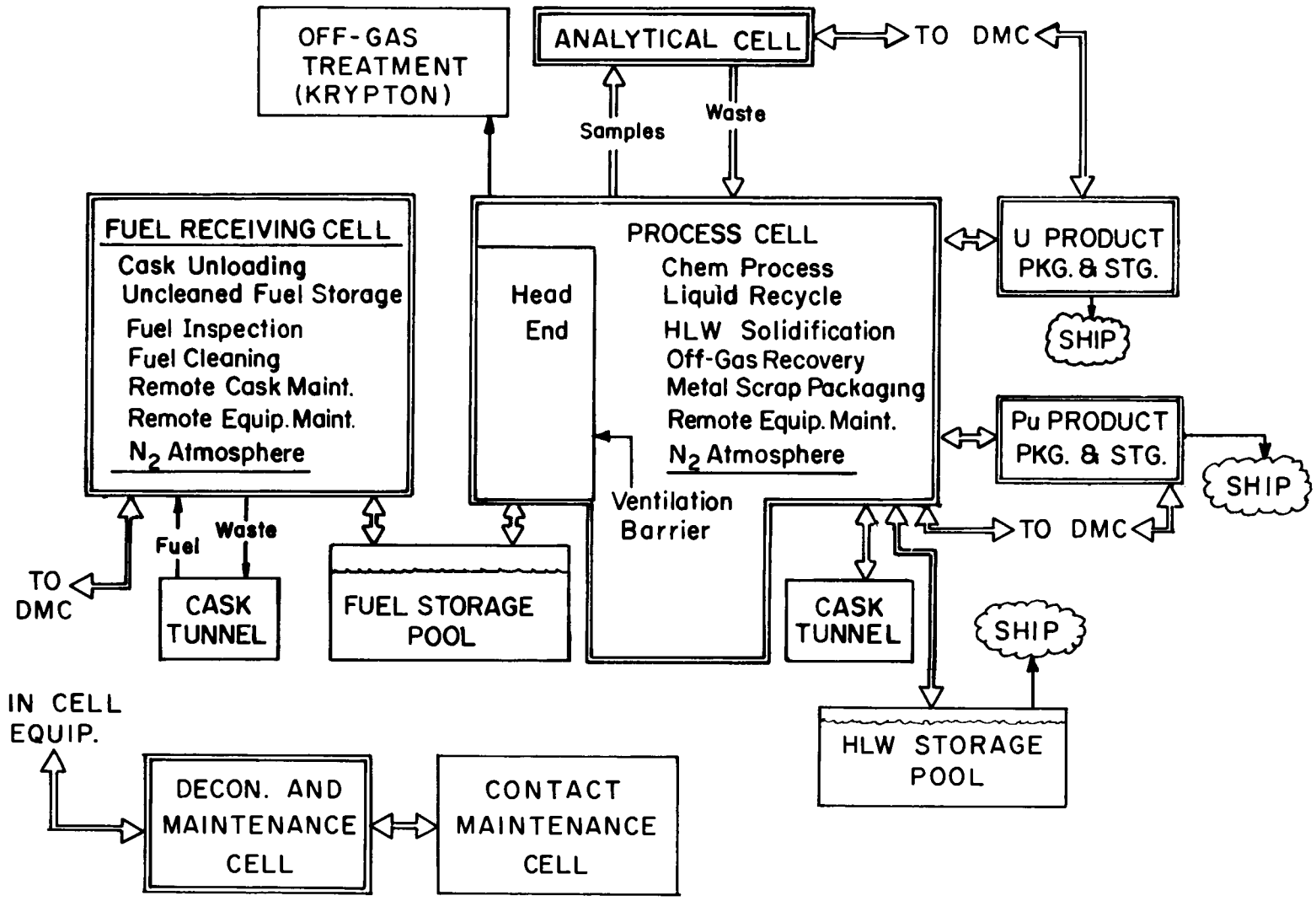

Fig. 2.1. HPP cell complex.

General-purpose in-cell equipment. The conceptual design of general-purpose in-cell equipment (material handling, manipulation, viewing, transfer hatches, service feed-through, etc.) will be performed by UCC-ND Engineering, with some assistance from specialty contractors. A draft of the design criteria for the in-cell material-handling system has been issued for project review.

3. PROCESS RESEARCH AND DEVELOPMENT

B. L. Vondra

Process research and development studies were continued in the laboratory and hot cells to define process parameters and conditions for an LMFBR reprocessing flowsheet. Work is in progress on the following: (1) the solubility of PuO_2 in hydriodic acid (HI), (2) the removal of impurities in aqueous recycle streams, (3) head-end parametric studies with irradiated fuel, (4) the recycle of nitrogen oxides for gaseous reagent usage, (5) solvent chemistry, and (6) iodine behavioral studies (IODOX).

Parametric tests using irradiated LMFBR fuel have been initiated in Building 4507. Three fuels have been processed and transferred to the facility for planned experiments. Initial-run data from shearing, voloxidizing, and dissolution are being collated.

A new task has been initiated to develop the technology for product conversion.

3.1 Hot-Cell Operations

V. C. A. Vaughen

3.1.1 Development of in-cell equipment

J. H. Goode, R. G. Stacy, G. K. Ford, E. C. Hendren, J. R. Travis, and C. S. Webster

Cold (unirradiated) shakedown tests of the hydraulic shear, the rotary voloxidizer, and the dissolver were completed in cells 2 and 3 of Building 4507, and the first experiments with zircaloy-clad UO_2 fuel segments from the H. B. Robinson-2 reactor were made. Operations appeared to be very satisfactory. Data from the initial LWR tests are being analyzed and will be reported elsewhere. The first LMFBR tests using highly irradiated, mechanically blended $(U,Pu)O_2$ were started late in the quarter. No data are available.

3.1.2 Dissolution studies

We reported last quarter[1] on a dissolution experiment with fuel rod ASOV-14 [containing VIPAC $(U_{0.8}Pu_{0.2})O_2$], which had been irradiated by Argonne National Laboratory (ANL) in EBR-2 to 10.7% burnup. The 1-in. sheared segments of the rod were leached for 2 hr in simmering 8 *M* HNO_3 and then washed with 3 *M* HNO_3. The undissolved solids were releached with 8 *M* HNO_3 and leached again with 8 *M* HNO_3–0.05 *M* KF to dissolve residual plutonia. Finally, the remaining residue was leached twice with 12 *M* HCl. The final residues were fused with sodium carbonate for material-balance purposes. We found that the two 2-hr leaches with 8 *M* HNO_3 dissolved 99.14% of the urania and 96.06% of the plutonia, which is fairly typical for nonhomogeneous, mechanically blended, mixed-oxide fuels. The HNO_3–KF mixture dissolved all the fissile material except 0.01% of the uranium and 0.07% of the plutonium. The HCl dissolved essentially all remaining material.

Residue characterization. The final residues from the leachings of the mixed-oxide fuel amounted to about 0.92% of the initial fuel weight. The scanning electron microscope showed images of very small particles ($\leq$2 μm in diam) and x-ray dispersion lines for Mo, Tc, Ba, Cs, and Ce. Emission spectroscopy indicated that the major constituents were Mo, Ru, Tc, Rh, and Pd. Spark-source mass spectrometry (SSMS) and semiquantitative emission spectroscopy data on three residue samples from rod ASOV-14 indicated quite similar compositions for the noble metal fission products (Table 3.1). Table 3.2 compares our results with other results using electron microprobe analyses of noble metal inclusions in irradiated $(U,Pu)O_2$ fuel specimens. The results are quite similar; some variation would be due to numerous chemical treatments of the dissolution residues.

Brown et al.[2] at ANL, in their postirradiation examination of sibling rods ASOV-5 and -6 at 2.7% burnup, commented on the metallic-appearing inclusions (of up to 6 μm in diam) in the columnar and equiaxed grain regions of those rods consisting mainly of Ru, Mo, and Tc, with small amounts of Rh and Pd. They noted that the ruthenium and molybdenum content varied with radial location; the ruthenium decreased and the molybdenum increased radially from the central void, that is, down the

Table 3.1. Composition[a] of residue after leaching with HNO_3, HNO_3–HF, and HCl acids

	Residue No.		
	7D1-S1	7D2-S1	7D4-7
Final residue weight, g	0.0822	0.3695	0.0718
Weight of noble metals (100%), g	0.0388	0.1375	0.0177
Noble metals	**Weight percent**		
Pd	8.5	2.2	7.9
Rh	2.1	2.2	2.8
Ru	63.4	53.7	61.0
Tc	11.1	18.6	7.9
Mo	14.7	23.3	20.3

[a]Composition without presence of Fe, Cr, Ni, Mn, Al, Si, and other materials introduced during sample fusion and dissolution.

Table 3.2. Noble metal inclusions in irradiated mixed oxide fuels

	Weight percent of particle or inclusion					
	This work	Ewart[a]	Sauvage[b]	Johnson[c]	Bramman[d]	O'Boyle[e]
Pd	2-9	5		2-7	2	2
Rh	2-3	11	3.3	8-16	7	13
Ru	54-63	37	34.4	30-51	32	49
Tc	8-19	10	16.7	12-20	15	17
Mo	15-23	38	45.6	22-51	41	20

[a]F. T. Ewart, *Electron Probe Analysis of Mixed Oxide Fuels from Experiment SP 993 ...*, AERE-R-7322 (May 1973).

[b]R. Sauvage, *Redistribution During Irradiation of Constituents and Fission Products in Uranium-Plutonium Mixed Oxide Fuel*, CEA-R-4649 (January 1975).

[c]C. E. Johnson, "Chemistry of Irradiated Fast Reactor Fuels and Materials," *Chemical Engineering Division Annual Report-1970*, ANL-7775 (April 1971).

[d]J. I. Bramman et al., "Metallic Fission Product Inclusions in Irradiated Oxide Fuels," *J. Nucl. Mater.* 25: 201-15 (1968).

[e]D. R. O'Boyle et al., *Trans. Am. Nucl. Soc.* 11: 101 (1968).

thermal gradient. The Ru-Mo-Tc inclusions were heavily concentrated at the juncture between long- and short-columnar grains and at the juncture between the columnar and equiaxed grains. The variations in composition of the inclusions are believed to be due to the radial changes in the oxidation state of the fuel[3,4] due to irradiation.

Material balances on some of the radioactive fission products reconfirmed earlier results that indicated very little ruthenium would dissolve (Table 3.3). Antimony and technetium were distributed between the residues and the leaches.

Table 3.3. Solubility of selected fission products

Fission product	Predicted[a] (total)	Found (total)	Insoluble (total)	Insoluble (% total found)
^{99}Tc, mg	136.4	86.7[b]	33.2	38.20
^{106}Ru, dis/sec	1.50×10^{11}	1.01×10^{10}	9.45×10^{10}	93.23
^{125}Sb, dis/sec	3.63×10^{10}	1.63×10^{10}	8.95×10^{9}	54.83
^{137}Cs, dis/sec	6.01×10^{11}	5.46×10^{11}	2.54×10^{9}	0.47
^{144}Ce, dis/sec	6.67×10^{11}	3.29×10^{11}	3.74×10^{9}	1.14

[a]Approximations predicted by ORIGEN; irradiation conditions uncertain.

[b]Since intermediate leaches were not analyzed for ^{99}Tc, the total found is probably low.

Volatile fission products. Volatile fission product concentrations were measured in the first nitric acid leach (dissolver solution), in a condensate vapor trap, and in two successive NaOH scrubbers (Table 3.4). The fraction of ^{129}I found in the dissolver solution is significantly larger than that found when LWR fuels are dissolved.

Dissolver solution. Analyses of the centrifuged first nitric acid leach of the mixed-oxide fuel rod are summarized in Table 3.5. Uranium and plutonium isotopic analyses are listed in Table 3.6.

Table 3.4. Distribution of volatile fission products during dissolution of $(U,Pu)O_2$ rod ASOV-14 (10.7% burnup)

Fission product	Total found	Percent ORIGEN[a]	Percent of total found in —			
			Dissolver solution	Vapor trap	Scrubber 1	Scrubber 2
^3H_2O, dis/sec	6.03×10^6	0.15	86.62	12.89	0.07	0.42
^{129}I, μg	1.62×10^4	30.00	30.81	0.41	69.93	0.85
^{14}C, dis/sec	1.40×10^6	34.00	NA[b]	Trace	100.00	Trace
^{106}Ru, dis/sec	1.01×10^{11}	67.00	5.66	0.003	0.012	<0.001

[a]Approximations only (uncertain irradiation conditions).

[b]Not analyzed but presumed small in highly acidic solution.

Table 3.5. Analysis of ASOV-14 dissolver solution

Fission product	Concentration	Fission product	Concentration
HNO_3	4.84 *M*	^{106}Ru	2.38×10^7 dis sec^{-1} ml^{-1}
Uranium	195.9 mg/ml	^{125}Sb	2.71×10^7 dis sec^{-1} ml^{-1}
Plutonium	39.2 mg/ml	^{129}I	21.8 μg/ml
Pu α	3.72×10^9 counts min^{-1} ml^{-1}	^{134}Cs	8.09×10^7 dis sec^{-1} ml^{-1}
Gross α	4.88×10^9 counts min^{-1} ml^{-1}[a]	^{137}Cs	1.92×10^9 dis sec^{-1} ml^{-1}
Am α	7.54×10^8 counts min^{-1} ml^{-1}	^{144}Ce	1.38×10^9 dis sec^{-1} ml^{-1}
$^3H_2$	2.28×10^4 dis sec^{-1} ml^{-1}	^{154}Eu	6.16×10^7 dis sec^{-1} ml^{-1}
^{90}Sr	2.24×10^9 dis sec^{-1} ml^{-1}	Molybdenum	500 μg/ml
^{99}Tc	233.6 μg/ml	Zirconium	1000 μg/ml

[a] 4.78 MeV α(U-233), 0.22%; 5.15 MeV α(Pu-239, Pu-240), 78.5%; 5.50 MeV α (Pu-238, Am-241), 20.1%; 5.80 MeV α(Cm-244), 0.03%; 6.11 MeV α(Cm-242), 1.2%.

Table 3.6. Isotopic analyses of uranium and plutonium before and after irradiation of ASOV-14 in EBR-2

Uranium			Plutonium		
Mass	Before	After	Mass	Before	After
^{233}U		≤0.002	^{238}Pu		0.035
^{234}U	1.06	0.901	^{239}Pu	90.21	89.01
^{235}U	93.00	84.14	^{240}Pu	8.27	10.32
^{236}U	0.80	2.30	^{241}Pu	0.78	0.58
^{238}U	5.13	12.66	^{242}Pu	0.04	0.06

Solution stability. Campbell has discussed the appearance of black solids in clarified LWR dissolver solutions.[5] These solids, originally thought to have been unusually fine dissolution residues not removed by centrifugation, were found to appear at the rate of 20-25 g per day per metric ton of uranium (MTU) until about 350 g/MTU had been produced; the rate of formation then decreased. Preliminary analyses showed the solids to be distinctly different from dissolution residues; typical emission spectrographic analyses indicated the presence of 3 to 4 wt % Pd, 5 to 10 wt % Ru, 8 to 14 wt % Rh, 1 to 6 wt % Mo, 0.2 to 6 wt % Zr, plus other elements.

The dissolver solution from ASOV-14 (Table 3.5) was recentrifuged after four days and again after 19 days (from the original clarification). Table 3.7 summarizes chemical and spark-source mass spectrometric analyses of the two solids that were centrifuged from the solution, washed, dried, and weighed. Table 3.7 shows that the 19.4 mg of solids [equivalent to about 300 g/metric ton of $(U,Pu)O_2$] that precipitated after the first four days were different from those removed after another 15 days of aging. The first solids were richer in uranium than the secondary solids [Pu:(U + Pu) = 0.06:0.25] and contained less of the noble metals. The second batch of precipitated solids also contained greater amounts of barium, cesium, tellurium, and the noble metals. Further investigation into this phenomenon is planned.

Table 3.7. Precipitates from clarified dissolver solution

	Sample No.	
	7D1-S2	7D1-S3
Days after first clarification	4	19
Weight, mg	19.4	17.2
Uranium, mg	16.1	1.2
Plutonium, mg	1.0	0.4
Pu: (U+ Pu)	0.06	0.25
Ba, μg/g	50,000	600,000
Cs, μg/g	20,000	300,000
Te, μg/g	<5,000	50,000
Pd, μg/g	3,000	30,000
Rh, μg/g	10,000	≤15,000
Ru, μg/g	30,000	80,000
Tc, μg/g	3,000	<2,000
Mo, μg/g	10,000	20,000
Zr, μg/g	<1,000	2,000
Fe, μg/g	50,000	100,000

Cladding. The stainless steel cladding of rod ASOV-14 was dissolved in dilute aqua regia (5 *M* HNO_3–2 *M* HCl). The cladding had previously gone through the first fuel dissolution in 8 *M* HNO_3, in two rinses with boiling 3 *M* HNO_3, and in four rinses with cold 3 *M* HNO_3. We obtained 0.41 g (about 1%) of insoluble residue from the original 34.47 g of cladding. The residue contained 0.0004 g of uranium and 0.0001 g of plutonium; the 750 ml of aqua regia solution contained 0.0015 g of uranium and 0.0001 g of plutonium. These totals are equivalent to 0.004% of the uranium and 0.012% of the plutonium in the rod. (Further tests are necessary to establish the variability of these quantities and to set limits on the possibility of cross-contamination of the leached cladding during handling in the hot cell.)

The only detectable fission product associated with the cladding was ^{137}Cs. Approximately 0.023% of the total ^{137}Cs was found in the aqua regia solution (about 1.6×10^5 dis sec^{-1} ml^{-1}). The activation products ^{54}Mn and ^{60}Co were factors of 46 and 41 higher respectively. More molybdenum was present in solution than could have come from type 304 stainless steel cladding (0.02 wt %); it may have been associated with the cesium.

3.2 Laboratory Studies

J. C. Mailen

3.2.1 Plutonium dioxide dissolution studies

O. K. Tallent and K. D. Williams

We are continuing to examine methods for dissolving plutonia-bearing residues left after nitric acid dissolution of LMFBR-type fuel rods. Criteria for acceptable dissolution methods for these residues require that the dissolvent volume be kept low, that the addition of foreign ions be kept to a minimum, and that as few as possible new steps be involved. A method presently being seriously considered involves the use of aqueous HI solutions to dissolve the residues.

It was reported last quarter[1] that 90 mg of residue from an irradiated LMFBR fuel rod was dissolved in 12 ml of 6 *M* HI at 124°C and that this dissolver solution was then evaporated to dryness and the remaining solids, including precipitated PuOI, were dissolved in 8.0 *M* of HNO_3. Additional data on the impurities and fission products dissolved along with the uranium and plutonium in the residue are now available.

The concentrations of the impurities (identified by SSMS analysis) in each of the dissolvents are listed in Table 3.8. Uncertainties in the analytical data at low concentrations appear to be large, so that attempts to calculate material balances for the impurities were unsuccessful. The principal significance of the data is that the impurity concentrations in the dissolvents are shown to be very low.

The fission product gamma emitters identified in the dissolvents include ^{106}Ru, ^{110}Ag, ^{125}Sb, ^{134}Cs, ^{137}Cs, ^{144}Ce, ^{154}Eu, and ^{155}Eu. The data for these gamma emitters are shown in Table 3.9. To calculate percent material balances for the individual gamma emitters, the total disintegrations per second in 12 ml of the 6 *M* HI solution was divided by the total disintegrations per second in 50 ml of the 8 *M* HNO_3 solution; the resulting quotient was multiplied by 100. Most of the material balances (Table 3.9) are within 100 ± 25%, which is probably within the accuracy of the data. Based on the data, it is assumed that

Table 3.8. Dissolved impurities[a] from irradiated LMFBR-type fuel residue[b]

Impurity	Concentration (μg/ml) in —	
	6.0 *M* HI[c]	8.0 *M* HNO_3[d]
Al	7	7
B	4	3
Ca	7	7
Cr	5	2
Fe	30	10
Mo	≤5	≤3
Na	50	70
Ru	≤5	≤2

[a]Determined by SSMS analysis.

[b]W. D. Burch et al., *LMFBR Fuel Reprocessing Program Progress Report for Period October 1 to December 31, 1976*, ORNL/TM-5768 (February 1977).

[c]12 ml of this solution contained 4.28 mg of plutonium and 3.85 mg of uranium.

[d]50 ml of this solution contained 4.36 mg of plutonium and 6.2 mg of uranium.

the same amounts of ^{106}Ru, ^{134}Cs, ^{137}Cs, ^{144}Ce, ^{154}Eu, and ^{155}Eu were dissolved in each dissolvent. Small amounts of Cl^- in the 8 *M* HNO_3 probably resulted in the precipitation of AgCl and thus in a decrease in the amount of ^{110}Ag in the 8 *M* HNO_3 solution. It is significant that there was 120% more ^{125}Sb in the 8 *M* HNO_3 than there was in the 6 *M* HI. The explanation of this result probably is that antimony has a low solubility in the HI dissolvent.

It was reported last quarter[1] that a vigorous reaction occurred when the HI dissolvent, which had been used to dissolve 90 mg of highly radioactive fuel residue, was evaporated to dryness. We have been unable to duplicate this vigorous reaction in evaporation tests of HI solutions containing various metal-ion impurities. We now believe it likely that the vigorous reaction in the "hot" test resulted from a minute exposure of the metal in the Teflon-coated magnetic stirring bar to the hot HI dissolver solution.

Table 3.9. Dissolved fission products from irradiated LMFBR-type fuel residue[a]

Fission product	Gamma activity (dis sec^{-1} ml^{-1}) in — 6.0 *M* HI	8.0 *M* HNO_3	Material balance[b] (%)
^{106}Ru	1.7×10^7	3.7×10^6	117
^{110}Ag	$\leqslant 3.4 \times 10^4$	$\leqslant 4.0 \times 10^3$	66
^{125}Sb	1.0×10^7	5.6×10^5	220
^{134}Cs	$\leqslant 6.8 \times 10^4$	$\leqslant 1.5 \times 10^4$	92
^{137}Cs	1.8×10^6	4.8×10^5	107
^{144}Ce	3.1×10^6	8.2×10^5	112
^{154}Eu	$\leqslant 4.7 \times 10^4$	8.6×10^3	76
^{155}Eu	$\leqslant 2.3 \times 10^5$	$\leqslant 5.2 \times 10^4$	103

[a]W. D. Burch et al., *LMFBR Fuel Reprocessing Program Progress Report for Period October 1 to December 31, 1976*, ORNL/TM-5768 (February 1977).

[b]Individual material balances were calculated from the total disintegrations per second in 12 ml of the HI solution divided by the total disintegrations per second in 50 ml of the HNO_3 solution.

Tests of alternative stabilizers for the HI dissolver solutions are in progress.

A topical report, *Cation Exchange in HI Solutions*, has been prepared and is in final draft form.

3.2.2 Hydroxylamine and hydrazine chemistry in Purex processing

Hydrazoic acid distribution (D. N. Browning, GLCA student participant in ORNL Chemistry Division, and A. D. Kelmers, ORNL Chemistry Division)

The measurement of the distribution of hydrazoic acid between nitric acid solutions and tributyl phosphate (TBP)–dodecane solutions has been completed. The experimental procedures were described previously.[6] Hydrazoic acid distribution-coefficient data were obtained from combinations of the following initial concentrations of solutions and temperatures:

Concentration in aqueous phase (*M*)		TBP concentration in organic phase (*M*)	Temperature (°C)
HN_3	HNO_3		
0.1	0.5	0.37	25
0.2	1.0	0.53	35
0.4	2.0	0.72	45
	4.0	0.89	55
		1.08	

The hydrazoic acid distribution coefficients (*E* O/A) are presented in Figs. 3.1-3.4 as log-log plots of *E* O/A vs free TBP concentration at 25, 35, 45, and 55°C respectively. Values of *E* O/A varied from about 1 to 10 over the range of conditions likely to be encountered in Purex processing and are in agreement with previous values.[7] The distribution reaction can be written as

$$HN_{3(aq)} + nTBP_{(org,free)} = HN_3 \cdot nTBP_{(org)} , \qquad (3.1)$$

where (org,free) denotes the free TBP in the organic phase and n is the number of moles of TBP bound per mole of HN_3. The free TBP concentration in the organic phase was calculated assuming the nitric acid in the organic phase to be present as a 1:1 complex with TBP.[8] The equilibrium constant for the reaction equals the respective concentrations times the activity coefficients

$$\frac{\gamma[HN_3 \cdot nTBP]_{org}}{\gamma[TBP]^n_{org,free}\ \gamma[HN_3]_{aq}} . \qquad (3.2)$$

Assuming the ratio of the activity coefficients to be constant, we can define the equilibrium quotient as

$$K' = \frac{[HN_3 \cdot nTBP]_{org}}{[TBP]^n_{org,free}[HN_3]_{aq}} . \qquad (3.3)$$

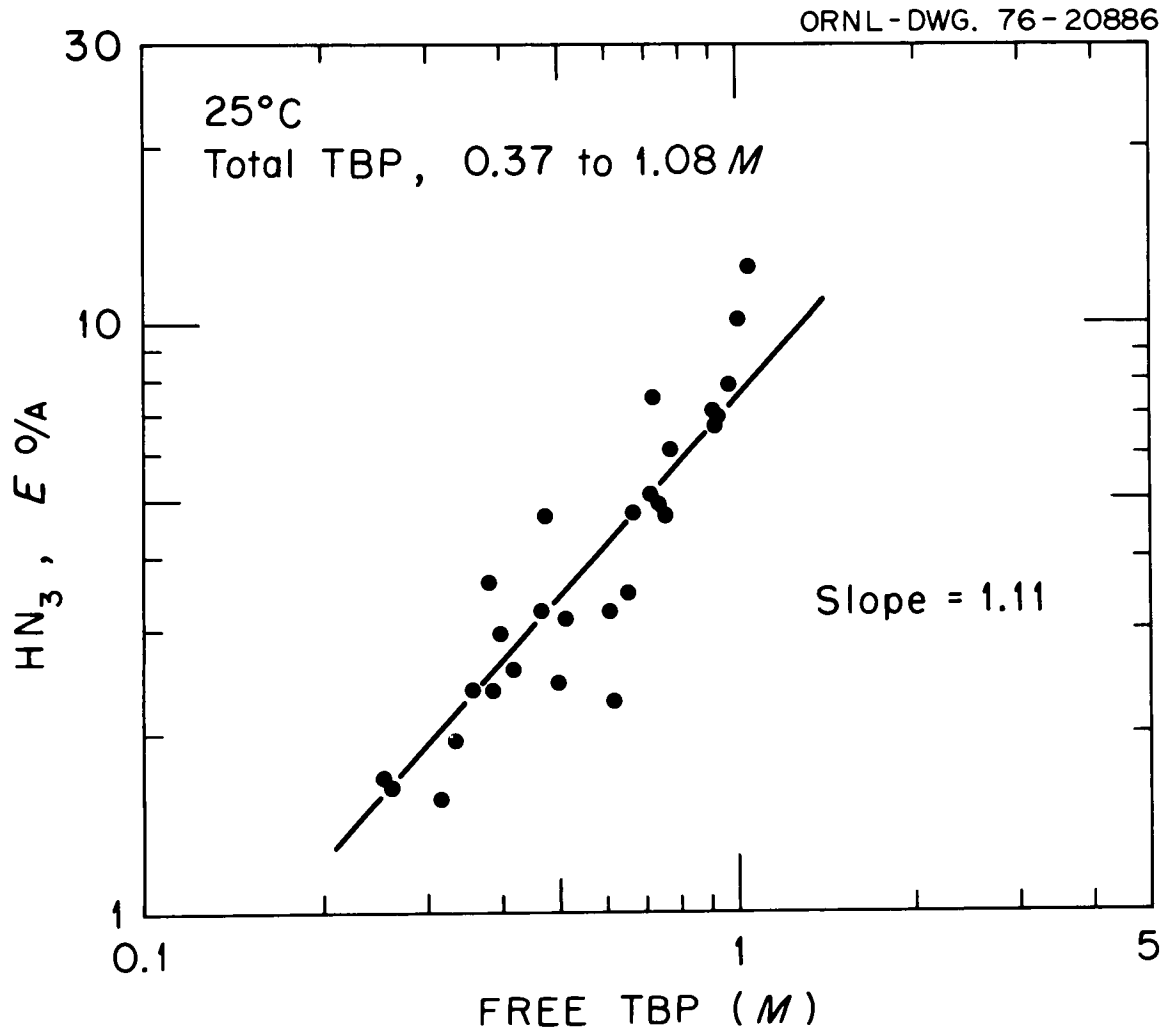

Fig. 3.1. Hydrazoic acid distribution coeficients at 25°C.

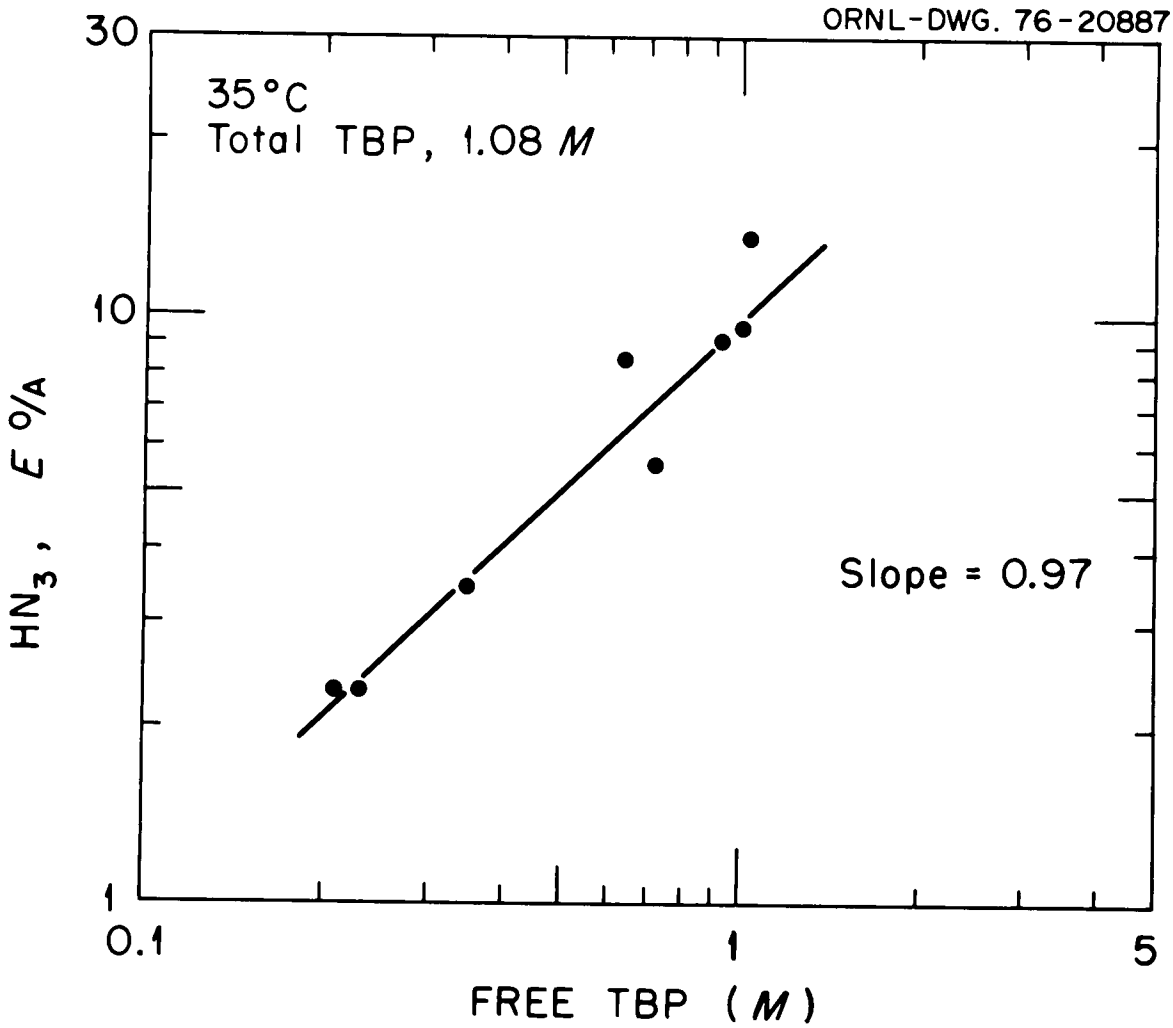

Fig. 3.2. Hydrazoic acid distribution coefficients at 35°C.

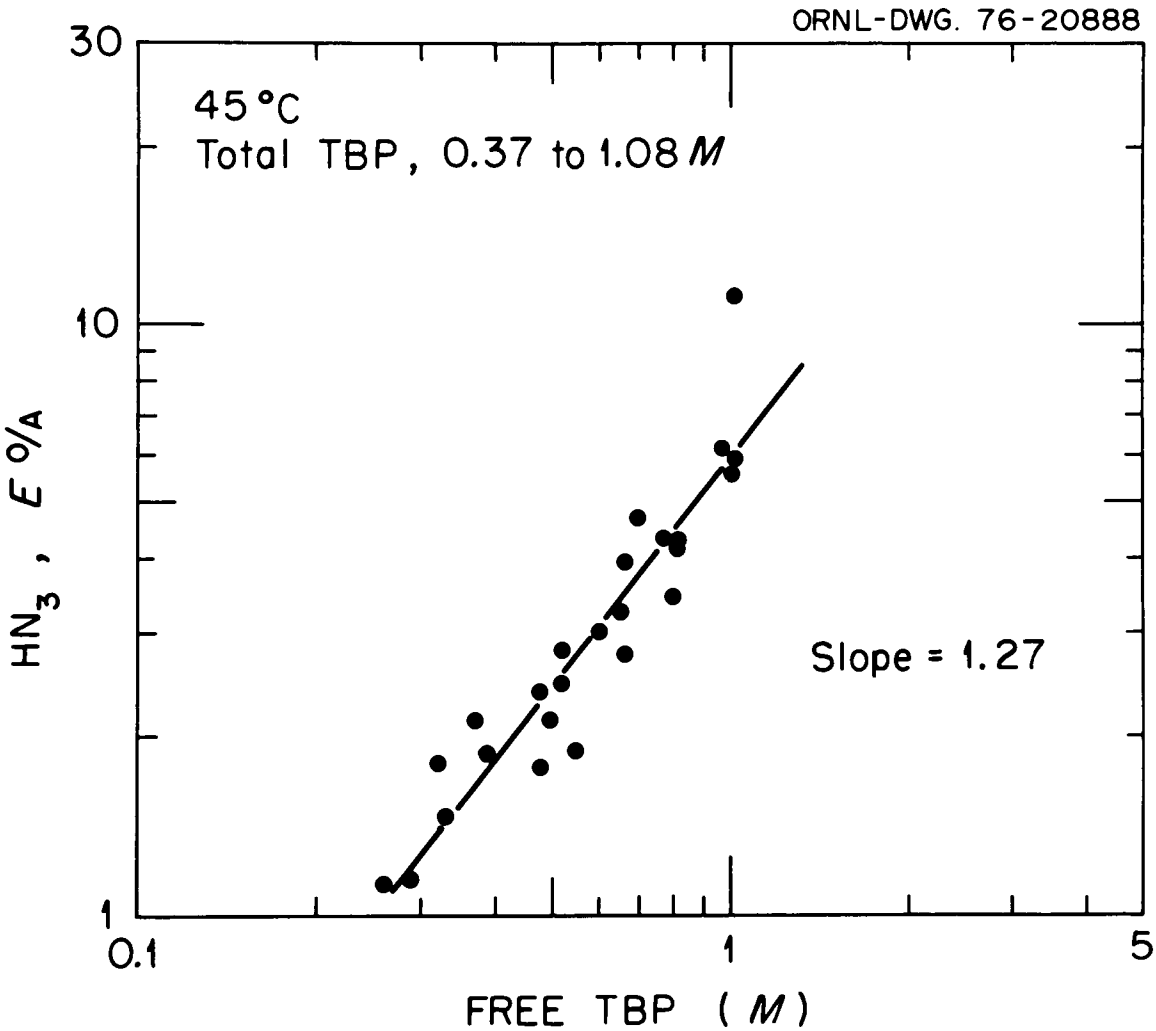

Fig. 3.3. Hydrazoic acid distribution coefficients at 45°C.

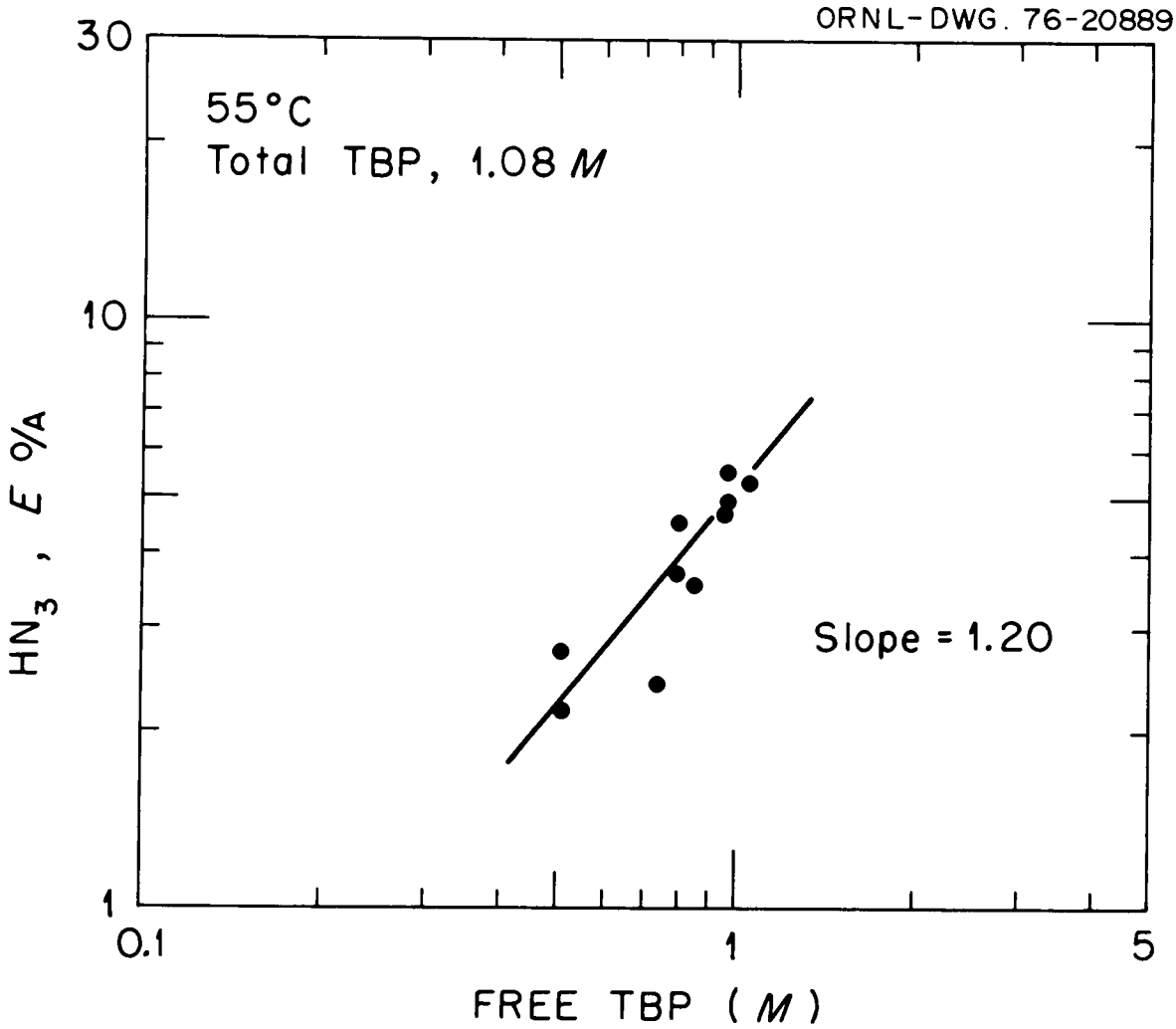

Fig. 3.4. Hydrazoic acid distribution coefficients at 55°C.

Since the distribution coefficient is

$$E\ O/A = \frac{[HN_3 \cdot nTBP]_{org}}{[HN_3]_{aq}} , \tag{3.4}$$

then

$$K' = \frac{(E\ O/A)}{[TBP]^n_{org,free}} , \tag{3.5}$$

or

$$\log (E\ O/A) = n \log [TBP]_{org,free} + \log K' . \tag{3.6}$$

Thus, the slope of each line (obtained by the least-squares fit of the experimental points in Figs. 3.1-3.4) gives the value of n for the complex $HN_3 \cdot nTBP$ at the indicated temperature. Slopes of 0.97 to 1.27 were obtained (Table 3.10), indicating that a 1:1 complex of HN_3 and TBP is formed.

Table 3.10. Values of the equilibrium quotients and values of n for $HN_3 \cdot nTBP$ complexes

Temperature (°C)	K'	n
25	7.40	1.11
35	9.85	1.27
45	5.84	0.97
55	5.06	1.20

The data did not show a marked temperature dependence, nor did the equilibrium quotients K' vary systematically with temperature (Table 3.10). This might be expected, since changes in K' reflect the cumulative changes in the activity coefficients with temperature.

The distribution coefficients obtained indicate that, during the reductive stripping of plutonium in Purex processing, most of the hydrazoic acid formed will be extracted into the organic phase and should follow the organic phase to the sodium carbonate scrub stages where it will be stripped into the carbonate waste stream as sodium azide.

Reaction of ammonium nitrate and nitric acid (D. N. Browning, GLCA student participant in ORNL Chemistry Division, and A. D. Kelmers, ORNL Chemistry Division)

There are several potential sources of ammonium nitrate in Purex processing flowsheets. These include:

1. The reaction of hydrazine with nitric acid[9] in nitric acid concentrators or during plutonium reoxidation by nitric acid

$$17N_2H_4 + 16HNO_3 \rightarrow 4NH_4NO_3 + 4HN_3 + 4N_2O + 11N_2 + 32H_2O \ . \qquad (3.7)$$

2. The reaction of hydrazine with plutonium(IV) during reductive stripping[10,11]

$$PuOH^{3+} + N_2H_5^{+} \rightarrow Pu^{3+} + NH_4^{+} + 0.5N_2 + H_2O \ . \qquad (3.8)$$

3. The spontaneous decomposition of hydrazine[12]

$$3N_2H_5^{+} + H^{+} \rightarrow 4NH_4^{+} + N_2 \ . \qquad (3.9)$$

4. Contaminants in feed chemicals such as hydrolylamine nitrate or hydrazine hydrate resulting from decomposition on storage.

It would be desirable to have available methods for the destruction of the ammonium ion in nitric acid solutions. We have been investigating the chloride-catalyzed decomposition of ammonium in nitric acid[13]

$$NH_4NO_3 \xrightarrow{C\ell^-} N_2O + 2H_2O \ . \qquad (3.10)$$

The kinetics and reaction intermediates are unknown, and an understanding of them may lead to catalysts other than chloride. The rate of disappearance of the ammonium ion is first order in 4 to 8 *M* HNO_3; above 8 *M* there is an abrupt change to second-order kinetics. Additional experiments are under way to further explain these effects.

An SR-52 calculator program for the calculation of the rate of plutonium(IV) reduction by hydroxylamine nitrate (D. Y. Valentine and A. D. Kelmers, ORNL Chemistry Division)

The kinetics of the reduction of plutonium(IV) by hydroxylamine were described[14] by a rate law

$$-\frac{d[Pu^{4+}]}{dt} = k' \frac{[Pu^{4+}]^2[NH_3OH^+]^2}{[Pu^{3+}]^2[H^+]^4(K_d + [NO_3^-])^2} , \qquad (3.11)$$

which relates the rate of reduction of plutonium(IV) to concentrations of Pu(IV), Pu(III), NH_3OH^+, H^+, and NO_3^-. The rate law was derived semiempirically and consistent with initial rate data. From the form of the expression, it is obvious that the rate will be sensitive to the total nitrate concentration and extremely sensitive to the hydrogen ion concentration.

Two separate mathematical techniques were applied to the above rate law and programmed on an SR-52 calculator with a PC-100 printer to calculate the reduction of plutonium(IV) to plutonium(III) as a function of time.

Technique (a) — Integration of the rate expression. The rate expression can be reduced to the form

$$-B\ dt = \frac{[Pu(IV)_i - x]^2}{x^2(c + x)^2}\ dx , \qquad (3.12)$$

where $Pu(IV)_i$ is the initial Pu(IV) concentration at time t = 0, x is the amount of Pu(IV) left as a function of time, (c + x) is the NH_3OH^+ concentration as a function of time (c = the initial NH_3OH^+ concentration), and

$$B = k'/(K_d + [NO_3^-])^2 \, [H^+]^4 \, . \qquad (3.13)$$

The assumptions are that both $[H^+]$ and $[NO_3^-]$ are invariant with time, that $\Delta Pu(IV)/\Delta NH_3OH^+ = 1$, and that K_d is independent of temperature. The expression for -B dt is integrable from standard tables.

Technique (b) — Finite difference evaluation. Numeric analysis with exceedingly small values of Δx was used as an alternative method of evaluating the expression for -B dt. Agreement with the integration technique (a) verified the correctness of both the integration and the programming of the expression for -B dt. Technique (a) was used in all subsequent calculations, since it is much faster.

A user's guide for the SR-52 program has been prepared and is available as ORNL/CF-77/27.

3.2.3 Solvent chemistry studies

L. Maya (Chemistry Division, ORNL) and C. D. Bopp (Chemical Technology Division, ORNL)

A study of the effect of butylaurylphosphoric acid (HBLPA) on the distribution of different fission products between TBP-organic and nitric acid solutions is continuing. As described in last quarter's report,[15] HBLPA was chosen as a model compound representative of the secondary degradation products of TBP and dodecane in the Purex process.

The distribution coefficient of zirconium between 3 *N* HNO_3 and 30% TBP in dodecane was examined as a function of HBLPA concentration. The zirconium solutions for these tests were prepared as follows: The tracer ^{95}Zr-Nb, in the oxalate form, was treated with boiling concentrated nitric acid and 30% hydrogen peroxide to eliminate the oxalic acid. The tracer was then added to a $ZrO(NO_3)_2$ solution; the mixture was neutralized with NH_4OH, filtered, and the zirconium hydroxide was redissolved in 10 *N* HNO_3. This treatment was repeated twice to ensure complete equilibration of the tracer and the carrier. Elimination of the ^{95}Nb activity was initially accomplished by contact with unfired Vycor glass;[16] however, this treatment still yielded a solution containing 10% of the gamma activity as ^{95}Nb. Better decontamination, with factors

of the order of 500, was obtained using a procedure[17] based on the absorption of both zirconium and niobium from 3 *N* HNO_3 on silica gel and the selective desorption of zirconium with 10 *N* HNO_3. Freshly decontaminated solution had to be prepared daily, since niobium activity ingrowth occurs at a rate of about 2% per day.

The distribution coefficients in the extraction runs were derived from Martin plots,[18] which are plots of concentration of the metal in the organic phase as a function of the concentration of the metal in the aqueous phase. A range of concentrations can be covered by changing the solvent-to-aqueous ratios and/or changing the initial concentrations in the aqueous phase. It is possible to detect the presence of different metal species in the system from these plots. A plot of log K_D as a function of log [HBLPA] is given in Fig. 3.5. Low loading factors, of the order of a few percent, were maintained in these determinations so that the final free HBLPA concentration was nearly the same as the initial concentration. The experimental points (Fig. 3.5) fall close to a line drawn with a slope of 2, showing that the mole ratio HBLPA:Zr of the extracted species is 2. In a parallel series of experiments in the absence of TBP, shown in Fig. 3.6, a similar result was found; however, the concentrations required to achieve the same distribution coefficients were about an order of magnitude lower. These results show that TBP lowers the activity of HBLPA, possibly through TBP–HBLPA association. The zirconium K_D values for HBLPA are very similar to those for zirconium with dibutylphosphoric acid. Also, the slopes for the log K_D vs [ligand] plots are the same in both cases, suggesting similar mechanisms of extraction.

Hardy et al.[19] postulated the following mechanism for the extraction of zirconium by hydrogen dibutyl phosphate (HDBP):

$$ZrO^{2+} + 2NO_3^- + 2[HDBP]_{org} \rightleftharpoons [Zr(NO_3)_2(DBP)_2]_{org} + H_2O \ . \qquad (3.14)$$

This mechanism was derived from a study of the zirconium extraction coefficient as a function of ligand, nitrate ion, and hydrogen ion concentrations. The equilibrium quotient for such a reaction in the

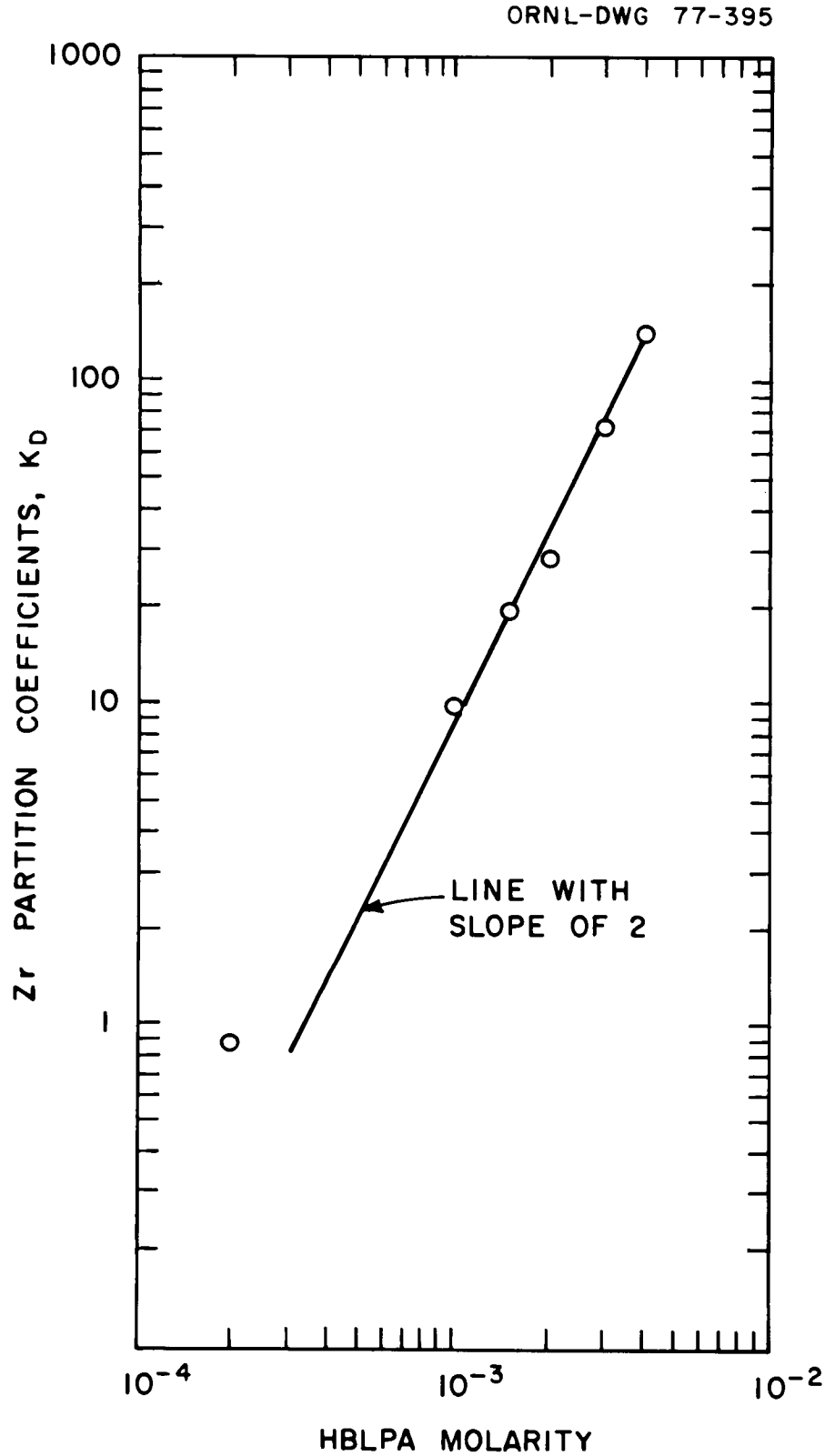

Fig. 3.5. Partition of zirconium between HBLPA–30% TBP–dodecane and 3 *N* HNO_3 at 21 ± 1°C; contact time, 15 min.

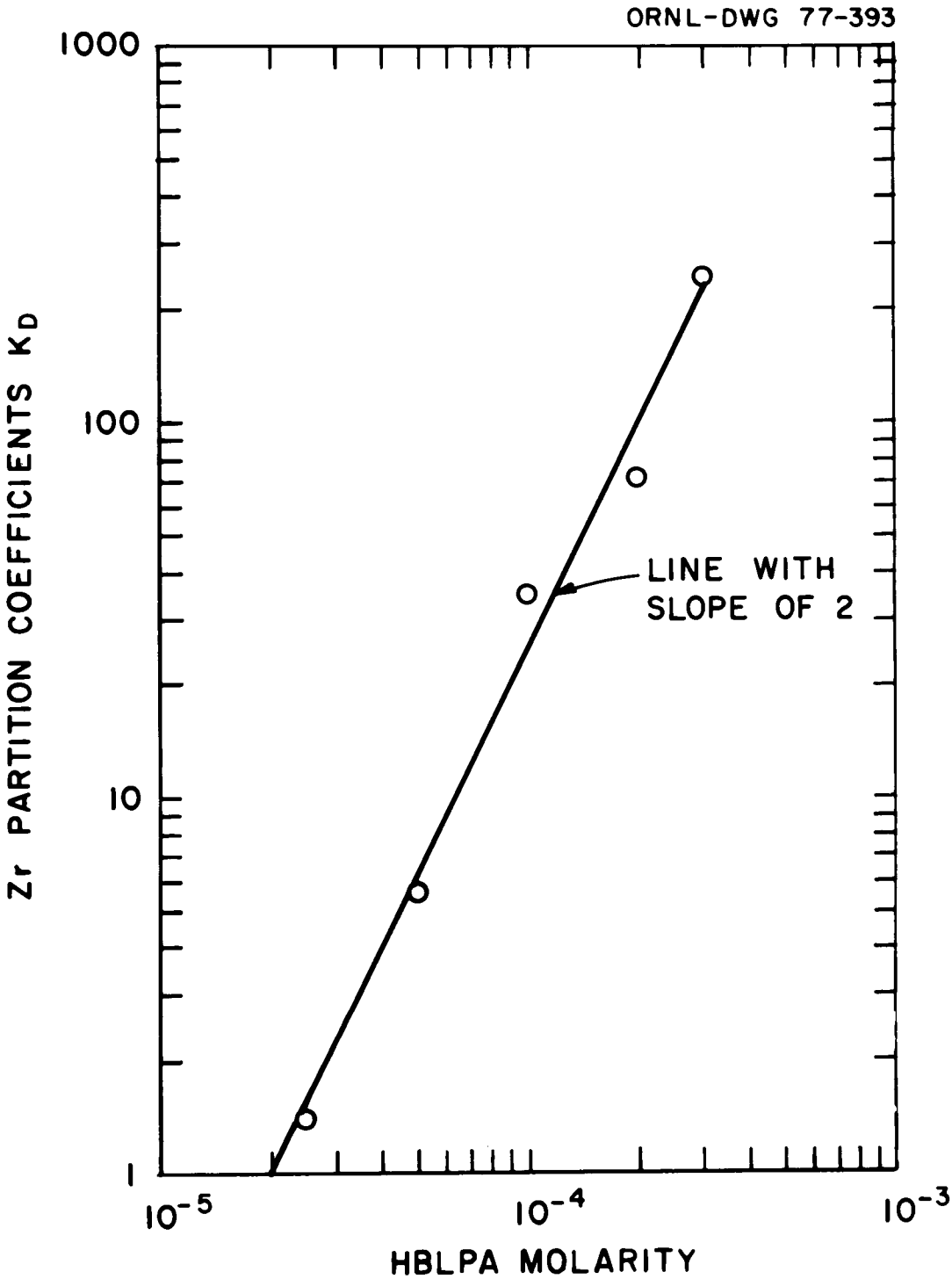

Fig. 3.6. Partition of zirconium between HBLPA–dodecane and 3 *N* HNO_3 at 21 ± 1°C; contact time, 15 min.

case of HBLPA is 4×10^9, assuming that a similar mechanism holds. This quotient indicates that the complexation of zirconium by HBLPA is strongly favored.

The hydrogen ion dependence of zirconium extraction at constant HBLPA and nitrate concentrations is given in Fig. 3.7. In this case, a behavior different than that with HDBP is observed. The extraction of zirconium by HDBP does not show a hydrogen ion concentration dependence in the 0.5-2 *N* HNO_3 concentration range,[20] whereas extraction by HBLPA shows a dependence that indicates participation of the hydrogen ion as a reactant in the extraction mechanism. This observation does not necessarily preclude this mechanism (extraction by HBLPA) from being similar to that of HDBP, but it may possibly indicate hydrogen ion association with the ligand.

The solubility effect of the HBLPA in the aqueous phase, especially at low acid concentrations (which is significant in the case of HDBP, causing K_D differences of one order of magnitude), seems to be of no consequence (in the case of HBLPA), which is an indication that HBLPA will not be removed from the organic phase with low-acidity washes.

Preliminary tests on the removal of HBLPA from TBP–dodecane solutions by a carbonate wash showed that three washes with 1 *M* Na_2CO_3 at solvent-to-aqueous ratios of 1 removed only about 20% of the HBLPA. This treatment is an extremely unfavorable case, since the solvent-wash step is usually performed with a much higher organic–aqueous ratio. The relatively limited removal accomplished by this treatment serves to demonstrate that HBLPA is a representative secondary degradation product, since it is known that secondary degradation products formed under process conditions are not removed in the solvent-wash step.

The plot of zirconium distribution coefficients between the solvent and 3 *N* HNO_3 (as a function of HBLPA concentration) can be used as an analytical tool to determine HBLPA concentrations in solvents with an unknown amount of this compound. This plot will be useful in future work to test the efficiency of different treatments aimed at removing HBLPA from solvent solutions.

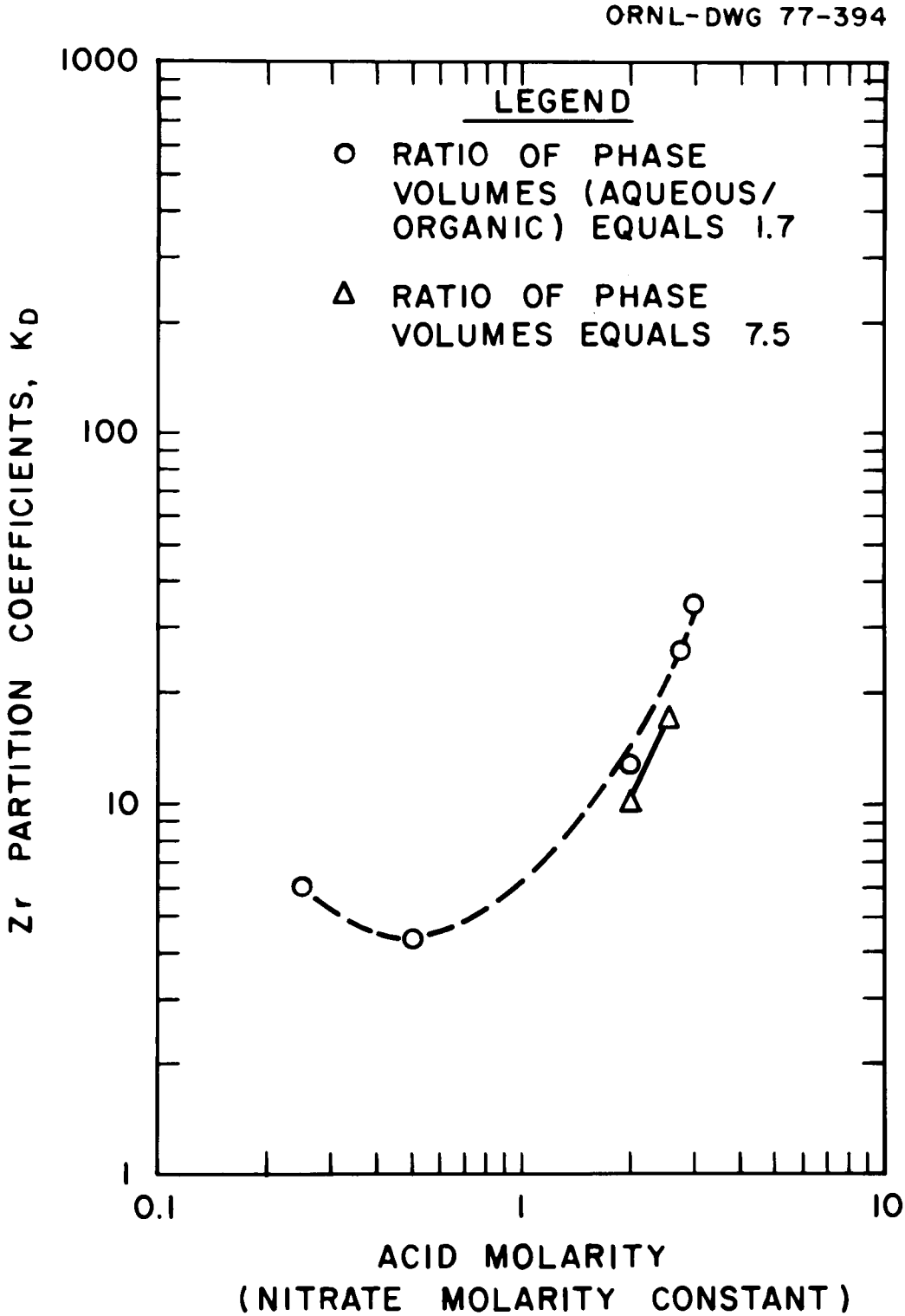

Fig. 3.7. Partition of zirconium between 10^{-4} *M* HBLPA–dodecane and HNO_3–$LiNO_3$ solutions at constant 3 *N* nitrate concentration at 21 ± 1°C; contact time, 15 min.

3.2.4 Reduction of Pu^{6+} using NO_x

M. R. Bennett, Chemisry Division, ORNL

Nitric oxide gas (NO) will reduce plutonium(VI) in nitric acid solution to plutonium(IV) according to the following reaction:

$$2NO + 3PuO_2^{2+} + 4H^+ = 3Pu^{4+} + 2NO_3^- + 2H_2O \ . \qquad (3.15)$$

We are currently evaluating the use of nitrogen dioxide gas (NO_2) as the initial reactant in obtaining comparable reduction of the plutonium(VI) to plutonium(IV). It is anticipated that the reduction will proceed in accordance with the following reactions:

$$3NO_2 + H_2O = 2HNO_3 + NO \ ; \qquad (3.16)$$

$$2NO + 3PuO_2^{2+} + 4H^+ = 3Pu^{4+} + 2NO_3^- + 2H_2O \ . \qquad (3.17)$$

Standard solutions of plutonium(VI) were prepared by heating a stock solution containing about 40 g/liter of plutonium(IV) in 1 *M* HNO_3 to a temperature of 90°C for 24 hr under total reflux. This heating was sufficient to oxidize about 80% of the plutonium(IV) to plutonium(VI). Test solutions containing about 3 g/liter of plutonium(VI) were then prepared by diluting 10 ml of the standard solution to a final volume of 100 ml with HNO_3 adjusted to the desired normality. In a typical experiment, 100 ml of the test solution is poured into an enclosed glass reaction vessel equipped with a glass-fritted sparge tube. After thorough mixing with a magnetic stirrer, a 1-ml sample of the solution is withdrawn, pipetted into 9 ml of 1 *N* HNO_3, and equilibrated with an equal volume of trifluoro-thenylacetone (TTA) to determine the plutonium(VI) and plutonium(IV) concentrations. [The extraction of plutonium(IV) into TTA is essentially quantitative, with the inextractable plutonium(VI) remaining in the aqueous phase.] After removal of all air from the system by sparging with nitrogen, NO_2 and/or NO gas is metered in at the prescribed flow rate. Samples are taken periodically through

a sample port located in the side of the glass vessel. These samples are equilibrated immediately with TTA in the manner previously described. In cases where the amount of plutonium(VI) reduced is in the proximity of 100%, a more precise measurement of the plutonium(VI) content is made from the absorption spectrum using a Carry-14 spectrophotometer. A series of experimental tests is in progress, in which the effect of temperature on the reduction kinetics of plutonium(VI) by NO_2 is being evaluated. Tests completed to date have demonstrated that the reduction proceeds very slowly, but with a strong temperature dependence over the range of 26 to 70°C (Table 3.11). Tests at 26 and 40°C, respectively, showed no detectable reduction of the plutonium(VI), even after ten times the stoichiometric amount of NO_2 was introduced. At temperatures of 60 and 70°C, respectively, complete reduction of the plutonium was achieved. Even at these temperatures, however, the reduction proceeded slowly, requiring 22 and 12 times, respectively, the stoichiometric amount of NO_2. The order of the reaction has not yet been defined.

Table 3.11. Effect of temperature on the reduction of plutonium(VI) in nitric acid with NO_2 gas

Initial Pu(VI) concentration (g/liter)	T (°C)	H^+ concentration (*N*)	NO_2 (mole equivalent)	Pu(VI) reduced (%)
2.8-3.2	26	3.0	10	nd[a]
2.8-3.2	40	3.0	10	nd[a]
2.8-3.2	60	3.0	10	26.2
2.8-3.2	60	3.0	22	100
2.8-3.2	70	3.0	12	100

[a]None detected.

In support of an earlier experiment by Horner and Crouse[20] in which plutonium(VI) was reported to have been reduced quantitatively with NO gas at 60°C using a calculated value of 1.8 times the number of mole equivalents, a test was made under identical conditions. The results of the test were in excellent agreement with those of Horner and Crouse,

with total reduction being achieved with less than two times the stoichiometric amount of NO gas. Due to the extremely low flow rate of the NO used in the reduction (2.8 sccm), a measure of the exact stoichiometry was not possible. This test will be followed up at a later date using a higher concentration of plutonium(VI) in an attempt to more accurately define the stoichiometry and to determine the order of the reaction.

Experimental studies are being continued. We plan to complete the temperature effect series using NO_2 with an additional test at 80°C, following which we will determine the effect of acid concentration.

3.3 Product Conversion

J. D. Sease

The primary objective of this task is to develop information that will allow the design and operation of the product conversion system in the Hot Pilot Plant (HPP) to proceed at an acceptable risk. Because the average plutonium content of both core and blanket FBR fuel entering an FBR reprocessing plant will be about 6% plutonium in uranium, and the plutonium content required for the refabrication of core FBR fuel will be about 20% plutonium in uranium, two conversion process systems must be included in an FBR reprocessing plant: one for uranium only and the other for plutonium. (The plutonium conversion system may process some uranium, depending upon the process adopted.) Major work this quarter has been in selecting the reference conversion process for the HPP and the development program and initiating the preparation of feed and product specifications for the product conversion system. A second draft of the product conversion work plan has been completed, including both internal and external comments.

3.3.1 Uranium conversion process

The selected reference process for uranium conversion will use a wiped film evaporator — a thermal denitration arrangement for the preparation of UO_3 directly from the uranium nitrate feed stream. The development work plan for this activity is to demonstrate the operation

of this type of process unit in the Integrated Prototype Equipment Test (IPET) Facility.

3.3.2 Plutonium conversion process

The selected reference process for plutonium conversion is a coprocessing [U(∿20 wt % Pu)O_2] flowsheet, probably by oxalate precipitation. Cothermal denitration has been tentatively selected as the backup to the reference process.

Research and development work will continue on both processes so that a determination can be made (by January 1979) as to which one will be used and which one will serve as backup.

REFERENCES FOR SECTION 3

1. W. D. Burch et al., *LMFBR Fuel Reprocessing Program Progress Report for Period October 1 to December 31, 1976*, ORNL/TM-5768 (February 1977).
2. F. L. Brown et al., *Performance of Vibratorily Compacted Mixed Oxide Fuel Elements in EBR-2 to 2.7 a/o Burnup*, ANL-7954 (June 1970).
3. C. E. Johnson, "Chemistry of Irradiated Fast Reactor Fuels and Materials," *Chemical Engineering Division Annual Report — 1970*, ANL-7775 (April 1971).
4. D. R. O'Boyle et al., *Trans. Am. Nucl. Soc.* 11: 101 (1968).
5. B. L. Vondra, *LWR Fuel Reprocessing and Recycle Program Quarterly Report for Period October 1 to December 31, 1976*, ORNL/TM-5760 (February 1977).
6. D. N. Browning and A. D. Kelmers, *LMFBR Fuel Reprocessing Program Progress Report for Period October 1 to December 31, 1976*, ORNL/TM-5768 (February 1977), pp. 3-14 to 3-20.
7. E. K. Dukes and R. M. Wallace, *Formation of Hydrazoic Acid from Hydrazine in Nitric Acid Solutions*, USAEC Report DP-728 (1962).
8. W. Davis, Jr., *Nucl. Sci. Eng.* 14: 169 (1962).
9. V. S. Koltunov, V. A. Nikolskii, and Yu. P. Agureev, *Kinet. Katal.* 3: 764 (1962).
10. V. S. Koltunov and G. I. Zhuravleva, *Sov. Radiochem.* 16: 80 (1974).
11. J. L. Swanson, *Platinum-Catalyzed Hydrazine Reductions of Plutonium(IV) and Uranium(VI)*, BNWL-1584 (1971).
12. L. F. Audrieth and B. A. Ogg, *The Chemistry of Hydrazine*, Wiley, New York, 1951, Chap. 6.
13. J. van R. Smit, *Chem. Ind.* (London) 1964: 2018.
14. G. S. Barney, *J. Inorg. Nucl. Chem.* 38: 1677 (1976).
15. L. Maya, *LMFBR Fuel Reprocessing Program Progress Report for Period October 1 to December 31, 1976*, ORNL/TM-5768 (February 1977), pp. 3-28 to 3-31.
16. J. G. Moore, *J. Inorg. Nucl. Chem.* 20: 166 (1961).
17. E. Akatsu and Y. Aratono, *Anal. Chim. Acta* 84: 347 (1976).

18. F. S. Martin and G. M. Gillies, *The Chemistry of Ruthenium*, AERE-C/R-816 (1951).

19. C. J. Hardy and D. Scargill, *J. Inorg. Nucl. Chem.* 17: 337 (1961).

20. D. E. Horner and D. J. Crouse, *Laboratory Development of Solvent Extraction Processes for Spent LMFBR Fuels*, ORNL/TM-5729 (January 1977), p. 6.

4. ENGINEERING RESEARCH

W. S. Groenier

Initial equipment concepts being developed and evaluated and engineering data on which to base equipment designs in various engineering research studies are reported. Studies of the dissolution, voloxidation, NO_x scrubbing, iodine evolution, and Iodox processes are in progress, and development efforts are defined.

Work directed toward the retention of krypton in the fluorocarbon absorption process and toward the development of instrumentation and control and solvent-extraction methods is also reported.

4.1 Voloxidation

M. E. Whatley

The voloxidation process has been proposed as a head-end method for removing tritium from the fuel prior to aqueous processing. Based on previous experimental work, it appears that this objective can be met by heating the oxide fuel to 450 to 600°C (723 to 873 K) in flowing oxygen or in air. Volatilization of tritium and other fission products results as the UO_2 in the mixed-oxide fuel is restructured during oxidation to U_3O_8. Early removal of the tritium from the fuel into a relatively small volume is desirable to avoid extensive dilution of the tritium with water in subsequent fuel dissolution. A secondary benefit of voloxidation is the oxidation of residual sodium in the fuel prior to dissolution.

The rotary-kiln studies are described and reported as part of the LWR Fuel Reprocessing and Recycle Program,[1] which now provides funding for voloxidation work. These studies are directly applicable to either LWR or LMFBR fuels; highlights of recent work follow.

The dispersion number, a measure of the spread of residence time in a rotary-kiln voloxidizer, has been found to be proportional to the square of the kiln diameter for kilns of equal length and is affected by feed-size distribution and kiln slope. Feed rate and rotational speed do not influence the dispersion number at low values of holdup.

The purchase order for a 0.5-metric-ton/day prototype voloxidizer has been approved and issued to the C-E Raymond-Bartlett-Snow Company.

4.2 Dissolution

The objective of the dissolution task is to ensure that LMFBR fuels can be dissolved in HNO_3 to give high metal recoveries. Dissolution characteristics of the fuels can vary widely, depending on plutonium content, method of preparation, and irradiation history. Consequently, extensive leaching data will be obtained in the overall program to determine the effects of such variables. Other efforts are directed toward understanding the behavior of iodine in the dissolver system. Criticality control and off-gas considerations call for dissolver design and operation to be performed within rather narrow limits. Continuous dissolving methods, which appear to offer superior solutions to these problems, are being emphasized.

During this report period major emphasis was on the ongoing development of a continuous, rotary dissolver.

4.2.1 Four-foot-diameter dissolver prototype

B. E. Lewis

Operational testing of the 4-ft-diam rotary dissolver prototype is continuing. During this report period, liquid backmixing tests were completed, rinsing studies were initiated, and preliminary plans were made for corrosion-erosion tests.

Liquid carryover studies. A design criteria of the continuous rotary dissolver is to minimize the amount of liquid backmixing, thereby achieving a higher recovery of heavy metals. Liquid backmixing can occur by diffusion against the normal countercurrent liquid flow or by carryover with solid materials. Backmixing can therefore cause an increase in heavy-metal contamination of fuel hulls, wires, etc., exiting the dissolver.

In experiments to determine the amount of liquid carryover, a measured amount of nitric acid solution was placed in the center section

of the dissolver along with a weighed quantity of sheared hulls and shrouds. The contents were agitated and the solids were transferred to the exit section by a single reverse rotation of the dissolver. A measured quantity of water was added to the exit section and mixed with the hulls and shrouds; the resulting weak-acid solution was then analyzed. The solids were next transferred out of the dissolver and into a receiver. The weight of the material in the receiver was used to determine the amount of liquid leaving the dissolver with the solids.

The degree of liquid carryover between stages was found to be highly dependent upon the amount of mixing that the hulls and shrouds received in the acid solution and is apparently related to how well the solids were wet by the liquid. For the case where the hulls and shrouds were completely wet by the acid, an average of about 266 g of solution was carried over with each kilogram of empty hulls and shrouds or <6% of the total liquid flow. The amount of liquid transferring out of the dissolver with the empty hulls and shrouds remained fairly constant at about 43 g/kg of solids.

These quantities of liquid carryover with solids transfer do not appear to be significant as long as sufficient stages are provided to adequately rinse and dilute the dissolved heavy metals before the sheared material exits the dissolver.

Rinsing studies. Experiments to determine the rinsing efficiency of the dissolver have been initiated. In these experiments, -325 mesh nickel powder is being used to represent fission products and slowly soluble plutonia.[2] The powder feed material was added to the dissolver through the flapper isolation valves in the first rinsing run to minimize the loss of metal powders by dusting. The water flow from the dissolver was filtered to remove all solids; the hulls and shrouds leaving the dissolver were collected in a receiver. Both the nickel powder remaining on these solids and that collected on the filter will be dissolved in nitric acid. We are preparing to dissolve the powder from the first rinsing run. Analysis of the data from several runs will determine the steady-state holdup of fines in the dissolver and the rinsing efficiency. We plan to look at the effects of liquid flow rate, percent fines in the

feed, and dissolver cycle time on the rinsing efficiency. Results will be compared with those obtained in earlier tests using a 1-ft-diam laboratory model rotary dissolver.

Corrosion-erosion tests. Plans are being made for the corrosion-erosion testing of various dissolver construction materials. In these tests, we plan to expose specimens of various candidate alloys to an environment of sliding and falling sheared materials and 8 *M* HNO_3 at 100°C. We are consulting with the Metals and Ceramics Division personnel in establishing a list of candidate materials and in setting up the experiments.

A decision will soon be made on whether to fabricate a new corrosion-erosion test unit, for which a design is nearly complete, or to modify the 4-ft-diam dissolver to accept hot nitric acid and material specimens. The costs of both systems appear to be similar; however, use of the rotary dissolver as a corrosion test device will prevent its use for other testing.

4.2.2 Operational testing of ferrofluidic seals

B. E. Lewis

The operational testing of ferrofluidic seals has been initiated to show their feasibility as a possible backup sealing system for the main concept of a purged housing for the rotary dissolver. A ferrofluidic seal is composed of a ferrofluid and permanent magnets. The ferrofluid fills the gap between the stationary and rotating parts and is held in place by permanent magnets mounted in the seal housing. The ferrofluid we had decided to use consists of colloidal iron (ferrite) particles permanently suspended in a polyphenyl ether medium that also includes various proprietary ingredients. However, because of difficulties in production, the manufacturer is unable to deliver this product and has suggested that we select a fluorocarbon-based ferrofluid. The manufacturer claims that this material offers an equally good resistance to radiation and that it provides a higher magnetic saturation. We have now obtained a supply of the fluorocarbon-based ferrofluid for evaluation;

a small aliquot will be irradiated to verify the claim of radiation stability. Instrumentation for the seal test stand is being purchased.

4.3 Feed Preparation

The aqueous feed discharged from the dissolver will contain solids (undissolved fission products, corrosion products, etc.) and will therefore require clarification prior to solvent extraction. Preparation of the feed for solvent extraction will also include adjustment of the plutonium valence and HNO_3 concentration as well as treatment to remove iodine.

Proposed iodine-removal methods include the use of NO_2-H_2O_2 or NO_2-O_3 gas mixtures in addition to steam as sparge streams in the digestion and feed preparation tanks. Since a large amount of NO_2 in vessel off-gas streams may have a deleterious effect on the performance of the Iodox process for iodine removal from gas streams, the development of a method for removing nitrogen oxides from the off-gas streams associated with feed preparation vessels has also been emphasized.

4.3.1 Nitrogen oxide scrubbing

R. M. Counce

Engineering studies to measure the removal of nitrogen oxides from mixtures of nitrogen oxides, air, and steam have continued. During this report period the experimental system for the NO_x scrubber development previously described[3-5] was removed from Building 4505 to Building 7603. With the addition of a packed column and other modifications, the experimental system has been reinstalled and shakedown activities have been concluded. Some initial NO_x scrubber experiments have been undertaken, and the data are being prepared for publication. Experiments are planned to determine the effect on the scrubber of iodine in the feed-gas and to measure steady-state phase distribution of I_2.

4.3.2 Iodine evolution

J. G. Morgan

The design was completed for a series of small-scale engineering tests to study iodine evolution from a simulated feed stream. Steam stripping in a packed bed shows promise as a method for removing iodine from the acid stream that leaves the dissolver digestion tank. A 4 *M* nitric acid stream containing 2.5×10^{-4} *M* iodine as a potassium or methyl iodide solution will be fed into the top of a column (packed with Intalox saddles) at 100°C; the solution will be spiked with an ^{131}I tracer for analysis purposes. As the feed flows down through the packing, it will be steam stripped of its iodine. Steam will be supplied from a reboiler at the bottom of the column. Distillation cuts will be varied from 5 to 25%. The iodine-rich exit vapor will be sampled using silver zeolite traps, which will be analyzed for ^{131}I. Previous small laboratory experiments indicate that it is important to avoid refluxing of the exit vapor to prevent recondensation of the evolved iodine. In the actual pilot plant, radiolytic decomposition and fuel dissolution produces hydrogen peroxide and nitrogen oxides, which are beneficial in decomposing any nonvolatile organic iodine compounds present in the feed. Our plans are to inject H_2O_2 and N_2O_3 into the column feed or reboiler to aid in iodine evolution. To obtain data that will allow the design of scaled-up equipment for the pilot plant, our experiments are ten times larger than were previous laboratory experiments. Purchase of equipment and fabrication of components have proceeded during this quarter.

4.4 Fluorocarbon Absorption Studies*

M. J. Stephenson

This program consists of the accelerated development of the krypton absorption process. The program includes expansion of the pilot-plant

---

*Jointly funded by LMFBR Fuel Reprocessing and LWR Fuel Reprocessing and Recycle programs.

development, performance of a proposed system reliability analysis, and a study of the chemical effects of impurities in the fluorocarbon solvent on the process and equipment.

4.4.1 Pilot plant operation

R. S. Eby, V. C. Huffstetler, and J. L. Patton (ORGDP)

Pilot plant tests continue to show that lower absorption pressures (i.e., 100 psig instead of 300 to 400 psig) are allowable in the performance of the packed column operation. Economics support the lower pressure, since only single-stage pumps and compressors are required to process the contaminated feed-gas. Figure 4.1 shows the effect of the lower pressure operation on the relative krypton concentration profiles in the absorber. Also in Fig. 4.1, the ratio of krypton concentration at various places within the column to that at the bottom or gas inlet section of the column is plotted as a function of position. Process measurements were made using an external scanning gamma scintillation detector and associated gamma-ray spectroscopy equipment. At the lower pressure, the fission-product removal is less than that in the run conducted at twice the pressure and at approximately the same solvent-to-gas flow-rate ratio. The solubility loss incurred at the lower pressure, however, can be compensated for by increasing the column contacting ratio. Figure 4.2 shows absorber concentration profiles taken at constant pressure but with varying L:G ratios. In these cases, increasing the L:G ratio by a factor of 2 resulted in a substantial improvement in column performance. The data indicate that, at an absorption pressure of 100 psig, an L:G ratio of 12 to 15 is needed in a 15-ft-high column to yield 95 to 99% removal of the feed-gas krypton.

Low-pressure tests conducted with xenon are summarized in Fig. 4.3, where the absorber decontamination factor is plotted as a function of the absorption ratio, kG:L;* krypton data are also plotted for comparison.

---

*k = distribution coefficient defined by y = kx; G = gas molar flow rate; L = solvent molar flow rate.

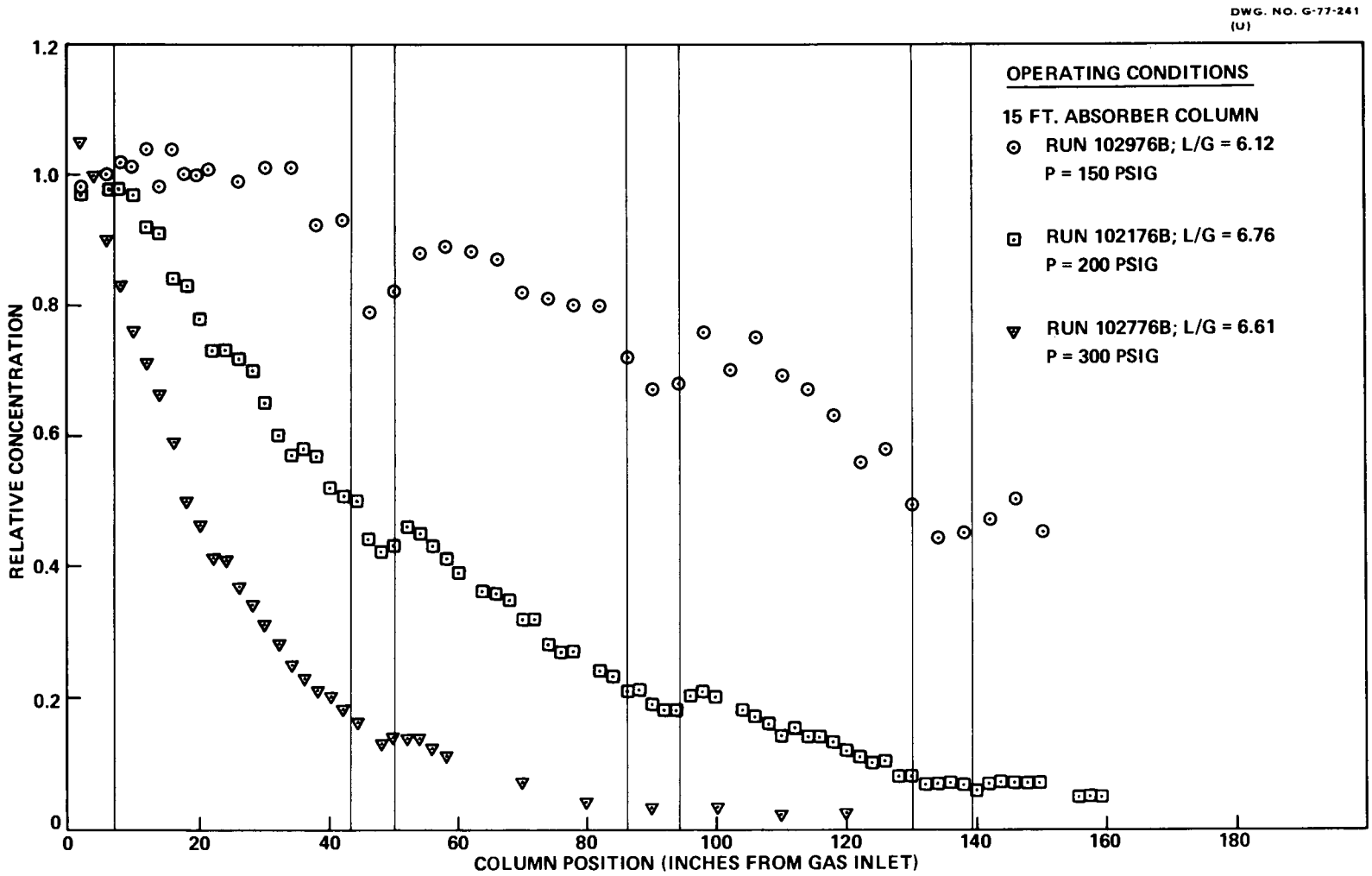

Fig. 4.1. Effect of absorber pressure on the column distribution of ^{85}Kr.

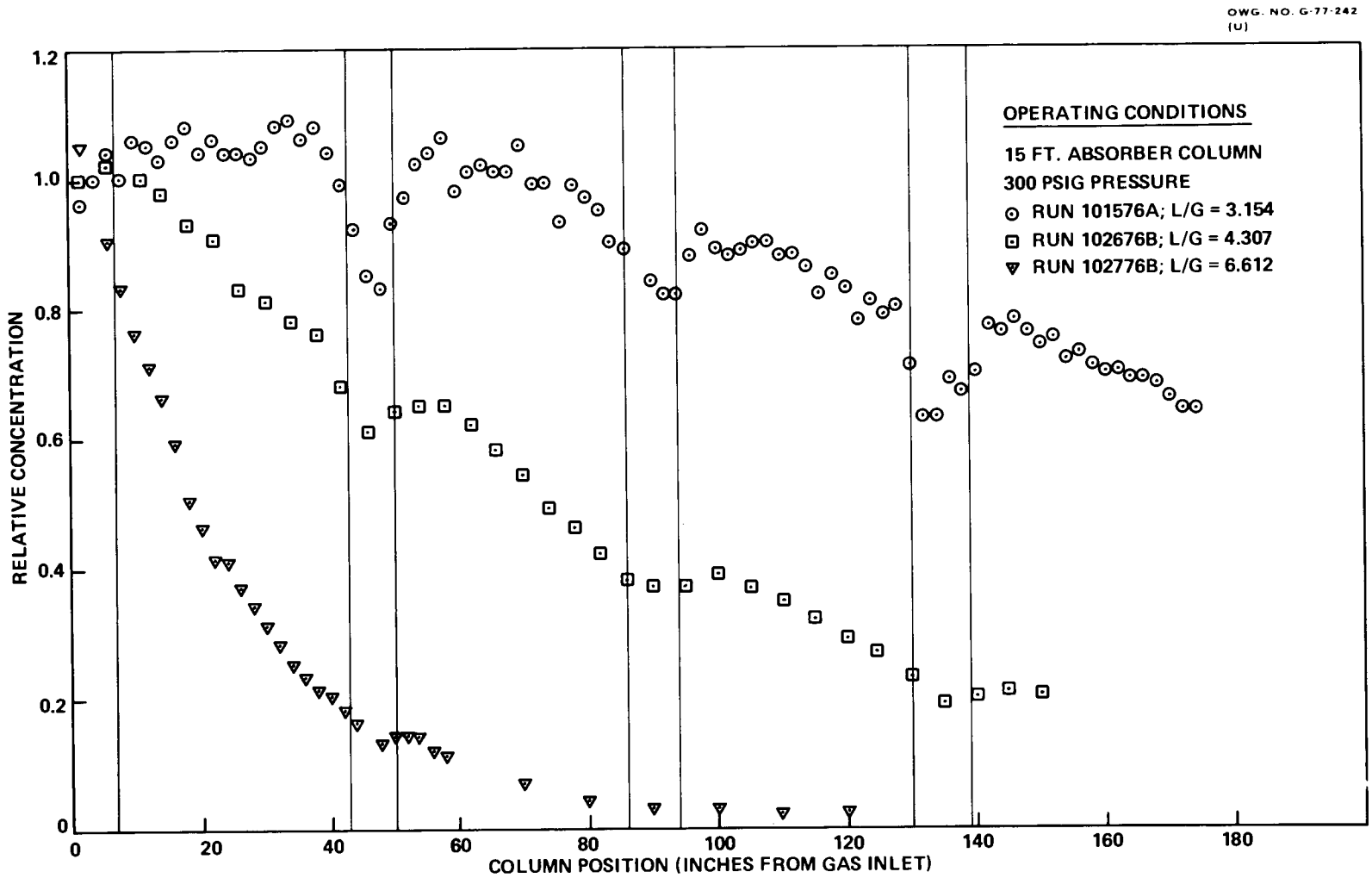

Fig. 4.2. Effect of absorber liquid-to-gas flow rate ratio on the column distribution of ^{85}Kr.

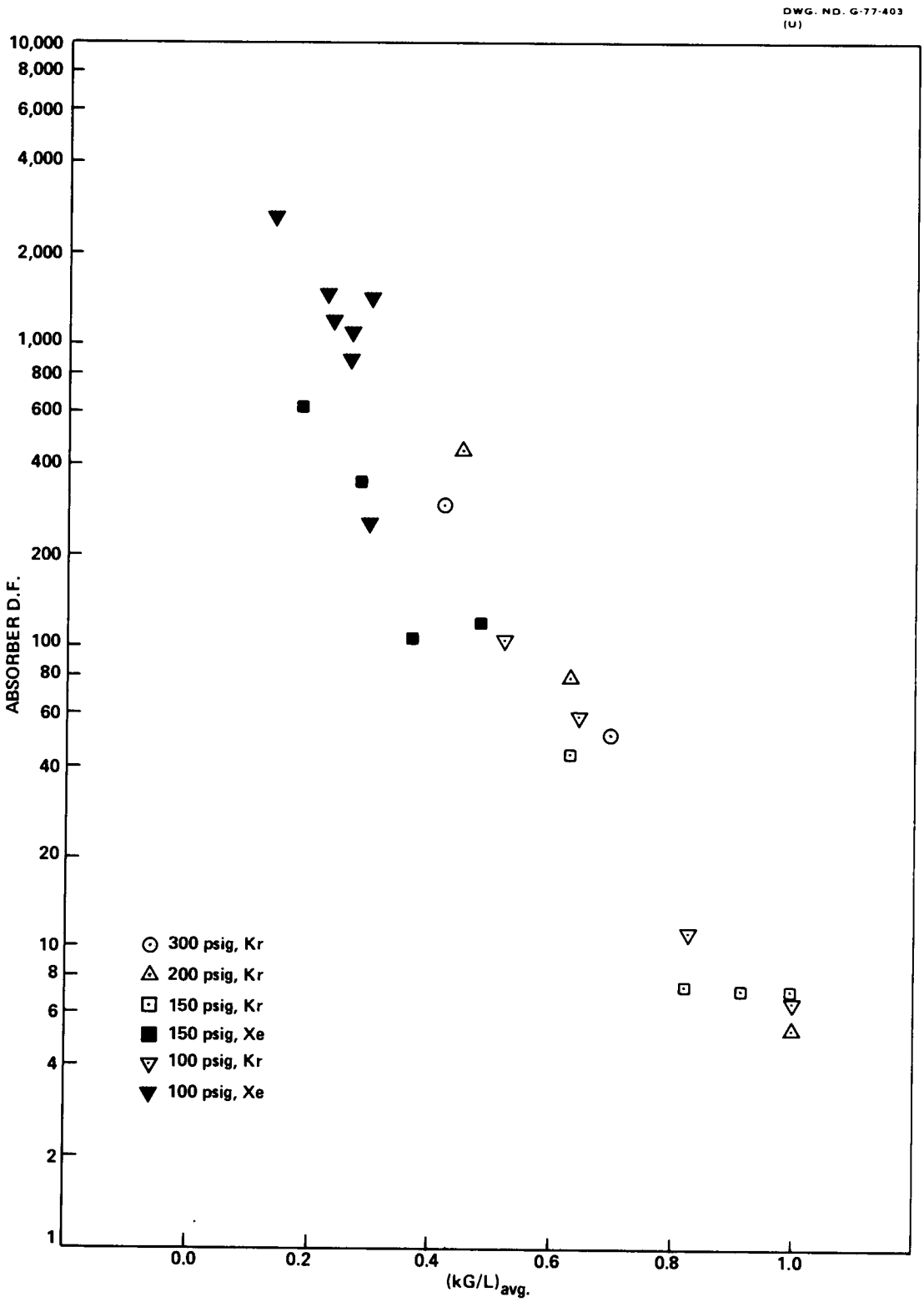

Fig. 4.3. Summary of low-pressure absorption tests with krypton and xenon.

Tests conducted at pressures and liquid-to-gas flow ratios that yield krypton removals between 90 to 99% resulted in xenon removals near 99.9%. Carbon dioxide removal tests were also conducted at the lower pressure. Concentrations of carbon dioxide in the process vent were less than our limit of detection; thus removal was probably >99.9%. Since carbon dioxide is slightly more soluble than xenon, at least 99.9% removal of the carbon is assured, even though we could not obtain a quantitative value.

The purpose of the fractionator is to remove the bulk of the co-absorbed carrier gas from the solvent that leaves the absorber prior to noble gas and ^{14}C collection in the stripper off-gas. The intermediate step is essential to achieve the desired fission product purity. All fractionated gas is recycled back to the process inlet; consequently, any desorbed krypton will increase the burden on the absorber and will decrease the overall efficiency of the process. The external gamma-scanning technique has been an especially valuable tool in analyzing the fractionator column. Figure 4.4 shows two typical ^{85}Kr concentration profiles taken from the fractionator while operating at 50 psig and at different liquid feed rates. In the case where the liquid rate was 8.55 lb-mole/hr the resulting process concentration factor was 3400; at the higher flow, the factor dropped to 2200. The krypton concentration peak is an intriguing effect brought about by a complex sorption-desorption phenomenon centered about a column krypton pinch-point. The pinch-point is an artifact of unconventional plant operation where the cold-loaded solvent leaving the bottom of the absorber is not preheated prior to introduction into the warmer fractionator. The effect is not only beneficial but desirable to the overall operation. While at first difficult to understand, the effect is now predictable and can be controlled.

Figure 4.5 shows the effect of fractionation pressure on the concentration profile. The higher pressure test conducted at approximately the same liquid flow resulted in a concentration factor of 2000, significantly less than that achieved at the lower pressure but still quite high. Additional tests have shown that a higher boilup rate can be used

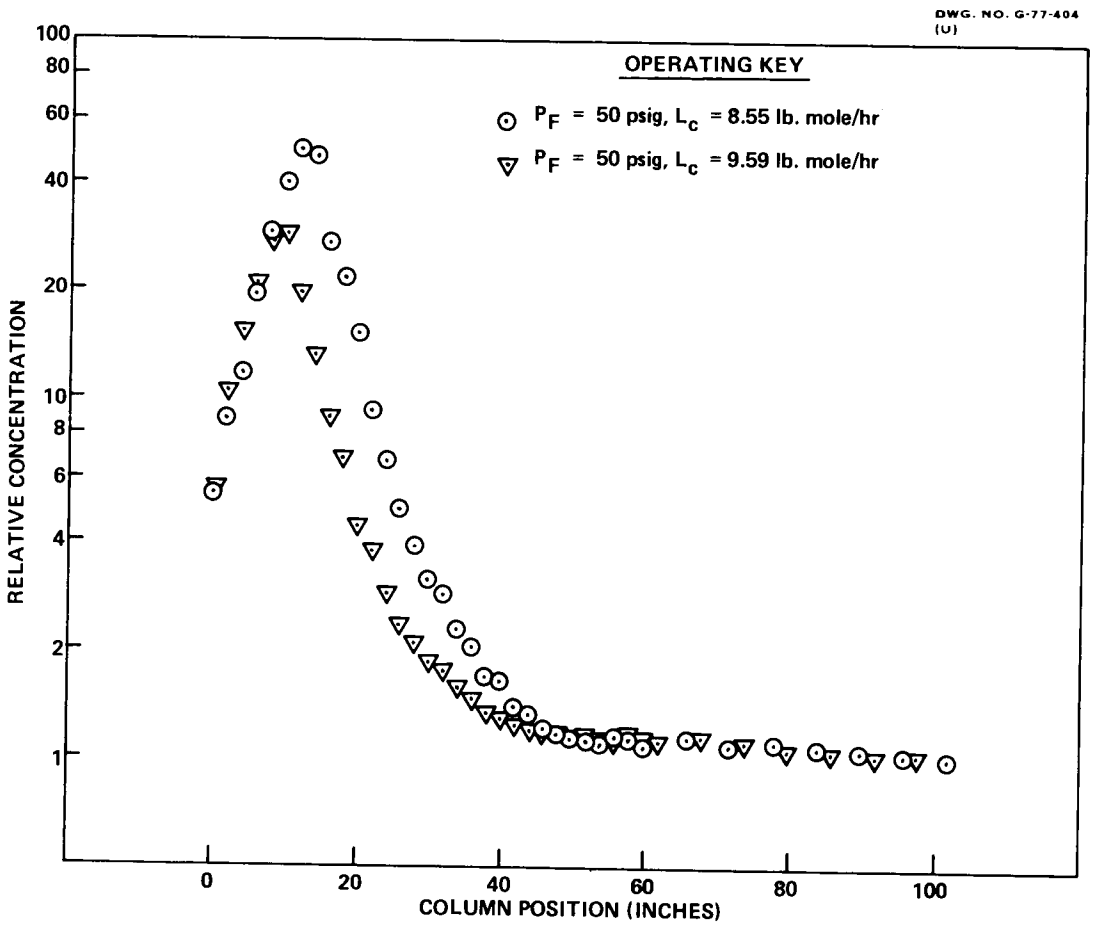

Fig. 4.4. Effect of liquid flow on the distribution of ^{85}Kr in the fractionator column.

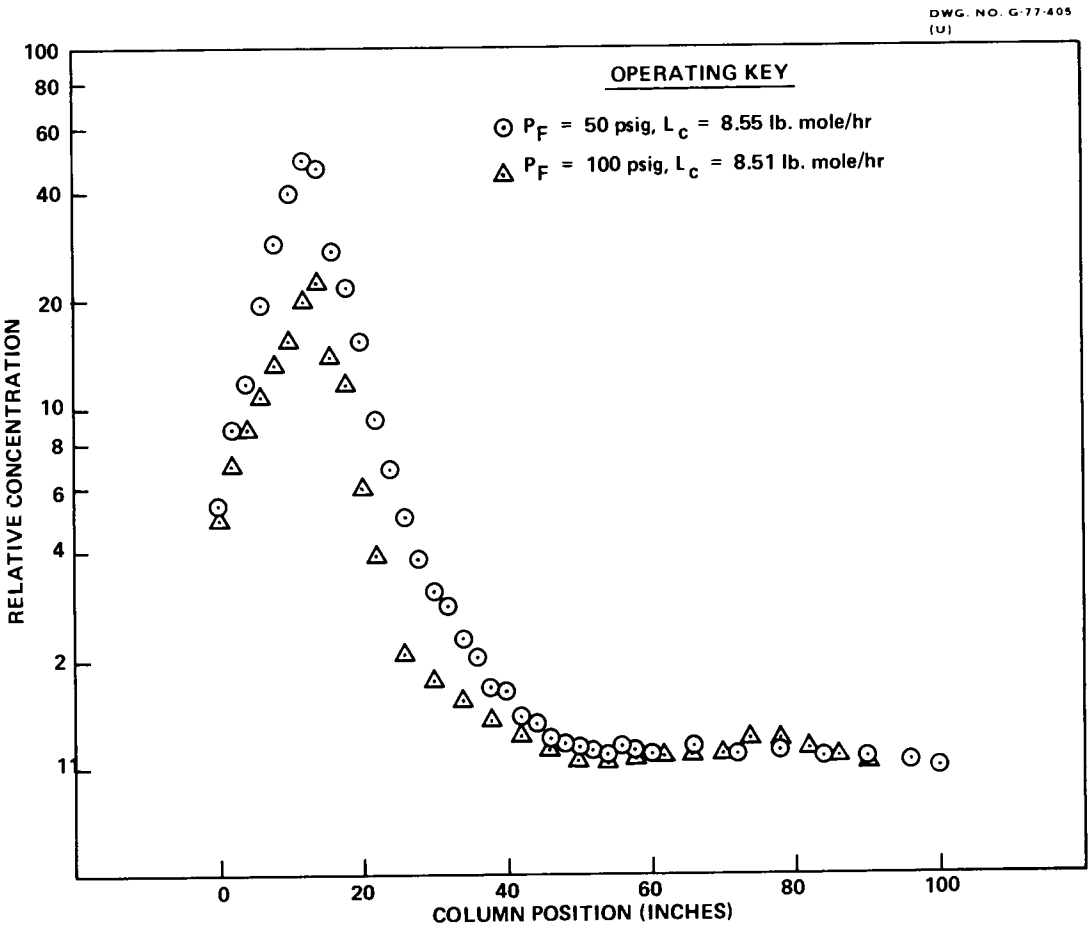

Fig. 4.5. Effect of operating pressure on the distribution of ^{85}Kr in the fractionator column.

to improve the fractionator performance at the higher pressure. Pilot plant operations with xenon show similar fractionator column concentration profiles.

Preliminary tests have been completed with the newly modified solvent still, which provides improved reflux control. A test series with nitrogen dioxide, iodine, methyl iodide, and water is being initiated. These tests will conclude campaign 4.

4.4.2 Process application

B. E. Kanak and M. J. Stephenson (ORGDP)

One of the objectives of this work is to identify flowsheet options and simplifications that lead to a more economical and/or reliable process. The pilot plant work conducted this quarter continues to support the viability of the proposed combination absorber-fractionator column. The intrinsic operational and economic advantages clearly mark the process employing this combination column as the preferred one over the conventional flowsheet.

Process modeling studies are continuing. Analysis of the fractionator column is confounded by the soluble gas pinch-point phenomenon, and allowance must be made for simultaneous absorption of multiple solutes and condensation of solvent under a sharp temperature gradient. Substantial progress is being made in this area, and it is expected that a rigorous model will be developed by midsummer.

4.4.3 Chemical studies of contaminants in LWR off-gas processing

L. M. Toth, D. W. Fuller, and J. T. Bell

After obtaining absorption coefficient data for NO_2 and N_2O_4 in the liquid and gaseous phases of R-12, the distribution coefficient data obtained earlier for "NO_2" (i.e., NO_2-N_2O_4 mixtures as found at equilibrium) in R-12 have been reduced to the standard form that was used previously:[1]

$$\log_{10} D = a + b/T \ . \qquad (4.1)$$

Here D represents the ratio of the mole fraction, x, in the liquid, L, to that in the vapor, V; a and b are constants; and T is the Kelvin temperature. Since "NO_2" occurs principally as the dimer in the liquid phase and as a monomer-dimer mixture in the R-12 gas phase, and since we can monitor the concentrations of these components separately with the absorption spectrophotometer, we have defined the distribution coefficient in Eq. (4.1) as:

$$D = \frac{x^L_{NO_2} + 2x^L_{N_2O_4}}{x^V_{NO_2} + 2x^V_{N_2O_4}} . \qquad (4.2)$$

In this manner, D represents the ratio of the "NO_2" mole fractions in the two phases after expressing the measured N_2O_4 as NO_2 and adding it to the measured amount of NO_2. We have obtained the following values of a and b as a function of the mole fraction of "NO_2" in solution:

$x_{"NO_2"}$	a	b
5.9×10^{-4}	-3.153	864
6.1×10^{-3}	-1.925	633
2.7×10^{-2}	-1.242	547

The change in these constants shows that the distribution coefficients decrease with the decrease in "NO_2" concentration in the liquid phase. The factor responsible for this decrease is most probably the shift in the NO_2-N_2O_4 gas phase equilibrium with pressure.

We have observed that the equilibrium constant for $2NO_2 = N_2O_4$ in the R-12 gas phase is equivalent to that of pure "NO_2" given earlier[1] (i.e., the equilibrium constant for "NO_2" with no diluent gas present) and that the constant expression in liquid R-12 is $\log_{10} K = -3.908 \times 10^3(1/T) + 10.26$ with K = 0.0015 mole/liter at 298 K. The expression yields values which are considerably higher than those of previously reported[6] equilibrium constants in other solvent systems, which indicates

that R-12 is less solvating than most solvents. This is consistent with our previous observations on I_2 and CH_3I in R-12, which demonstrated that the CCl_2F_2 molecule does not associate appreciably with solute molecules.

Interactions between I_2, NO_2, and R-12 were sought in a study of an R-12 solution containing approximately 5×10^{-3} and 6×10^{-4} mole/liter of "NO_2" and I_2 respectively. Spectra of these solutes in the mixed system over the temperature range -40 to 20°C were identical to those where each solute was measured separately, suggesting that there are no interactions whatsoever between the solute species.

Tributyl phosphate (TBP) and CO_2 have also been studied in R-12 solutions to determine their distribution coefficients and their general physical-chemical behavior. The vapor pressure of TBP in R-12 is so low that no detectable amount of TBP occurred in the vapor, thus precluding the determination of distribution coefficients. Nevertheless, concentrations of TBP up to 33 vol % were found to be totally miscible from -40 to 20°C and behaved as normal unsaturated solutions. The CO_2 study is not complete.

4.5 Iodox Process

B. A. Hannaford

The removal of volatile fission products from process and effluent streams is an important part of LMFBR fuel reprocessing. Iodine retention factors approaching 10^7 are desired when processing 90-day-decayed fuel. The Iodox demonstration system incorporates iodine scrubbing, collection of the solid pentavalent iodine, and acid recovery. Studies were continued of the Iodox process, which uses hyperazeotropic HNO_3 to scrub volatile iodine compounds from air and to convert the iodine to the nonvolatile pentavalent form.

Iodox experiment IXD-9 with elemental iodine resulted in the highest decontamination factors observed to date, despite the presence of NO_2 and water vapor in the feed-gas. The key to the performance apparently was the high acid concentration (22.5-22.8 *M* HNO_3) maintained throughout most of the column. This experiment combined elemental iodine vapor,

NO_2, and water vapor in the feed-gas for the first time in the current series of tests. To maximize the ^{131}I activity, the experiment was carried out as soon as possible after receiving the tracer (∿4 days). A 40-g charge of elemental iodine was employed in the $^{131}I_2$-I_2 generator, as in run IXD-8, to ensure an adequate excess.

Counting results for IXD-9 (Fig. 4.6) were based entirely on post-run counting of 2-ml samples in glass because of significant background activity in the flow cell for all samples. Precipitation of iodine occurred on plate 1 in 20.9 *M* HNO_3 at 25°C, presumably as iodine tetroxide; the measured concentration of dissolved iodine (0.34 to 0.73 g/liter) ranged from about 50 to 100% of reference solubility data. Counting results for plate 8 may be biased by the higher ^{131}I concentration in the raffinate sample, which precedes the sequence of samples taken from the Iodox column, plates 8 through 1 respectively. Iodine-131 concentrations taken from the figure at a run time of 360 min were used to calculate decontamination factors, except for plate 6 for which an average concentration (2.9 cpm/ml) over a sequence of four samples was taken to be a more representative value than the 360-min concentration. The calculated overall decontamination factor (DF) value (Table 4.1) was larger than observed in any previous experiment. Compared with IXD-8, the only other experiment with elemental iodine, the performance was enhanced by the increase in average acid concentration (21.3 to 22.6 *M*) and not lessened to any substantial degree by the presence of NO_2 in the feed-gas. These conclusions are based on empirical correlations of experimental DF as a function of nitric acid concentration, which will be presented in a future report.

Modifications to the $^{131}I_2$-I_2 metering system prior to IXD-9 included the replacement of a few stainless steel components with Teflon and provision of a dry-air purge to lower the partial pressure of iodine in the Teflon feed line to the feed-gas manifold. Post-run rinsing of the feed line with ethanol demonstrated that very little iodine ($<10^{-5}$ fraction) had condensed between the generator and feed-gas manifold. A preliminary iodine balance confirmed the concentration of 0.000233 g of iodine per liter of feed-gas, but because of unexplained variations in iodine-specific activity, further analyses were planned.

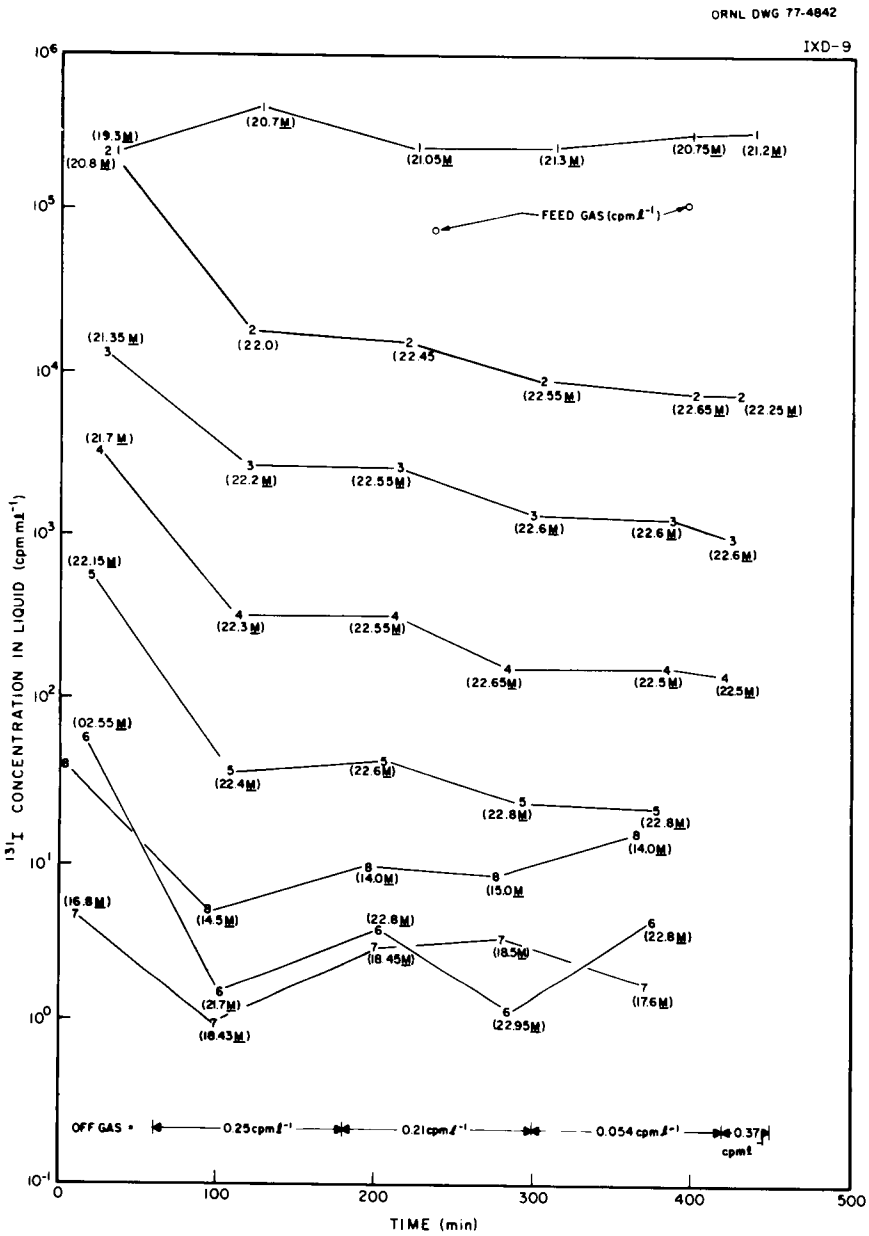

Fig. 4.6. Run IXD-9. Concentration of iodine in liquid and gas streams vs time for scrubbing ^{131}I–traced I_2 from air – 2% NO_2–2.4% H_2O with fuming nitric acid [feed rate of gas mixture = 96 std liters/min (1.59×10^{-3} m^3/sec); feed rate of 23.5 *M* HNO_3 = 55 ml/min (9.17×10^{-7} m^3/sec); feed rate of water = 5.9 ml/min (9.83×10^{-8} m^3/sec); concentration of I_2 in feed gas = 0.000233 g of iodine per liter (nominal); nitric acid concentrations are given in parentheses; temperature: 23°C, plate 1; 27°C, plate 6; 50°C, plate 8].

Table 4.1. Run IXD-9: decontamination factors (DF) for ^{131}I-traced I_2 in air — 2% NO_2–2.4% H_2O[a]

Plate number	Decontamination factor
1	34.2
2	6.43
3	8.45
4	6.97
5	6.44
6	3.65
Average[b]	8.20
Column, overall	3.04×10^5
Column, overall[c]	4.95×10^5

[a]At a run time of 360 min.

[b]Average = $[(DF)_1 \times (DF)_2 \times \ldots (DF)_6]^{1/6}$.

[c]Based on ^{131}I concentrations and flow rates of gas streams only, taking the average of two feed-gas samples (104,000 counts min^{-1} $liter^{-1}$) divided by the average of the two final off-gas samples (0.21 counts min^{-1} $liter^{-1}$).

Iodine leaving the iodine concentrator (T3) in the vapor phase amounted to only 2000-3000 cpm/min, with only 1 cpm/min reporting to the condenser off-gas zeolite trap. From the resulting condensate, which was fed to the extractive distillation system, about 2% of the iodine content reported to the raffinate and about 7% to the acid product, leaving about 90% of this iodine stream accumulating in the magnesium nitrate inventory. The ^{131}I concentration in the acid product (∿4 to 10 cpm/ml) was substantially the same as the concentration measured on the plate to which it was fed (plate 6).

Preparations are under way for an extended run. Additional silver-zeolite final traps were fabricated, and two Dynatrol in-line acid (density) analyzers were installed. A purge pump was installed for supplying feed-plate acid to one Dynatrol analyzer; a similar pump is on order for sampling the extractive distillation system product line.

4.6 Instrumentation and Control Systems

N. C. Bradley

The overall objectives of this task are to develop instrument systems and engineering techniques for the fuel reprocessing program and to provide a basic instrumentation and control technology for application to commercial plants. In addition, instrumentation and control systems are required in support of laboratory experiments and highly specialized tests associated with the components and process development tasks in the LMFBR Fuel Reprocessing Program.

4.6.1 Nondestructive assay of spent fuel

G. L. Ragan, C. W. Ricker, T. J. Burns, D. T. Ingersoll,
J. D. Jenkins, F. R. Mynatt, and J. E. Rushton

The objective of this subtask is to develop a nondestructive assay system for the determination of the total fissile content of spent fuel and blanket subassemblies. The effort to date has been concentrated on the active neutron interrogation assay method. A conceptual design of a proof-of-principle experiment has been completed, and experimental investigations of detector performance have been initiated.

During this quarter the detector evaluation program has continued. Energy calibrations of a 5-atm methane-filled detector and a 10-atm ^{3}He-filled detector have been completed. The sources used for the calibrations were a ^{232}U + Be source, which produces 0.85-MeV neutrons, and a ^{232}U + D_2O source, which produces 0.20-MeV neutrons. Despite the low intensities of these sources, adequate calibrations were obtained. The acquisition of sources of higher intensities is being investigated for future calibrations.

In addition to the proton-recoil and ^{3}He types of detectors, fission detectors using ^{238}U- and ^{237}Np-coated electrodes are being studied because of their lower operating voltages, inherent simplicity of operation, and ability to operate in high-gamma environments.

To evaluate the potential problems of both gamma-ray and neutron pileup in the detection system, a source mock-up has been designed to

simulate both the normal and the background signals expected in the proof-of-principle experiment. A ^{252}Cf source will be used to simulate, both in energy and intensity, the normal and fuel background signals. To simulate the interrogation neutron flux and the gamma background field, a 100-Ci ^{124}Sb-Be source will be used. The Sb-Be source materials have been procured, and the antimony will be activated in the ORR.

Both the detector evaluation program and the proof-of-principle experiment will use a single 100-Ci ^{124}Sb-Be source. The use of this source in the Thorium-Uranium Recycle Facility (TURF) requires an appropriately monitored and interlocked storage shield that has been designed and is under construction. A request to use the Sb-Be source in the TURF will be submitted to the Safety and Radiation Control Committee for approval.

As indicated in the previous quarterly report,[5] the use of borated polyethylene end-pieces was investigated. The calculational results show that the axial portion of the subassembly under assay is more clearly defined with the use of borated polyethylene end-pieces than without and that there is little difference between the use of 5 and 20 wt % of boron. Since the system performance is improved by the end-pieces and since the 5% borated polyethylene is considerably cheaper and more easily machined than the 30% material, end-pieces fabricated from 5% borated polyethylene will be incorporated in the design of the proof-of-principle experiment.

The mechanical design of the proof-of-principle experiment was initiated during this quarter. To simplify the design and to provide the capability of simulating the use of a pulsed neutron source, four detectors and four source positions will be used instead of six of each, as reported previously. The use of four-way rather than six-way symmetry does not compromise any of the design criteria and, in fact, allows for greater experimental flexibility and for lower component and fabrication costs.

Although the design and fabrication of the storage shield and the source mock-up have delayed the design and construction of the proof-of-principle experiment, it is expected that the schedule for this subtask will be met this fiscal year.

4.6.2 Process sensors and control

N. C. Bradley, D. N. Fry, J. M. Googe,* J. M. Jansen, Jr.,
W. F. Johnson, G. N. Miller, W. P. Murray, H. H. Ross,
A. A. Shourbaji, C. M. Smith, J. E. Strain, and R. M. Tate

Vibration analysis instrumentation for the rotary dissolver. As reported last quarter, recordings of vibration measurement signals from accelerometers mounted on the pillow-block bearing supports were taken during several special tests of the 4-ft-diam dissolver.[5] Analysis of these recorded vibration signals is being performed to develop a method of detecting blockages in the dissolver.

We have analyzed the vibration signals from one of these tests in which two loads of simulated chopped fuel hulls were introduced into the dissolver. Figure 4.7 schematically follows the hulls as they pass through the dissolver during the test; the figure also shows the input of hulls into the dissolver, their transfer into the central dissolution section, hull mixing in the dissolution section, and hull transfer from the outlet section of the dissolver. The first load of hulls was introduced 1 min (three dissolver revolutions) from the beginning of the test (schematic A and B) and the second after 3 additional min (schematic E). This double load of hulls was allowed to mix in the dissolution section for approximately 6 additional min (schematic F and G), at which time the dissolver reversed for one revolution and transferred the hulls to the outlet section (schematic H) where they were continuously transferred out of the dissolver during additional forward dissolver revolutions (schematic I).

To identify the movement of the hulls through the dissolver, two special fast Fourier transform (FFT) analysis programs were employed. These programs divide a revolution of the dissolver into ten divisions, with division 10 being adjacent to division 1 for successive revolutions. This allows the investigation of position-dependent vibration signals in the dissolver. Using this method, frequency spectra were obtained

---

*University of Tennessee consultant.

ORNL DWG 77-6865

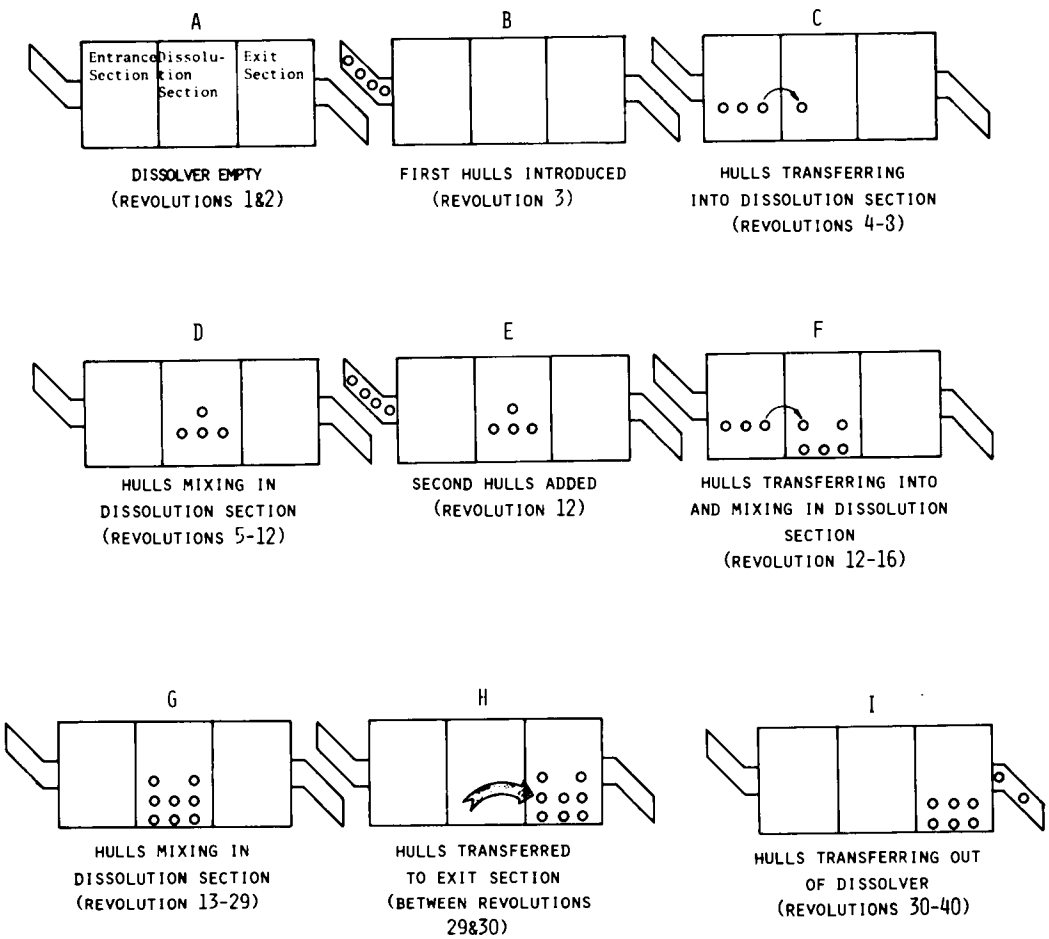

Fig. 4.7. Schematic flow diagram of hull movement in the dissolver during operation.

that consisted of vibration signal power spectral density (PSD) values. These spectra covered the useful bandwidth of the accelerometers (0-5 kHz) and were obtained for each of the ten divisions of a dissolver revolution. It was observed that the frequency spectra between 0 and 1 kHz were nearly identical for each of the ten divisions, and also that hull transfer did not affect the vibrations in the 0 to 1 kHz range. Therefore, we tentatively conclude that there is little significant information about hull transfer or mixing in this frequency range (0 to 1 kHz).

From these frequency spectra, two broadband rms levels were computed that covered the frequency ranges of 1 to 5 kHz and 4 to 5 kHz, as shown in Figs. 4.8 and 4.9; the figures do not include details of the transfer of material from the dissolution section to the outlet section, as is shown in Fig. 4.7 (H), which constitutes a separate analysis. Each of the dissolver functions has a characteristic response in the 1 to 5 kHz rms noise range. During the first two dissolver revolutions, there was no material present in the dissolver. This gave a low rms value (Fig. 4.8). In revolution 3, the first load of material was introduced that produced a large rms peak. During revolution 4, the material was transferring into the central dissolution section, which we believe is apparent as a small peak above the general noise level. In revolutions 5 through 29, a definite peak is apparent at approximately division 10 or 1. Since this analysis was conducted while material was residing in the dissolution section of the dissolver, we tentatively conclude that the change in rms at division 10 or 1 is caused by the material passing over the transfer scoop in the dissolution section.

In revolution 12 a large peak occurs in division 7 in addition to the normal peak at division 10 or 1. This corresponds to the addition of the second load to the dissolver. After revolution 29, the dissolver reversed and transferred the hulls into the outlet section. Since FFT analysis was not performed on this reverse revolution, it is not shown in Figs. 4.8 or 4.9. In revolutions 30 through 40, there are numerous peaks that we believe may correspond to the hulls being transferred out of the dissolver by the outlet scoops.

When the analysis bandwidth is decreased to 4 to 5 kHz (Fig. 4.9), different rms responses develop that are characteristic of hull transfer.

ORNL DWG 77-6863

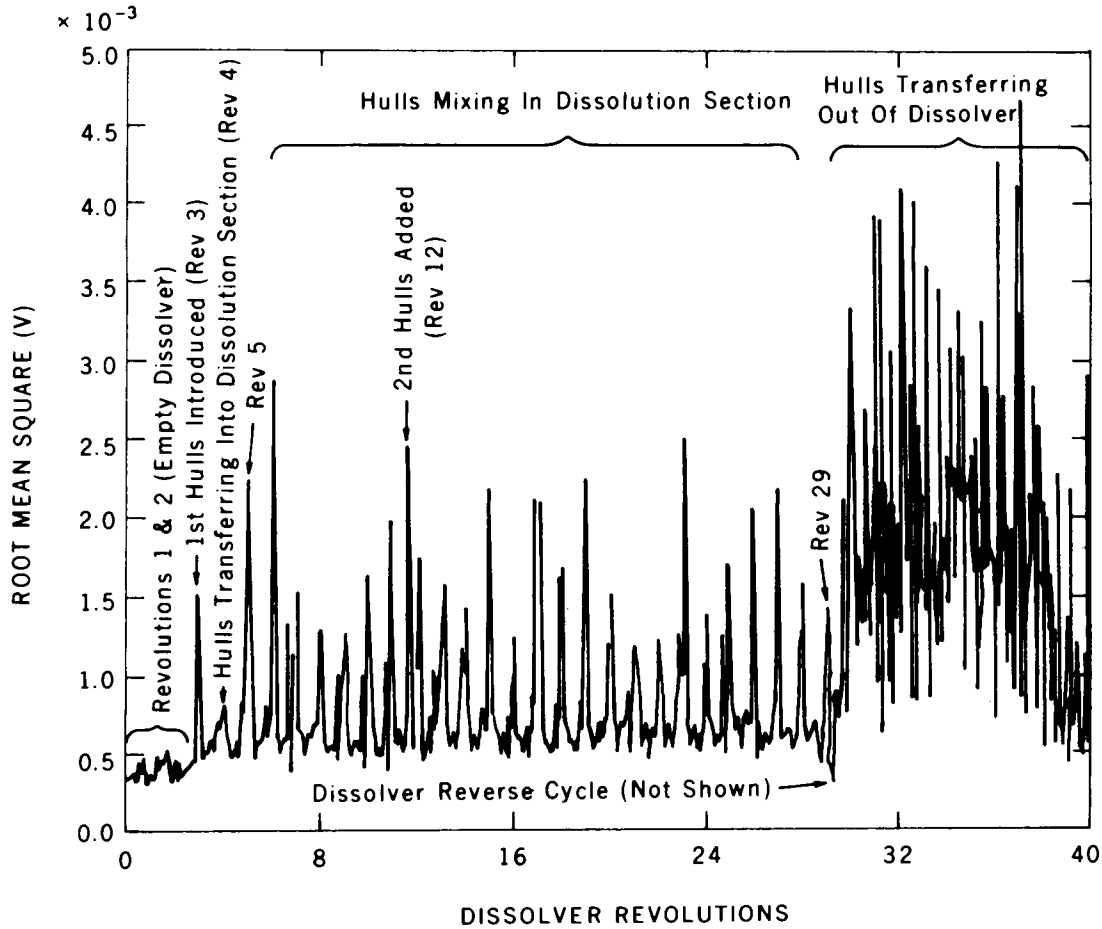

Fig. 4.8. Rms vibration level in 1 to 5 kHz frequency range during dissolver operation.

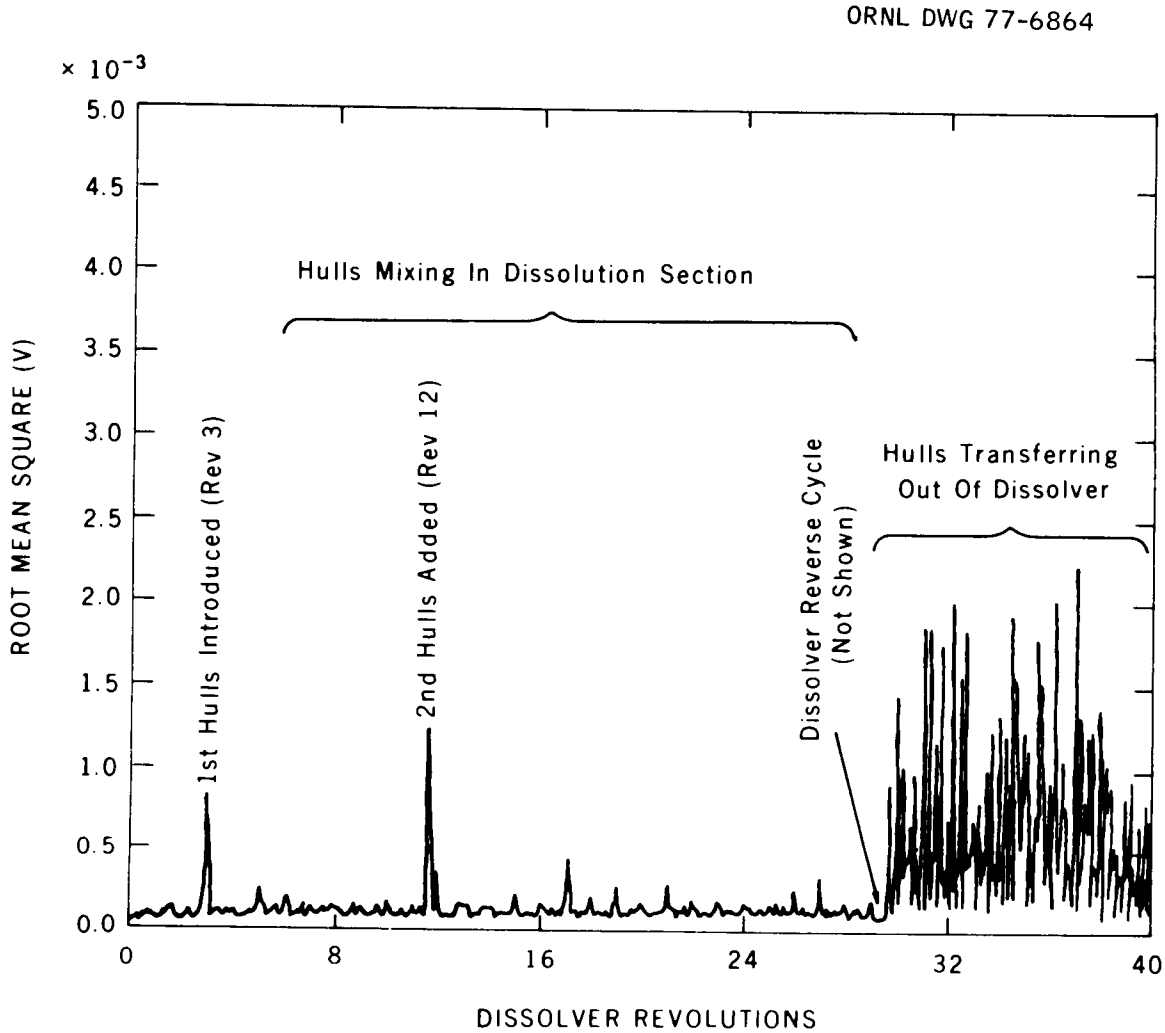

Fig. 4.9. Rms vibration level in 4 to 5 kHz frequency range during dissolver operation.

The peaks at revolutions 3 and 12, the point of hull addition, are very prominent. The peaks at division 10 and 1 in each revolution have been eliminated by frequency bandlimiting. Furthermore, the peaks beyond revolution 29, which are believed to be associated with material transfer from the outlet section, are also prominent. From this, we tentatively conclude that material transfers result in high-frequency vibrations, whereas the vibrations associated with material mixing in the dissolution sections are of a lower frequency.

Sensor development for process analysis. The Analytical Chemistry Division has been invited to cooperate with the Instrumentation and Controls Division on the development of chemical measurement systems for process analysis. The primary responsibilities of the Analytical Chemistry Division are:

1. to help identify required chemical measurements for proper process control,
2. to recommend off-the-shelf commercial instrumentation where available,
3. to suggest modifications of commercial devices to perform specific analyses when possible,
4. to aid in testing and calibration of chemical (or physical) measurement systems,
5. to investigate the development of new and unique methods of analyses for problems where no conventional system is known to exist.

During the past month, we have studied the overall process analysis system with the objective of making a preliminary assessment of required analyses for each process analysis subsystem. These projected analyses were further identified as being relatively routine, moderately difficult (small R&D effort needed), and quite difficult (significant R&D required). A statement is being completed that details those measurement areas where an R&D effort appears needed. This statement will indicate not only the required analytical measurements (i.e., uranium concentration, pH, etc.) but will include other information such as the state of the chemical system, possible interfering materials, and proposed accuracy and precision requirements.

Testing and evaluating density measuring instruments. Two Dynatrol* density instruments (for two different density ranges) have been purchased for use in the Iodox process system to measure nitric acid concentration (molarity) in the Iodox column. A test loop was set up to test and evaluate the instruments and to verify the manufacturer's specifications as well as to carry out the calibration. Testing and calibration of both instruments were completed satisfactorily, and they are being installed. An evaluation report is being prepared and will be available in the near future.

One-fourth-scale dissolver seal test instrumentation. This system is designed to study the performance of ferrofluid as a seal between rotary and stationary components. A programmable logic controller (PLC) will be used to simulate the 4-ft dissolver sequential operation. System control involves two variables, namely, temperature and pressure (vacuum), where the seal performance could be tested under different combinations of the two. Instrument flowsheet and instrument layout drawings have been completed. Procurement has been initiated for those instruments to be ordered from outside vendors, and fabrication is expected to start on the remainder by the end of March.

Digital unit process controller evaluation. The Bristol UCS-3000** unit process controller has operated continuously for approximately six months on the mock-up process while undergoing various performance tests. Its overall performance has been quite good and has demonstrated suitability for use in the Integrated Process Equipment Test (IPET). After evaluating proposals from competitive systems, the decision was made to use a UCS-3000 to control the dissolver process. Specifications for purchase of the new unit are being formulated, and a requisition has been initiated for the purchase of the ACCOL B compiler for use with the UCS-3000.

---

*Automation Products, Inc.

**American Chain and Cable Company, Inc., Bristol Division.

Infrared temperature measurement. A system for measurement of the internal temperatures of the voloxidizer kiln by a noncontact method is being studied. An infrared (single color) measurement system has been specified for procurement. A periscope has been designed and is being fabricated that will be used to view specific points within the kiln. In addition, a two-color system of measurement is being studied for possible use to determine if the emissivity effect could possibly be eliminated.

Programmable logic controller development. The study and evaluation of a large programmable logic controller (Modicon 384) was delayed by the vendor's loss of the purchase order for the programming panel. The mistake was corrected and the programming panel has been received.

The development of a computer program, designed to convert control logic state diagrams to a set of boolean algebra equations representing a minimum solution of the control task, has been completed. The program has been tested on small logic models with success, and will be further tested with a real control application on the multirod shear system. An engineer-derived program will also be designed and compared to the computer-generated control for comparison of program size and engineering effort.

Four-foot-diameter dissolver prototype. The eddy current probes for the measurement of the rotating drum deflections have been ordered; the sensor mounting hardware has been designed and is being fabricated.

An instrumentation flowsheet has been prepared for nitric acid concentration control for the corrosion-erosion tests; procurement of instrumentation is awaiting funding approval.

Prototype voloxidizer. The voloxidizer control system has been studied, and an instrument flowsheet has been prepared for review.

The material feeder-weight system has been studied with the major objective of good control and accurate measurement of material fed. A system has been designed and is being evaluated on paper. The system involves a smart PLC (one that can do computation and has memory), a pneumatic feeder, a weigh system based on weight loss principle, and an incremental measurement system to achieve accuracy.

Portions of the weighing system have been specified and placed for procurement. A conceptual design has been completed for a tare-weight-corrected weigh-table system.

4.7 Solvent Extraction

M. E. Whatley

An effort has begun at Argonne National Laboratory to emphasize the development of a critically (nuclear) safe centrifugal solvent extraction contactor for LMFBR fuel reprocessing. The work will be directed toward the Purex process at about 0.5-metric-ton/day capacity. Centrifugal (fast) contactors are believed to provide several benefits as compared to conventional pulsed columns for the initial coextraction cycle, and to include decreased fission product extraction, decreased solvent degradation, better operational control, and compact size.

The design will retain the features of high throughput, low holdup, ease of start-up–shutdown, and operating reliability that have been demonstrated by an 18-stage bank of contactors for first-cycle extraction and scrubbing at the Savannah River Plant (SRP). The development is based on previous work at ANL that led to a modification of the SRP design; the modification simplifies fabrication of the contactor, makes it more suitable for remote maintenance, and improves the hydraulic performance. The principal change is elimination of the separate mixing chamber and paddle that are used in the SRP units. In the ANL contactor, the aqueous and organic process streams are fed into the annulus between the rotating bowl and the casing and are mixed as they flow downward toward the rotator inlet. This design eliminates the mixing chamber, mixing paddle, straightening vanes, and injection nozzle of the SRP unit. The rotor assembly can consequently be made lighter and shorter, easier to balance dynamically, and easier to remove remotely.

In the SRP design, the mixing paddle is held captive in the mixing chamber so that removal of the rotor assembly requires disassembly of the housing. A complex drive shaft, spindle, and circumferential air seal (for the air-controlled weir) are employed to permit remote replacement of a motor or spindle if the need arises. In the ANL annular

design, the rotor is attached directly to a motorized spindle that has a hollow shaft. A simple rotary air seal is mounted at the top to admit air for weir control. The entire rotor assembly can be readily removed and replaced without disturbing the housing, thus simplifying maintenance. The overall design is adaptable to commercially available components, a feature which should contribute to reduction of fabrication costs. Industrial firms qualified to produce these units on a production basis will be brought into the program at appropriate times. The scope of the program will also include testing of the contactor to demonstrate its performance under representative Purex flowsheet conditions. Extraction efficiency will be tested with unirradiated uranium.

Mechanical and hydraulic stability during momentary or extended departures from normal process flow conditions will be investigated. The effect of solids in the process solutions resulting from inadequately clarified feed solutions or precipitated impurities will be investigated.

Design features for remote maintenance will be developed and incorporated into the prototype unit. This aspect of the development program will be closely coordinated with ORNL pilot plant design to achieve compatibility between the contactor design and the remote handling equipment.

The program includes general chemical studies in support of contactor development. These will include studies of extraction kinetics for uranium, plutonium, and fission products applicable to high-plutonium, high-fission-product Purex systems. Plutonium reduction techniques and kinetics, as they affect plutonium-uranium separation in short residence centrifugal contactors, will also be studied. Formation of interfacial precipitates and their effect on contactor performance and plutonium losses will be examined. Applicable solvent washing techniques designed to avoid formation of interfacial precipitates will be applied as necessary to maintain contactor efficiency. Studies will also be conducted on possible third phase formation and Pu(IV) precipitation in the centrifugal contactor. During the past quarter the conceptual design for the contactor system experiment (single stage) was completed, the motor drive procurement was initiated, and facility preparations were begun.

REFERENCES FOR SECTION 4

1. B. L. Vondra, *LWR Fuel Reprocessing and Recycle Program Quarterly Report for Period October 1 to December 31, 1976*, ORNL/TM-5760 (February 1977).
2. J. H. Goode, C. L. Fitzgerald, and V. C. A. Vaughen, *The Dissolution of Unirradiated and Irradiated $(U,Pu)O_2$ in Nitric Acid*, ORNL-5015 (February 1975).
3. W. D. Burch et al., *LMFBR Fuel Reprocessing Program Progress Report for Period April 1 to June 30, 1976*, ORNL/TM-5556 (August 1976).
4. W. D. Burch et al., *LMFBR Fuel Reprocessing Program Progress Report for Period July 1 to September 30, 1976*, ORNL/TM-5668 (November 1976).
5. W. D. Burch et al., *LMFBR Fuel Reprocessing Program Progress Report for Period October 1 to December 31, 1976*, ORNL/TM-5768 (February 1977).
6. T. F. Redmond and B. B. Wayland, *J. Phys. Chem.* 72: 1626 (1968).

5. COMPONENT DEVELOPMENT

N. R. Grant

The component development effort is a general follow-on to the engineering research effort. Chemical concepts applicable to the effort, which are projected by the research and development area and subjected to model testing in the engineering research area, are screened for engineering application to the program. In the component development area, both capacity and remote maintenance and operation criteria are applied. The design, fabrication, and operation of full-scale, remotely operable process equipment are component development goals.

5.1 Disassembly and Fuel Cutting — Contracted Work

C. D. Watson and B. S. Weil

The component development effort in disassembly and shearing is charged with the mechanical preparation of fuel materials for the succeeding steps of voloxidation and dissolution. The work is being carried out with in-house effort (Sect. 5.2) and with a subcontract to the Gulf + Western Advanced Development and Engineering Center (G+W). Both short-range development and testing and longer-range process improvement technologies are being pursued, with the major effort in those activities directly applicable to the Hot-Pilot-Plant (HPP) design.

This portion of component development is being performed by G+W. The work is divided into four tasks: machining (rotary shearing), disassembly, shearing, and subassembly cutting. During this report period, work was continued on all tasks.

5.1.1 Machining

Rotary shearing (machining) tests conducted at G+W's Folcroft 2 facility demonstrated that unshrouded prototype fuel rods could be cut successfully at a feeding rate of 1.3 cm (0.5 in.)/min in the rotary cutter turning at 9 rpm. The rotary cutter driven by a 75-hp motor was

equipped with six staggered cutters. None of the cutters were damaged significantly during the three test runs.

Visually, the product appeared to be equally as good as the highly acceptable one produced by the ORNL multirod shear. However, rotary shearing of precompacted shrouded rods was unsuccessful. Although cutting took place, the product was very poor, as demonstrated by powder and flattened cladding. It appeared that the cut shroud fragments were acting as the cutter blades. A few additional tests with a better feeding mechanism and raked cutters to prevent blade loading are projected for the first week in April.

5.1.2 Disassembly

The overall design concept of the disassembly "push" system to be interfaced with the existing ORNL straight-sided 250-ton shear was completed. All layout work is finished; detail design is about 20% complete and is scheduled for completion by the end of May. A 1/4-scale working model of the disassembly unit is being fabricated and is scheduled for delivery by April 30, 1977.

Joint ORNL–G+W review of the program resulted in the following:

1. Additional G+W manpower has been put on the program, and the longest lead equipment items have been ordered.
2. The target date for a fabricated disassembly "push" unit ready for onsite testing is December 31, 1977.
3. The unit is to be fabricated of carbon steel with stainless steel bearings and wear plates. Use of essentially carbon steel is expected to effect a savings of $250,000 over an all-stainless version. Where carbon steel is used, G+W will ensure that stainless steel could be substituted if required on an in-cell machine.
4. A plasma torch (model PT-7 or PCM 250) is to be used for removal of the inlet nozzle, whereas roll pipe cutters will be used to remove the outlet nozzle.

5.1.3 Shearing

The G+W design of shear tooling for the ORNL straight-sided shear has been completed. The design package consists of fixed and moving blade sets, blade holders, backup shoes, blade sets, and wear plates.

At ORNL's request, G+W prepared a formal proposal (No. 17018), "Engineering and Design of a Remotely Operated and Maintained Straight-Sided Shear." The concept is based on the modular concept suggested by ORNL in which the fixed and moving blades and the gag-compactor would be modularized as a replaceable unit. The G+W concept proposal eliminated the gibs used in the present ORNL shear. Detailed layouts are scheduled to be completed in about seven months.

5.1.4 Subassembly cutting

G+W has performed a series of roll cutting tests in which dummy 0.305-cm (0.120 in.) LMFBR shrouds are severed at a reference position 23.88 cm (9.4 in.) from the end of the outlet nozzle. A total of 112 cuts were made on sections of type 304 stainless steel shroud using opposing pairs of standard commercial 7.1-cm-diam (2.8-in.) pipe cutters. At the beginning of the tests, sections rotated at 20 rpm were severed in 25 to 35 sec with a calculated radial applied force of 2640 kg (1200 lb). The average cutting time increased to about 45 sec at the end of the test. A detailed report of the tests is in preparation.

Retech Incorporated (formerly Max P. Schlienger, Inc.) has rebuilt the electric-arc subassembly cropping saw in preparation for LMFBR cropping and cutting tests. A new power source was shipped to Retech in March; Retech will install a control console, and definitive cutting tests could begin by mid-April.

5.2 Disassembly and Fuel Cutting — ORNL Program

C. D. Watson, B. S. Weil, and M. E. Clifton

The overall disassembly and cutting program was reviewed in light of potentially accelerating the HPP schedule. If the time to develop machines is reduced, the available funding must be directed toward the

established base. The areas of investigation would then be divided into three parts:

1. Phase I:
   a. Remotely operated, straight-sided shear (interface with b),
   b. Push-type disassembly (with whole assembly shearing feeder),
   c. Plasma-arc cutting (for inlet nozzle),
   d. Roll cutter (for outlet nozzle).
2. Special consideration:
   a. Shear tooling (cutting and compacting),
   b. Laser cutting.
3. Phase II:
   a. Alligator shear (interface with b),
   b. Pull-type disassembly (with whole assembly shearing feeder),
   c. Electric-arc saw cutting,
   d. Other options.

All funding and scheduling will be based on Phase I receiving the highest priority. Work on Phase II items will be accomplished on a time and money availability basis except for current commitments. Two items are noted for special consideration: (1) Shear tooling is still involved in a selection of options. It is estimated that the best tooling for cutting shrouded and unshrouded subassemblies can be selected in less than a year, and April 1978 is considered to be a firm deadline. (2) The other item is use of a laser for slitting the shroud and possibly for circumferential cutting of the shroud at the inlet and outlet nozzles. We have gotten a late start on applying a laser to subassembly shroud cutting, but we propose to add it to the disassembly machine by FY 1980 for the final system checkout in component development. The major achievement dates for Phase I are as follows:

1.	Disassembly machine ready for testing with old shear	April 1978
2.	Decision on best shear tooling	April 1978
3.	Complete fabrication and checkout of new shear	June 1979
4.	Prototype disassembly-shear system ready to operate	August 1979
5.	Testing complete, ready to move to Integrated Process Equipment Test (IPET)	July 1980

The testing activity has been reduced this quarter so that modifications to the shear could be completed. The acquisition of equipment for the fabrication of prototype fuel is proceeding smoothly, and a new shear data acquisition and control system is nearly ready for installation. Estimates for FY 1978 and FY 1979 expenditures and the first iteration of a program plan covering shear development up to the HPP operation began this quarter.

5.2.1 Shear

The ORNL straight-sided shear has been down for modifications during the entire quarter. The new compound ram (Fig. 5.1) required some field customizing, and changes in the swing-out components for the new compactor and fixed blade holder (Fig. 5.2) were made. Some field milling on the main shear housing casting was needed so that it would accept the new swing-out designs. All tooling has now been successfully custom fitted, and experimental work will resume early next quarter.

These new sets of tooling will be used to test the feasibility of both push-pull and pinking-type shearing. The new compactor tooling was designed to break the shroud prior to the actual shearing operation (Fig. 5.3). In addition, tooling modifications to the slice-shearing equipment that would permit the uniform slices to spontaneously release the chopped fuel from the shroud segment will be tested.

A new control system for the shear has been built by the Instrumentation and Controls Division, and installation began during this quarter. The system controls the shear, compactor, feed mechanism, and fuel unit positioner. Later, the control can be interfaced with the new PDP 11/40 computer. Additional planning and preparation for next quarter's experimental campaign includes the adaptation of the closed-circuit video system to the compound ram and the acquisition of a millipore particle analyzer for analysis of airborne particulates created by shearing.

Design specifications were prepared for a new straight-sided shear. This shear concept would depart from the present ORNL–Birdsboro design by being remotely operable–maintainable and of modular construction. The shear tooling, bearings, and compactor dies are to be contained in

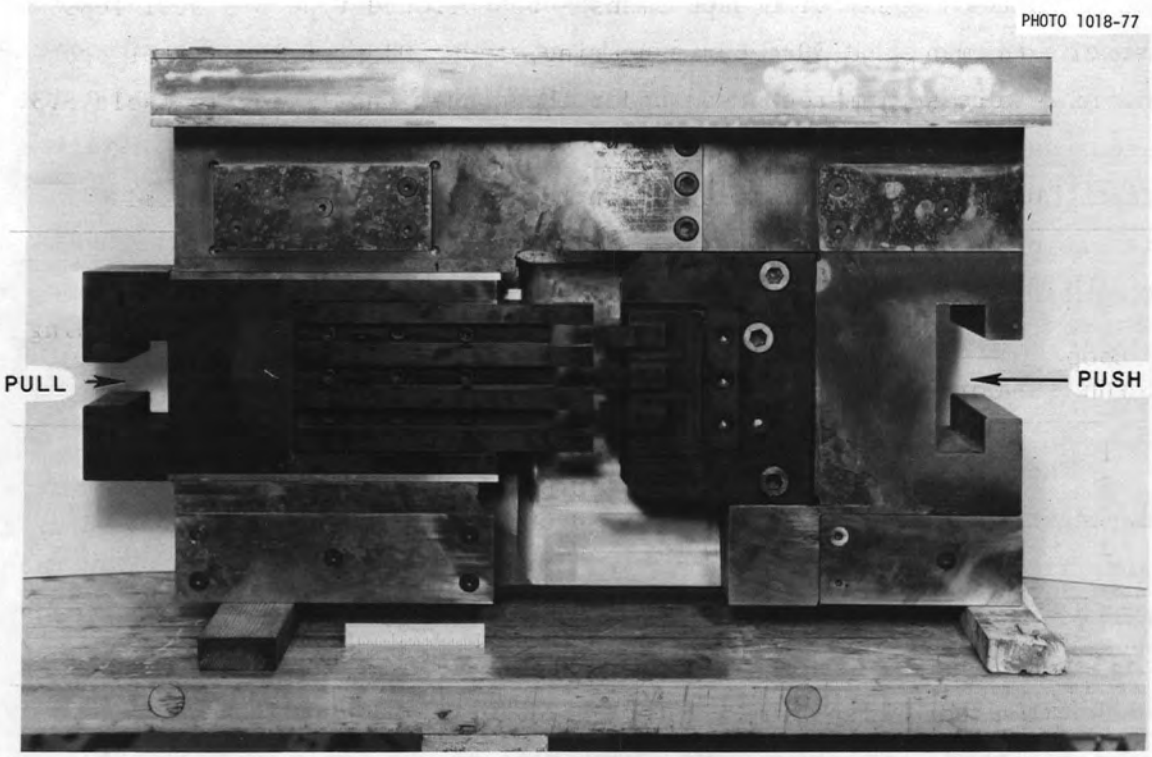

Fig. 5.1. New compound ram for push-pull and pinking type shearing.

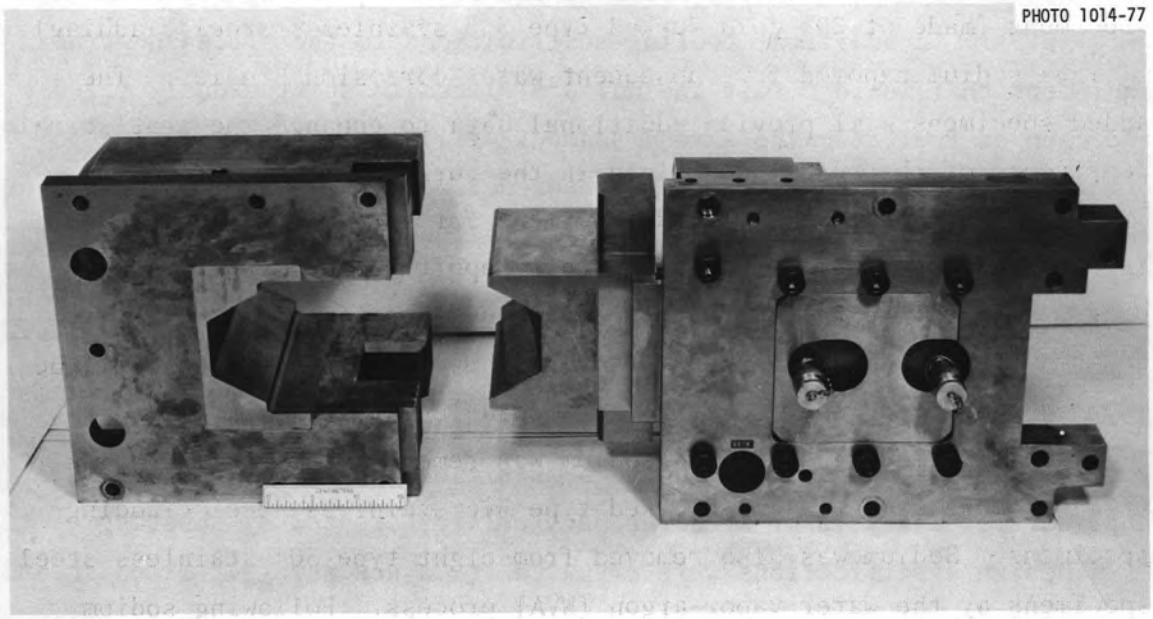

Fig. 5.2. New fixed blade holder (left) and new 200-ton gag compactor (right).

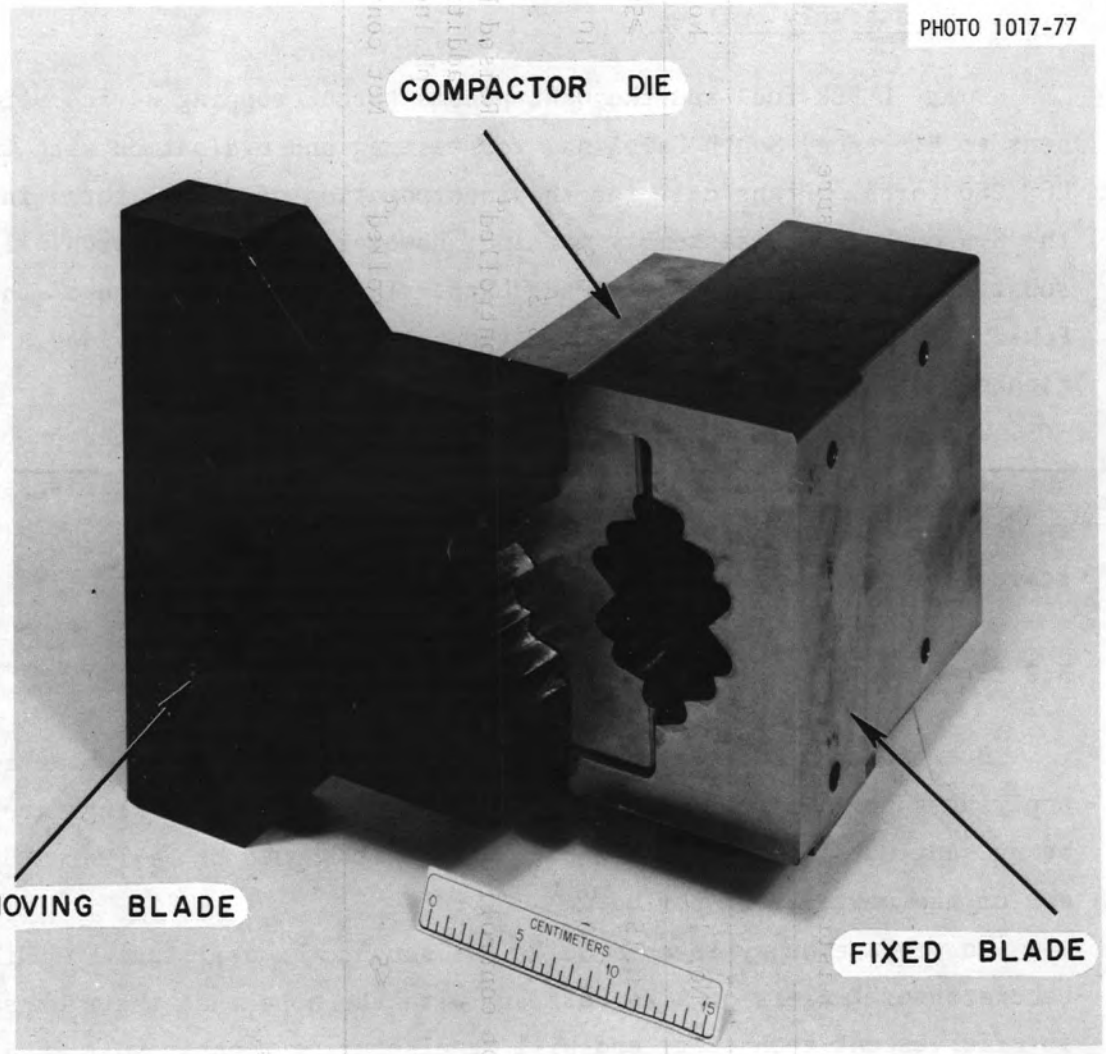

Fig. 5.3. New gag-compaction shape designed to tear shroud prior to shearing, also to slice type shear blade (shown in black) that will permit chopped fuel ejection.

one easily replaceable prealigned package. The specification will be used as a basis for the G+W concept design.

5.2.2 Subassembly cutting

Dummy LMFBR fuel and the ORNL plasma torch cropping device were sent to Florence, South Carolina, for testing and evaluation with the PCM-250 torch. Plans call for the incorporation of a PT-7 torch into the G+W push-type disassembly machine; however, a PCM-250 torch will be substituted if it proves to be adequate. The major advantage of the PCM-250 torch is that it has automatic arc control that provides a cleaner cut and produces less swarth.

Design criteria for a laser-cutting test device have been prepared. The device will initially be used to extend the work done on disassembly in England and France. Later, the device can be converted to a full-scale remotely operated unit and incorporated into the HPP.

5.2.3 Prototype fuel

Drawings were completed this quarter for a wire-wrap machine for applying spacer wires to dummy LMFBR fuel rods. These drawings are being sent out for fabrication bids; the unit should be delivered by the end of the next report period.

To produce dummy leached hulls, we sought the assistance of Miles Laboratories (makers of Alka Seltzer) with the hope that their expertise in effervescent technology and pill manufacturing might result in a supply of hard, water-soluble pellet materials. We did find a soluble material, but their pill-making machines could not produce a pellet geometry necessary to prevent the fuel tube ends from collapsing during shearing. We are therefore attempting to fill tubing with a saturated sugar solution or a liquid magnesium nitrate solution that will crystallize and provide the necessary rigidity to prevent fuel hull collapse.

A core pellet-sorting machine (Fig. 5.4) was acquired recently and is undergoing acceptance tests. The machine inspects pellets for straightness, length, and diameter and is capable of inspecting up to 60

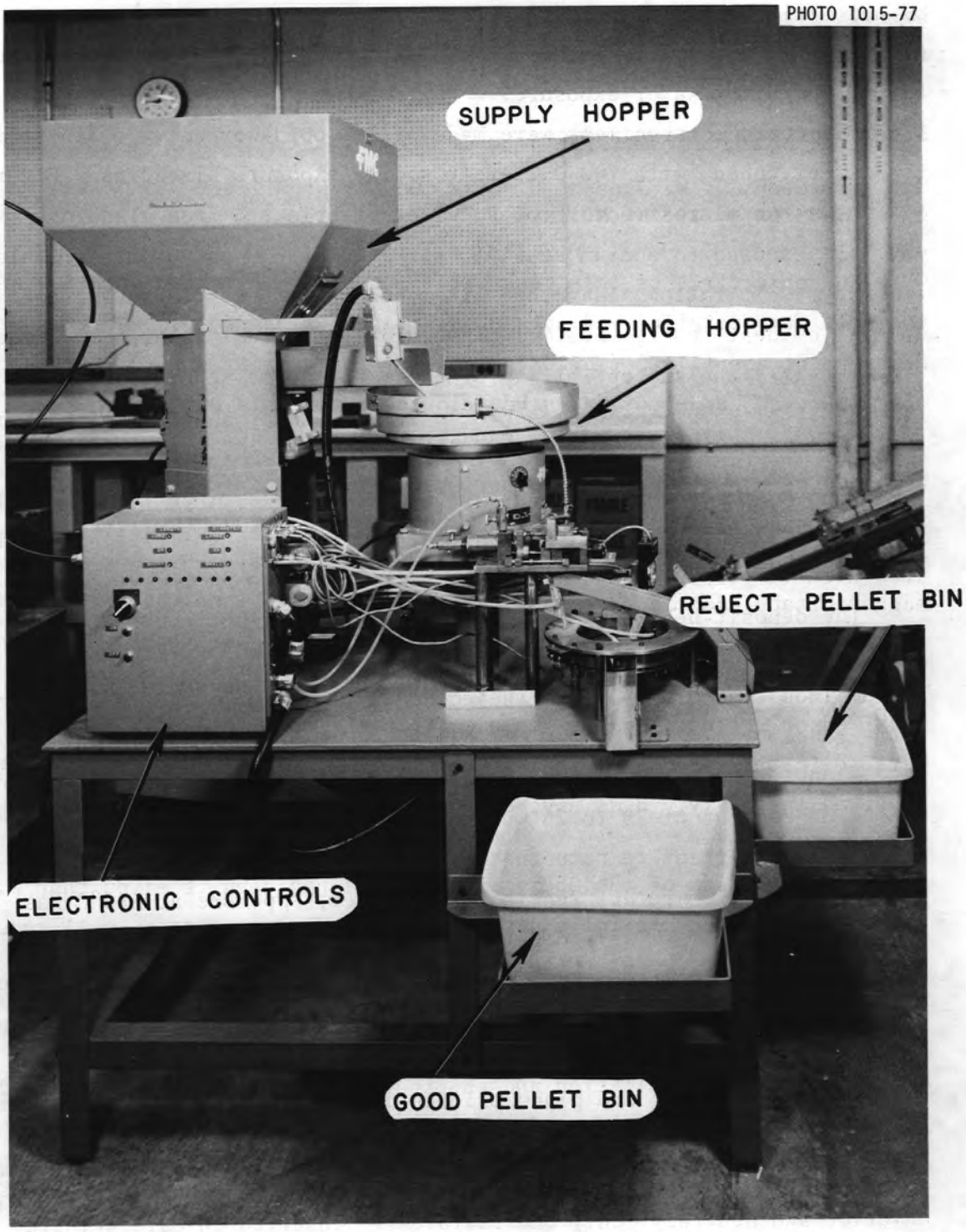

Fig. 5.4. LMFBR dummy cove and axial blanket steatite pellet sorter.

pellets per minute. A second machine for sorting radial blanket pellets is being fabricated for delivery next quarter.

5.2.4 Instrumentation and controls

N. C. Bradley, J. M. Jansen, D. D. McCue, G. N. Miller,
A. A. Shourbaji, and R. M. Tate

The objectives of this task are (1) to provide instrumentation and controls for operation and data acquisition during process and component development and (2) to provide a facility for testing and evaluating new, improved, adapted, and/or developed instruments and controls.

Data acquisition computer for straight-sided shear. Requisitions have now been approved for all peripheral equipment for the PDP 11/40 computer system. The hard copy unit, cathode ray tube (CRT), and medium-speed line printer have been installed and are in operation. The magnetic tape addition has been received, but cannot be installed until the vendor obtains and provides the correct interconnecting cable. The core memory expansion received previously has been rejected and is to be repaired or replaced by the vendor within the next 30 days. New bids were solicited for the digital input–output system because no bids were received initially. Bids have been requested on the high-speed analog input subsystem.

A new version of the operating software has been received that will correct errors and provide additional features; installation will require approximately two weeks. Plans are to move the computer to the LMFBR fuel reprocessing building when the computer room is completed.

Shear instrumentation and control. The control system has been fabricated, and installation and checkout are in progress. The installation is to allow transfer of the control rack from the component development position to its final destination in the IPET control room.

The fuel loader fabrication was completed during this period, and the control system is being installed, along with the fuel loader.

Shear dust particle-size analyzer. A particle-size analyzer for use to determine the particle-size distribution of the dust generated in the shearing operation has been borrowed from the Isotopes Department.

A faulty particle counter module was repaired, and the unit has been delivered to the operation site.

Fuel assembly shroud slitting plasma torch control. The torch control system has been modified, and the operation appears to be improved. A test is being set up to qualitatively evaluate the control system.

Multirod shear control systems. The operation of the shear will be controlled either manually or automatically. Automation of the shear is accomplished with the programmable logic controller (PLC) in command of both the pneumatic feed and the hydraulic shear operating systems. Analysis efforts are on producing an instrument flowsheet for the control of the system's dynamic functions.

5.3 Voloxidation

The work previously described[1] in this section involved the procurement of a prototype voloxidizer. Because of a lack of bids on the first specification submitted, the bid request was rewritten, deleting the requirements for remote operation and maintenance. Consequently, the voloxidizer is considered to be an engineering research model rather than a prototype unit and is therefore reported in Sect. 4 of this report.

5.4 Dissolution

J. Q. Kirkman

Component development effort in the dissolution area is directed toward designing, constructing, and demonstrating the operability of a 0.5-metric-ton/day pilot-plant-scale dissolver system, which consists of a remotely maintainable rotary dissolver integrated with the support equipment necessary to produce a functional dissolution.

5.4.1 Prototypical rotary dissolver

Fabrication work on the pilot-plant-scale rotary dissolver started in early January 1977. This work is expected to consume approximately 13,000 man-hours and is scheduled for completion in August 1977.

Figure 5.5 is a cut-away isometric drawing of the dissolver. The unit is approximately 6 m (19 ft) in overall length, 1.2 m (4 ft) wide, and about 116 m (5 ft) in height from bedplate to shroud top. The 75-cm-diam (30-in.) cylindrical drum is about 2.4 m (8 ft) in overall length. A description of dissolver mechanical features and overall operation was provided in the last progress report.[1]

Dissolver fabrication during this report period was concentrated in three areas. First, construction of the main equipment bedplate was completed. This is the rather massive horizontal structure (Fig. 5.5) that underlies and supports the entire dissolver machine.

The second area of concentration was the dissolver drum. The drum assembly procedure consists of butt-welding nine cylindrical shells (one for each stage) in a fixed sequence. This method allows assembly and welding of the drum and its internals in a series of steps beginning at the feed-end of the drum. To date, the nine cylindrical drum shells have been rolled, the circumferential butt-weld joints prepared, and the flanged inspection ports welded in place in each shell. These cylindrical sections are undergoing stress relief and annealing treatment. In addition to the drum sections, the seven conical transfer ducts contained in the internal dissolving stages have been formed, and the circular bulkheads separating the stages of the drum have been manufactured. Milling of the circumferential liquid transfer slots in the circular bulkheads is scheduled next.

The final area of effort involved a wide variety of machined parts. The following items were completed: the large drum-end flanges, roller support rings, shroud reinforcing flanges, motor drive shaft, gear-reducer lead screw, and the remotely operable hold-down studs.

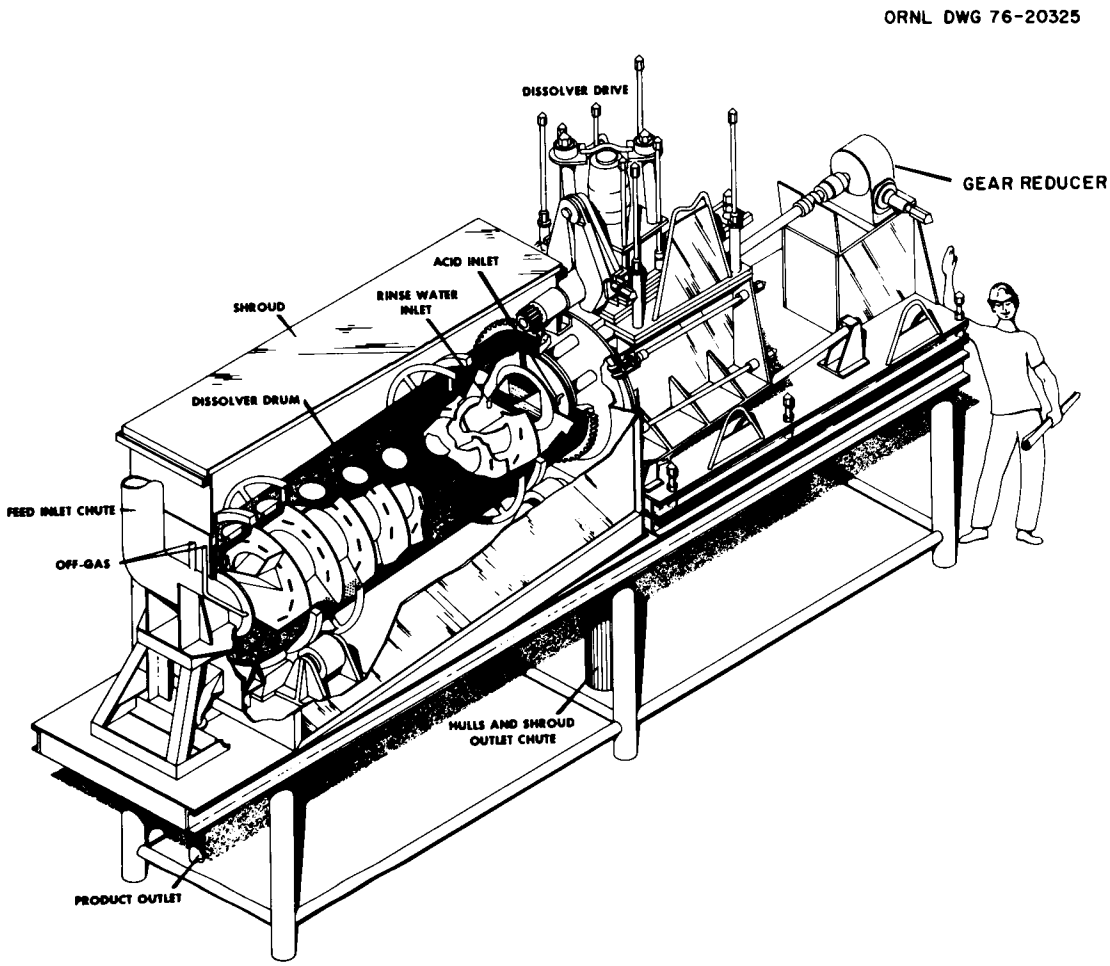

Fig. 5.5. Dissolver.

5.4.2 Dissolver support system and process equipment

Figure 5.6 is a flowsheet showing the support equipment associated with the rotary dissolver. This system breaks down naturally into a set of functional subsystems necessary to provide dissolver off-gas scrubbing, recovered acid recycle, liquid dissolvent additions, shroud steam purge, product collection and handling, and solids feeding.

Fabrication work on the NO_x scrubber and the scrubber bottoms hold tank, initiated late last quarter, has continued, with completion expected about May 1977. These components are key items in the off-gas scrubbing subsystem that converts NO_x gases contained in the process component vent streams into nitric acid for recycle.

Procurement–fabrication orders for stainless steel process tanks, stainless steel jacketed tanks, process pumps, and process heat exchangers were completed and placed during this period. These components constitute the major equipment items contained in the liquid and gaseous process subsystems of the dissolver system. In general, the pumps and heat exchangers are standard, off-the-shelf items with short delivery times, whereas the tanks are shop-fabricated components with deliveries up to 16 weeks.

Work was initiated in the ORNL fabrication shops on several special mechanical and process components, including the iodine stripper, recovered acid head tank, acid flow control loop, hulls collection equipment, and the dissolver liquid product diversion valve.

Procurement actions during this period concluded with placement of purchase orders for the process instrumentation and flow control valves and with requests for bids on the product clarification centrifuge and the recycle acid chillers.

Detailed design work on mechanical components in the solids-feeding subsystem has continued. Design of the contained screw feeder equipment, which accurately meters U_3O_8 powder to the dissolver, was completed early in March 1977. Design of the remainder of the feeding system, consisting of a set of vibratory trays that feed sheared hulls, wire, and shroud fractions, will be completed next quarter. Design reviews of the feeding system have been started.

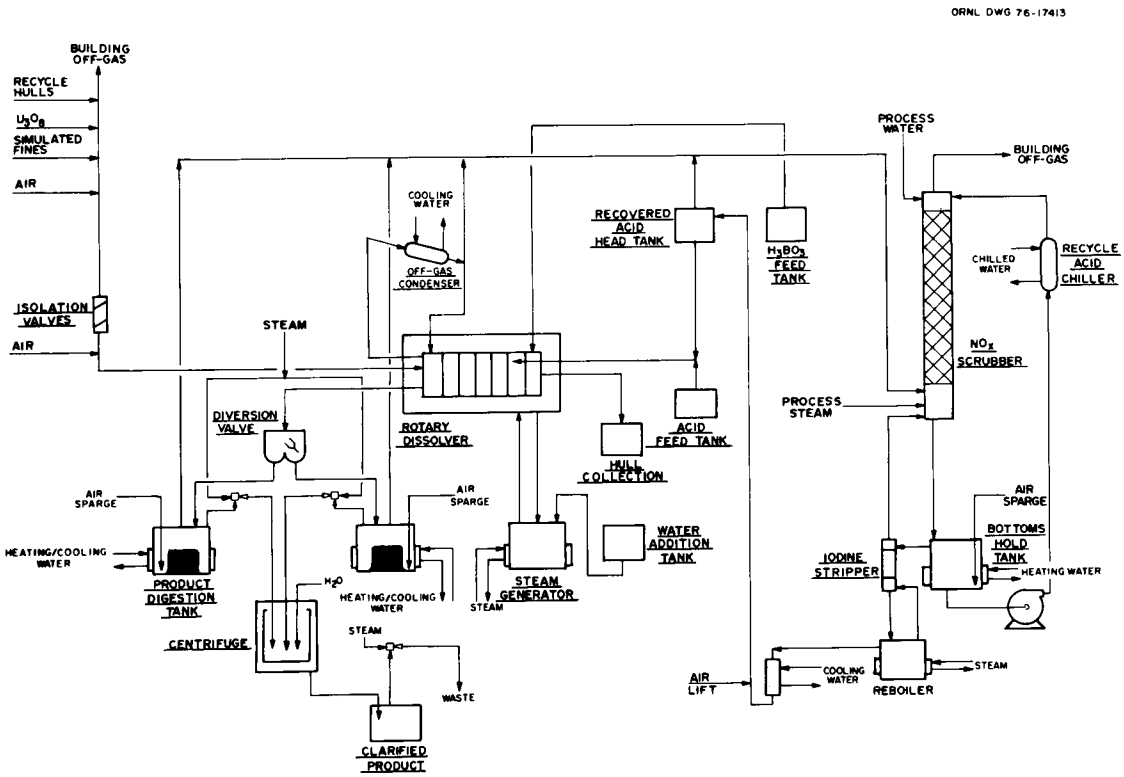

Fig. 5.6. Dissolver equipment flowsheet.

Review of the feed isolation valve preliminary designs was completed in January 1977. Detailed design and drafting work is proceeding on a course that will produce a set of valves that satisfactorily segregate the atmosphere of the dissolver from that in the voloxidizer and that can be remotely operated and maintained.

Work on the overall system has been directed toward development of a complete installation package. Important elements in this package include general arrangement drawings, detailed piping layout drawings, electrical and instrumentation drawings, structural support drawings, and details of tie-ins to essential building services. Progress on the detailed piping layout drawings has been sufficient to allow issuance of a bill of materials for stainless steel piping system items. Procurement of these stainless steel items will start early next quarter, so they will be available for the start of system installation.

5.4.3 Instrumentation and controls

N. C. Bradley, W. F. Johnson, and G. N. Miller

Drafts of the specifications and requisitions for the process instruments associated with dissolution, NO_x scrubbing, and acid recycling phases of the dissolver system were prepared and circulated for comments. Purchase requisitions and specifications have been corrected and submitted for procurement of these instruments, and most of the instrumentation is on order.

Construction sketches have been prepared. They show (1) the arrangement of the instruments in the transmitter racks, (2) the interconnecting wiring between both the transmitter rack, field-mounted instruments, and the unit process controller, and (3) typical field installation of the various flow transmitters. These drawings should be completed and construction should be well under way on the transmitter racks during the next quarter.

The instrument flowsheet has been completed for the dissolver disassembly and reassembly instrumentation, which will indicate remotely the position and limits of critical elements during maintenance operations.

The material feed system for the dissolver has been studied, and the weigh and control functions have been defined. The feed system rate is to be manually set and will have the capability to monitor the weight of material fed.

The control system for the drum operation has been defined, and instrumentation has been identified for procurement.

5.5 Receiving and Storage

S. A. Meacham*

The overall work plan for the receiving and storage task was completed and submitted for approval during this quarter. In addition, the projected budgets and manpower requirements for FY 1978 through FY 1981 were submitted.

This task has been divided into seven areas. The objective of each subtask is described below.

Subtask 1 — Receiving and storage systems integration. To provide task management for the design and development of receiving and storage subsystems and to contribute to the establishment of the proper interfaces with the preceding and succeeding process steps. The interface with advanced or modified subassembly designs will also be established.

Subtask 2 — Sodium removal system. To design, construct, and evaluate a system that will remove sodium and/or sodium compounds from core, blanket, and control rod subassemblies. The removal system must be adequate to permit subsequent water pool storage.

Subtask 3 — Fuel transporter. To design, construct, and evaluate a system(s) that will unload, confine, and transfer sodium and/or nonsodium-wet core components to either a sodium-removal system or to a water pool storage facility.

---

*Westinghouse Advanced Reactors Division (WARD), Madison, Pa.; on loan to ORNL.

Subtask 4 — Fuel handling system. To design, construct, and evaluate systems that will be required to operate within the water pool storage areas and to transport subassemblies to the disassembly area.

Subtask 5 — Fuel identification system. The incorporation of the existing Fast-Flux Test Facility (FFTF) and Clinch River Breeder Reactor (CRBR) fuel identification system within the HPP will allow for the remote identification of core components. In addition, an interface with Gas-Cooled Fast Reactor (GCFR) and Prototype Large Breeder Reactor (PLBR) fuel designers would permit the standardization of a remote identification system.

Subyask 6 — Sodium-removal experiments. To establish the optimum sodium-removal process and sodium-removal cycle.

Subtask 7 — Research and development corrosion program. To establish the feasibility of the water pool storage of LMFBR spent fuel cladding by determining the effects of various sodium-removal procedures and water pool parameters.

5.5.1 Systems integration

The first draft of the HPP Work Task Description 5.3.0-4, HPP Fuel Storage Pool — Design Criteria, was completed. An evaluation was made of the heat rejection capability to be provided by the pool-heat-exchange system. The heat load was based on the most recent predictions for spent-fuel storage and for solidified high-level-waste storage. Table 5.1 is the current assessment of the decay heat associated with the different LMFBR driver fuels.

Table 5.1. Heat dissipation of LMFBR fuels[a]

Facility	Kilograms of heavy metal per subassembly	Days cooled (kW per subassembly)				
		60	90	120	180	400
FFTF	34.5	3.3	2.4	2.0	1.4	0.7
CRBR	57.5	6.8	5.8	4.6	3.3	1.0
PLBR	169	15.0	12.2	10.8	8.8	5.0

[a]Based on average power of 44,000 MWd/metric ton for FFTF, 79,000 MWd/metric ton for CRBR, and 110,000 Mwd/metric ton for PLBR.

We are currently considering component development hardware and equipment to initially handle spent fuel assemblies with decay heat to 10 kW. Transfer times within the receiving and storage areas have been qualitatively estimated under noncooling conditions and are given in Table 5.2. The estimates were extrapolated from ORNL/TM-2906, Appendix C, which used heat generation rates computed with the ORNL ORIGEN code. The significance of the current estimates is that the transfer and handling times considered are adequate in the event that forced cooling is lost in an emergency situation. Quantitative values will be obtained when the actual transfer sequences are identified and when better estimates are available on the heat dissipation of the spent fuel.

Table 5.2. Estimated time–temperature relationship of the center pin (without cooling — emissivity assumed to be 0.5)[a]

Days cooled	Time required to reach 650°C (min)	Time required to reach 980°C (min)	Maximum temperature (°C)
		FFTF	
60	50	180[b]	955
90	75	195[b]	845
120	95	200[b]	800
180	170	300[b]	695
400	420		540
		CRBR	
60	20	40	1370
90	25	55	1260
120	30	65	1205
180	45	100	1095
400	60		730

[a]The values are estimates only and are considered as an order of magnitude.

[b]Minutes required to reach maximum temperature.

5.5.2 Sodium-removal system and fuel transporter

A contract has been initiated with Aerojet Manufacturing Company (AMCO) of Fullterton, California, to have them prepare a scoping study

for the sodium-removal system and the fuel transporter (subtasks 2 and 3). The study will briefly describe different methods to transport a subassembly or a group of subassemblies from the cask into or through a sodium-cleaning operation and on to the storage pool. The scoping study will be complete in approximately ten weeks.

5.5.3 Fuel identification system

Discussions with ORNL and General Atomic personnel involved with the GCFR are continuing. A recommendation has been made to consider the fuel identification system to be used at the FFTF and the CRBR. Adoption of such a system would facilitate fuel handling and identification within the HPP. The significance of standardizing the fuel identification system is at least twofold: it leads to lower overall costs and provides a common interface between the fuel designers and the reprocessing plant. Discussions relative to a fuel identification system are also being held with Prototype Large Breeder Reactor (PLBR) personnel.

5.5.4 Corrosion program

The Westinghouse Advanced Reactor Division (WARD)–ORNL program,* which has the objective of determining the corrosion behavior of sodium-exposed stainless steels after various sodium-removal procedures and under water-pit storage conditions, continued on schedule. The results of this study will be used to define whether a problem exists in the storage of sodium-exposed fuel assemblies under water. Progress made during this quarter is described in detail for four areas within the current program, as reported by WARD.

Sodium recondition. All specimens requiring sodium reconditioning, as defined in the test matrices of the current program, have been exposed

---

*The WARD–ORNL Fuel Reprocessing Work Program on Sodium Cleaning and Subsequent Corrosion of Sodium-Exposed Stainless Steel Under Water Pit Storage Conditions," ORNL Subcontract No. 7168, Westinghouse Electric Corporation.

to sodium. A total of 60 specimens — 30 corroded type 316 stainless steel specimens and 30 deposit-bearing, type 304 stainless steel specimens — were sodium-reexposed under the conditions listed in Table 5.3.

Table 5.3. Sodium recondition history of the test material

Loop run	Temperature (°C)/No. of specimens		Loop operating conditions		Sodium reconditioning time (hr)
	Corroded	Deposited	Oxygen (ppm)[a]	Velocity (m/sec)	
1	718/8		0.31	2.1	334
2	718/7		0.50	2.1	330
3	643/8	399/6	0.60	2.1	335
4	649/7	399/1	0.59	2.1	340
4		399/7	0.59	2.1	340
5		399/4	0.50	2.1	340
6		399/8	0.50	2.1	340

[a]Measured by vanadium wire equilibration method.

Extension of corrosion-study program. As an extension of the current WARD—ORNL LMFBR Fuel Reprocessing Corrosion Program, 120 new specimens (made ot 20% cold-worked type 316 stainlesss steel cladding) will be sodium exposed for subsequent water-corrosion studies. The added specimens will provide additional data to enhance the statistical confidence of the results obtained in the current investigation.

The fabrication of 60 clad specimens for hot-leg (718°C) sodium exposure has been completed during this report period. Work is in progress to fabricate the four required test-section legs that will contain the specimens during exposure. The other 60 specimens will be exposed (beginning next quarter) in a cold leg at 371°C.

Sodium removal. Residual sodium was removed by the steam—argon (KNK) process from six cold-worked type 316 stainless steel cladding specimens. Sodium was also removed from eight type 304 stainless steel specimens by the water vapor—argon (WVA) process. Following sodium removal, the samples were removed from the cleaning vessel, photographed, and visually examined. Samples cleaned by the KNK process have a thin,

black coating, probably caused by caustic reaction at the higher temperature (140°C) used with this process (Fig. 5.7).

Water exposure. All specimens defined in the test matrices are now undergoing water exposure or have been withdrawn from water following exposure. Table 5.4 defines the water bath conditions. Table 5.5 lists conditions for corroded type 316 stainless steel specimens. The water exposure of alcohol-cleaned specimens was initiated early in this reporting period, whereas the majority of the specimens, with sodium removed by the WVA process and/or by the KNK process, has completed water exposure (defined in Table 5.5). To date, none of the type 316 stainless steel cladding specimens have failed. One specimen from each bath, after water exposure, will be destructively analyzed to provide metallurgical information. The remaining specimens will be subjected to extended exposure after visual examination.

The current status of type 304 stainless steel specimens is shown in Table 5.6. Three more specimens have failed during the present report period, making a total of five failures thus far. All failures occurred in high chloride baths, four in neutral bath 3, and one in high pH bath 4. Three of the failures in bath 3 occurred in a relatively short time (∿72 hr). The remaining failure occurred after about 10 days of exposure. The failure observed in bath 4 occcurred after about 18 days of exposure. All failures are characterized by the development of a pinhole and the subsequent slow release of the pressurizing gas.

The problems in maintaining bath conditions appear to be resolved, and conditions are relatively stable. High chloride baths still tend to accumulate a brown precipitate. The material has been identified as ferric hydroxide. It is assumed that the precipitation must be preceded by the chlorination of iron; however, the mechanisms of the reaction are not clear.

Specimen characterization. Two types of sodium-preexposed stainless steel tubing were studied in the present investigation. Corroded type 316 stainless steel tubing was previously exposed to sodium in a corrosion region of a flowing sodium loop, whereas type 304 stainless steel was exposed in a deposition area. Specimens made of these materials were reexposed to sodium in loop system MTL-4 for two weeks in corrosion

Fig. 5.7. Typical surface condition of type 316 stainless steel specimens after sodium removal by the steam–argon process.

Table 5.4. Chemistry of water baths for cladding material exposure

Property	Water bath conditions			
	No. 1	No. 2	No. 3	No. 4
Chloride,[a] ppm	≤0.15	≤0.15	≥500	≥500
pH	7.0 ± 0.5	10 ± 1[b]	7.0 ± 0.5	10 ± 1[b]
Oxygen content,[c] mg/cm^3	5.3	5.3	5.3	5.3
Sodium ion content	Not controlled[d]	Raised by NaOH addition for pH increase	Not controlled[d]	Raised by NaOH addition for pH increase
Conductivity, micromhos	≤5	Not controlled[d]	Not controlled[d]	Not controlled[d]

[a]Adjusted with NaCl.

[b]Raised by NaOH additions.

[c]Saturated at 82°C.

[d]Will be measured.

Table 5.5. Test matrix (hot leg, 718°C) for sodium removal and water exposure of sodium-exposed cladding material (type 316 stainlesss steel)

Sodium removal methods	Test period (months)	Water bath[a] No. 1	No. 2	No. 3	No. 4
Alcohol	1				
	2				
	3	X	X	X	X
Water vapor–argon	1		X^c	X^c	X^c
	2		X^c	X^c	X^c
	3	X^cX^c	X^cX^c	X^cX^c	X
Steam–argon	1		X^c	X^c	X^c
	2		X	X	X
	3	X^cX^c	X^cX^c	X^cX^c	X^c

[a]X = one specimen; X^c = exposure completed, specimens removed for examination.

Table 5.6. Test matrix (cold leg, 371°C) for sodium removal and water exposure of sodium-exposed cladding material (type 304 stainless steel)

Sodium removal methods	Test period (months)	Water bath[a] No. 1	No. 2	No. 3	No. 4
Alcohol	1				
	2				
	3	X	X	X	X
Water vapor–argon	1		X	X^r	X
	2		X	X^r	X
	3	XX	XX	X^rX^r	X
Steam–argon	1		X^c	X^c	X^r
	2		X	X	X
	3	XX	XX	X^rX	X

[a]X = one specimen; XX = two specimens; X^r = specimen ruptured, removed for examination; X^c = exposure completed, specimens removed for examination.

or deposition regions typical of their prior history. The materials were studied by metallographic characterization and electron microscopy before and after water exposure.

The corroded specimens were made of 20% cold-worked type 316 stainless steel tubing with two different sodium-exposure histories. Figure 5.8 shows the microstructure of specimens fabricated from cladding material exposed to sodium at 649°C for 5300 hr. Massive intragranular carbide precipitation along the slip lines resulting from severe cold work is evident in Fig. 5.8(a). The cold-work effect apparently reduces significantly the susceptibility of the material to sensitization. Figure 5.8(b) shows the presence of a ferrite layer and the molybdenum-chromium intermetallic compound at the alloy–sodium interface. The formation of these phases in the austenitic alloy surface is due mainly to the preferential depletion of nickel (austenite stabilizer) resulting from high-temperature sodium exposure.

The deposit-bearing type 304 stainless steel specimens were manufactured from an economizer (liquid-metal heat exchanger) tube from sodium loop system MTL-1-10. The economizer was subjected to a temperature gradient across the tubing wall and a temperature differential (ΔT) along its entire length. The economizer was exposed to an oxygen in sodium content of 20 to 25 ppm for 3500 hr.

It is important to note that sturctures resulting from sodium exposure at 454°C are not sensitized; however, exposure at 580°C has sensitized the alloy, as indicated by the presence of intergranular carbides. An extensive Strauss test of the specimen materials has been initiated to determine the significance of sensitization in the present investigation.

Surface cracking and pinhole leaks developed on the deposit-bearing type 304 stainless steel specimens after exposure in high chloride baths. The majority of failures resulted from exposure in bath 3 (high chloride and neutral); only one failure was observed in bath 4 (high chloride and high pH). Therefore, a high pH solution apparently enhances the cracking resistance of the test material in a high chloride environment.

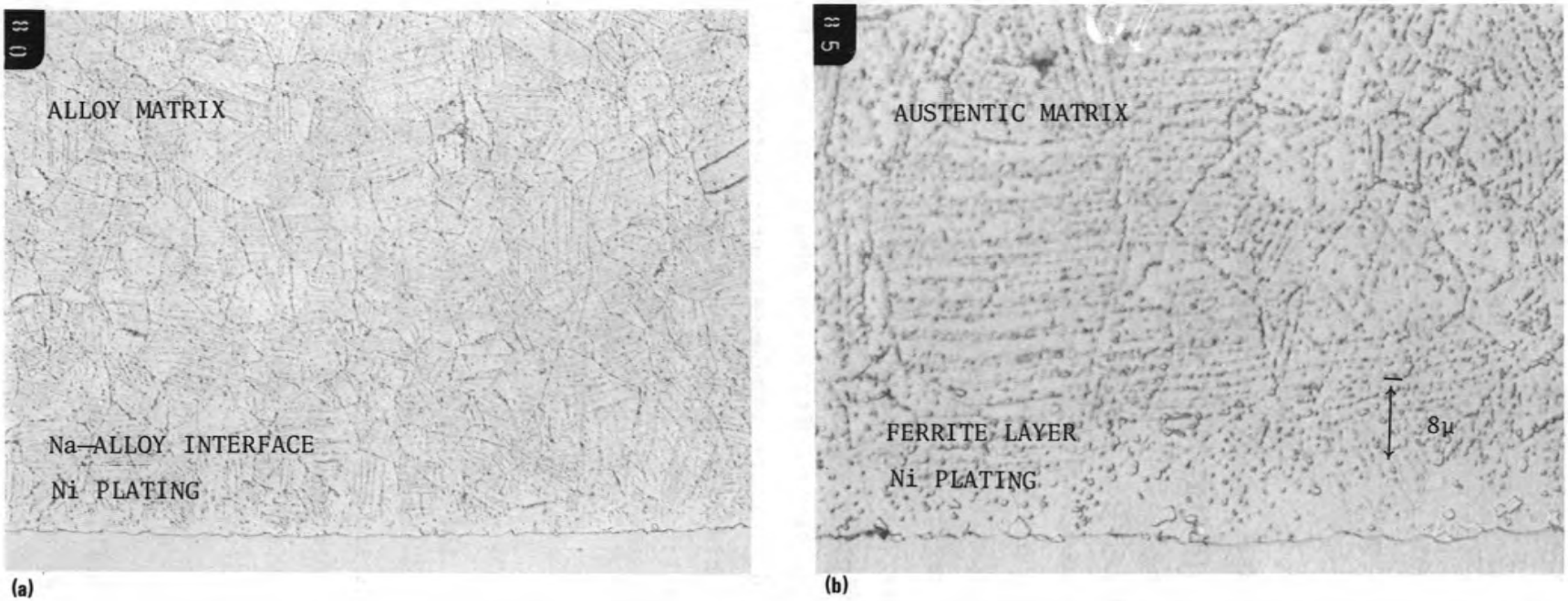

Fig. 5.8. Microstructure of corroded 20% cold-worked type 316 stainless seeel specimens exposed to 2.1 m/sec of sodium at 649°C for 5300 hr. (a) Intragranular carbide precipitation along slip lines within the matrix. Etch: Gly HCl HNO_3. 500×. (b) Formation of the ferrite layer and the molybdenum-chromium compound intermetallic compound. 1450×

Typical surfaces of failed deposit-bearing type 304 stainless steel specimens are shown in Figs. 5.9 and 5.10. Based on these results, it can be concluded that failure was apparently initiated by severe localized pitting. The subsequent formation of transition metal chlorides accelerated the development of cracks via a wedging effect due to volume expansion.

Conclusion. Based on the results obtained to date, it can be concluded that the satisfactory performance of corroded type 316 stainless steel specimens in high chloride water solutions is due mainly to two factors: (1) the massive intragranular carbide precipitation due to severe cold work prevented the alloy from sensitizing during high-temperature sodium exposure, which in turn reduced the susceptibility of the alloy to intergranular attack; and (2) the presence of a ferrite layer with high molybdenum content enhanced the alloy's resistance to localized pitting corrosion.

The failure observed on deposit-bearing type 304 stainless steel specimens in high chloride water solutions (baths 3 and 4) was apparently initiated by localized severe pitting and was accelerated by the wedging effect due to chloride formation. Consequently, stress appeared to be a secondary factor in this failure; however, additional testing is being conducted to substantiate this observation.

5.6 Remote Maintenance

J. D. Sease

The objective of the remote maintenance task is to develop information that will allow the design and operation of general-purpose maintenance equipment and facilities for a pilot-scale LMFBR reprocessing plant to proceed at an acceptably low risk. The remote maintenance task includes development work in the following areas: (1) electromechanical systems, (2) remote viewing, (3) mechanical manipulators, (4) welding and joining, (5) connectors and jumpers, (6) locks and seals, and (7) sampling.

The major effort this quarter has been in the electromechanical systems development area.

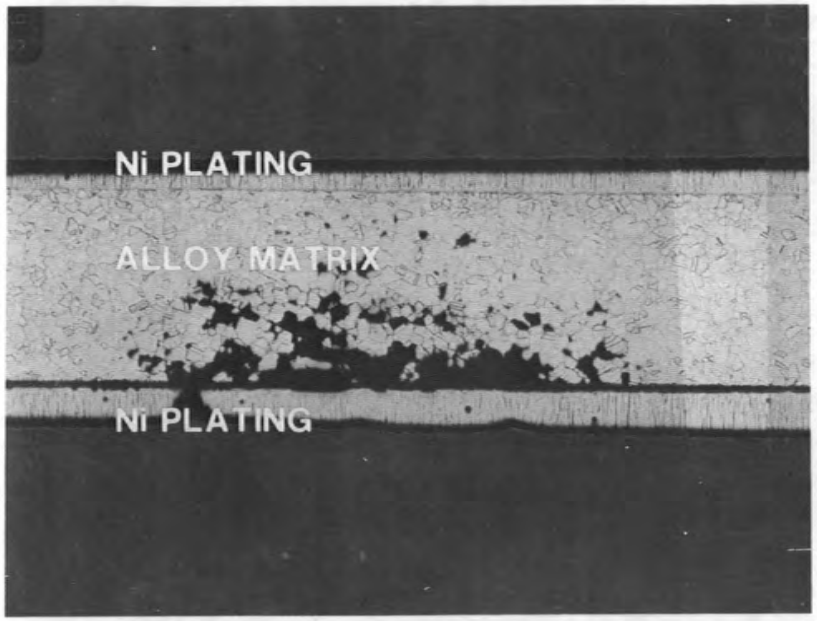

(a)

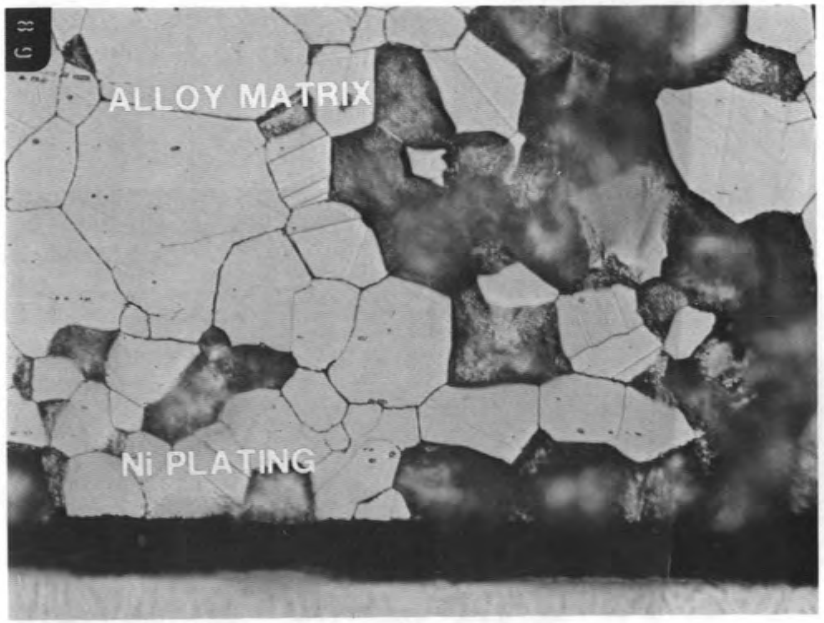

(b)

Fig. 5.9. Microstructure of deposit-bearing type 304 stainless steel after neutral and high chloride water exposure (82°C, 10 days). (a) Severe localized pitting. Etch: Gly HCl HNO_3. 50×. (b) Intergranular cracking of the alloy matrix. 500×

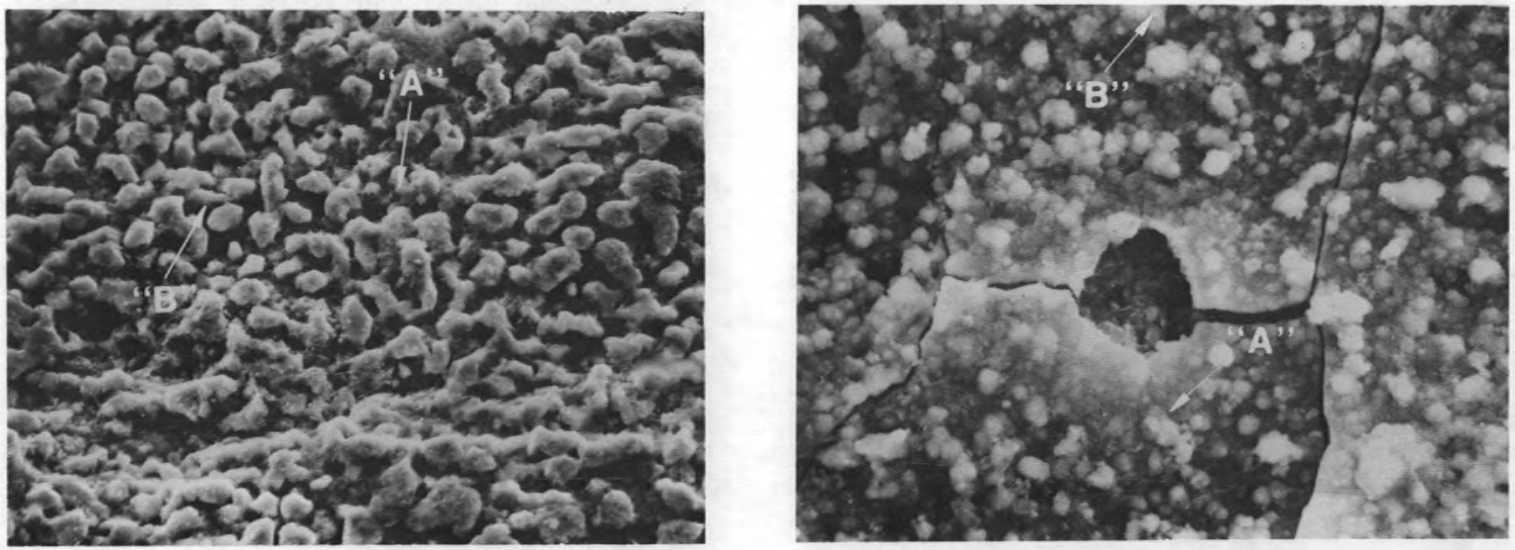

(a) (b)

Fig. 5.10. Scanning electron microscopy photomicrograph of deposit-bearing sodium-exposed type 304 stainless steel. (a) Specimen exposed to sodium for 3500 hr at 454°C, sodium removal by steam–argon process. Specimens water exposed in high chloride and neutral bath for 72 hr at 82°C.

5.6.1 Electromechanical systems

N. C. Bradley, W. R. Harmel, J. O. Hylton, and R. C. Muller

This activity involves the design and development of crane systems and electromechanical manipulators required for an LMFBR reprocessing pilot plant. Initial work is being directed toward the problems of signal and power transmission to a remotely operated and maintained electromechanical system.

Signal transmission. For signal transmission, multiconductor cables can be eliminated by multiplexing and transmitting all signals over a single carrier. The carrier can be a single coaxial cable or a wireless medium such as radio, microwave, or optical (laser or light beam).

A survey of current technology suggests that an optical data link would be best suited for hot-cell use. This technique has been used successfully for video transmission, for computer data links, and for remote control of warehouse cranes. The hardware is commercially available and is relatively simple and inexpensive in comparison to radio or microwave systems.

A small-scale bench test of a typical optical telemetry system is being planned. The test will be used to evaluate available hardware and to determine performance and design criteria for a representative system to be installed for developmental testing.

Power transmission. Power transmission to mobile equipment has traditionally been accomplished by the use of either festooned cables or bus bars. Literature studies show that it is within the capability of current technology to provide a wireless power source for hot-cell manipulators. For example, the PaR 3000 manipulator and bridge system operates at a nominal power level of 100 to 200 W, with a peak level of around 1600 W. A lead-acid battery pack weighing 250 lb can provide this power level for around 20 hr without recharging.

Microwave beams can also be used to transmit power to mobile equipment. While the transmitting equipment is fairly complex, the receiving equipment, which would be inside the cell, consists of essentially an antenna and a diode. Further study into the practical aspects

of these systems is under way to determine if they can provide an attractive alternative to cables and bus bars.

Position indication. Methods for measuring the position of mobile equipment inside the cells have been investigated. Rotary and linear displacement transducers, such as resolvers, inductosyns, and limit switches, are widely used to control servo mechanisms. These devices, which will meet many of our requirements, require sensing instruments inside the cell environment. The possibility of using a remote radar or laser range finder has been studied.

Conventional radar does not appear suitable for use within the confines of a hot cell because of multiple reflections from surfaces other than the target.

A laser interferometer, which is used on large machine tools for displacement measurements, appears promising. We plan to borrow such a unit from the Y-12 Plant for evaluation.

An optical range finder developed by MIT's Draper Laboratories for use with a robot manipulator is another possibility. If the commercially available devices do not prove satisfactory, tentative plans have been prepared to build a modified version of the MIT device for evaluation.

Thorium-Uranium Recycle Facility (TURF) overhead system. Many of the mechanical features of the TURF interactive bridge and transfer system are considered to be representative of what might be used in the HPP. A portion of this activity is to investigate the TURF system and determine what design changes will be required to make it representative of a modern system, from both a mechanical and a control and operational viewpoint.

Specifications for upgrading the TURF system are being prepared. A meeting with the PaR Corporation will be arranged in the near future to discuss their possible involvement in the work.

5.6.2 Remote viewing

Remote operations in the HPP will require the use of TV viewing systems, both mobile and fixed locations, to provide adequate visual feedback for the performance of maintenance tasks away from windows and

periscope locations. This activity includes the evaluation of available TV systems to determine which are best suited and how best to use them.

A file of information from equipment vendors and users is being compiled. Commercially available TV systems include conventional high resolution (1000 line raster) and 3D systems in both black and white and color. Some users who have tried different systems for remote process maintenance operations have made the following observations:

1. Color television does not offer a significant advantage and is considerably more expensive and complicated.
2. The advantages of depth perception in 3D systems are offset by the lack of close-up resolution. Also, many operators experience headaches and eye fatigue more rapidly than with conventional TV.
3. Good results in performing dexterous tasks have been obtained with a dual-camera high-resolution system mounted on a manipulator arm. One camera was for wide-angle and the other for close-up viewing.

5.6.3 Connectors and jumpers

W. F. Schaffer, Jr.

The success of remote maintenance is highly dependent on the ability to reliably remove connecting pipes and electrical and instrument lines from failed process and auxiliary equipment. Conversely, one must be able to reconnect (with high reliability) a repaired or new equipment item to the system.

Radiation levels in most cells of the HPP preclude the use of elastomers and plastics in connectors for pipelines. The development and testing of pipe connectors and the associated connecting lines or jumpers are directed toward mechanisms that are fully radiation resistant and acceptable from the standpoint of corrosion resistance, strength, temperature and pressure cycling, vibration, and other environmental conditions. Connectors being investigated in this category in general will employ metal seals to ensure system integrity and longevity; the only known exception may be Grafoil, a high-temperature chemical and radiation-resistant carbon product.

Because of the anticipated longer development schedule, the primary effort to date has been devoted to pipe connectors. The Hanford-Purex model has been designated as the reference pipe connector; alternate connector types also being studied, along with the remote mechanisms that are needed.

Preliminary studies on the Hanford-Purex connector indicate that modifications which replace the present Teflon seal with a metal seal are feasible. Current engineering drawings specifying recent design changes and current materials of construction have been requested from Atlantic Richfield Hanford Company (ARHCO) to enable us to continue this design investigation. We plan to subcontract work relating to the seal modifications of the Hanford-Purex connector to industrial concerns specializing in metal seals.

Reports, test data, and industrial literature on possible alternate pipe and tubing connectors have been collected and reviewed. This study indicates that a number of pipe connectors with metal seals are available in the industrial market; several have remote operation features. Further evaluation of these alternate connectors will be necessary to determine their suitability for use in the HPP. We plan to make this evaluation by requesting formal proposals from several manufacturers for a remotely operable pipe connector. A preliminary specification for these proposals has been prepared and circulated for comments.

In addition to remotely operable pipe connectors, we are considering the application of standard connectors, such as pipe flanges, unions, and tubing fittings, that could be joined or disjoined by remote control. The study would allow us to evaluate the desirability and economics of this approach vs specially designed connectors.

5.6.4 Sampling

The sampling activity will involve work in four areas: (1) sample transfer, (2) mechanical handling of sample containers in a sample "blister," (3) liquid samplers, and (4) solid samplers. A work plan outlining these activities has been drafted.

A visit was made to the Reactor Experiments Company (RE), San Carlos, California, January 24, 1977, to discuss remote sampling and RE's possible involvement in the remote sampling activity. RE can offer expertise in area (1) and possibly area (2). They also indicated that they would be interested in doing development work in these areas.

REFERENCE FOR SECTION 5

1. W. D. Burch et al., *LMFBR Fuel Reprocessing Program Progress Report for Period October 1 to December 31, 1976*, ORNL/TM-5768 (February 1977).

6. INTEGRATED PROTOTYPE EQUIPMENT TEST FACILITY (IPET)

Pre-Title I planning for the IPET project was completed in January 1977. During this initial phase, work was accomplished on a number of tasks that must be completed prior to the start of Title I design. These tasks included a project management plan, a project reporting plan, communication and documentation guidelines, and a personnel index. The IPET conceptual design report[1] was screened by various disciplines to clarify the IPET scope and to identify unanswered questions. The list of subtasks was reviewed, and schedules for the input of information for each subtask were tabulated. Titles I and II manpower requirements were estimated according to current information; document lists for Title I were prepared.

Figure 6.1 shows the IPET design and construction schedule. The UCC-ND Engineering manpower estimates for IPET are listed in Table 6.1, along with estimated costs. The manpower data show a total of 32,735 man-hours for Title I design, 58,003 man-hours for Title II design, $970,200 for Title III Engineering, and a total engineering cost of $2.5 million.

IPET Title I design began February 1, 1977, using authorized construction planning and design (CP&D) funds. The design criteria were prepared according to the work breakdown structure generated during the pre-Title I planning exercises. The Project Management review of the criteria was scheduled for late March. Table 6.2 lists the IPET work breakdown structure, which consists of five major groupings: (1) general plant facility, (2) integrated process demonstration, (3) remote operation and maintenance demonstration, (4) operations support, and (5) general project support. The five major groupings are further segregated into subtasks for management purposes.

An earlier Line Item Construction funds request (Schedule 44) for $16 million has been changed to reflect ERDA's proposal that $600,000 in CP&D funding in FY 1977 be used to conduct IPET Title I design, that $3 million in FY 1978 funding be used for Title II design and procurement of long-lead-time equipment items, and that the remaining $12,400,000 for construction be requested for FY 1979 authorization and appropriation.

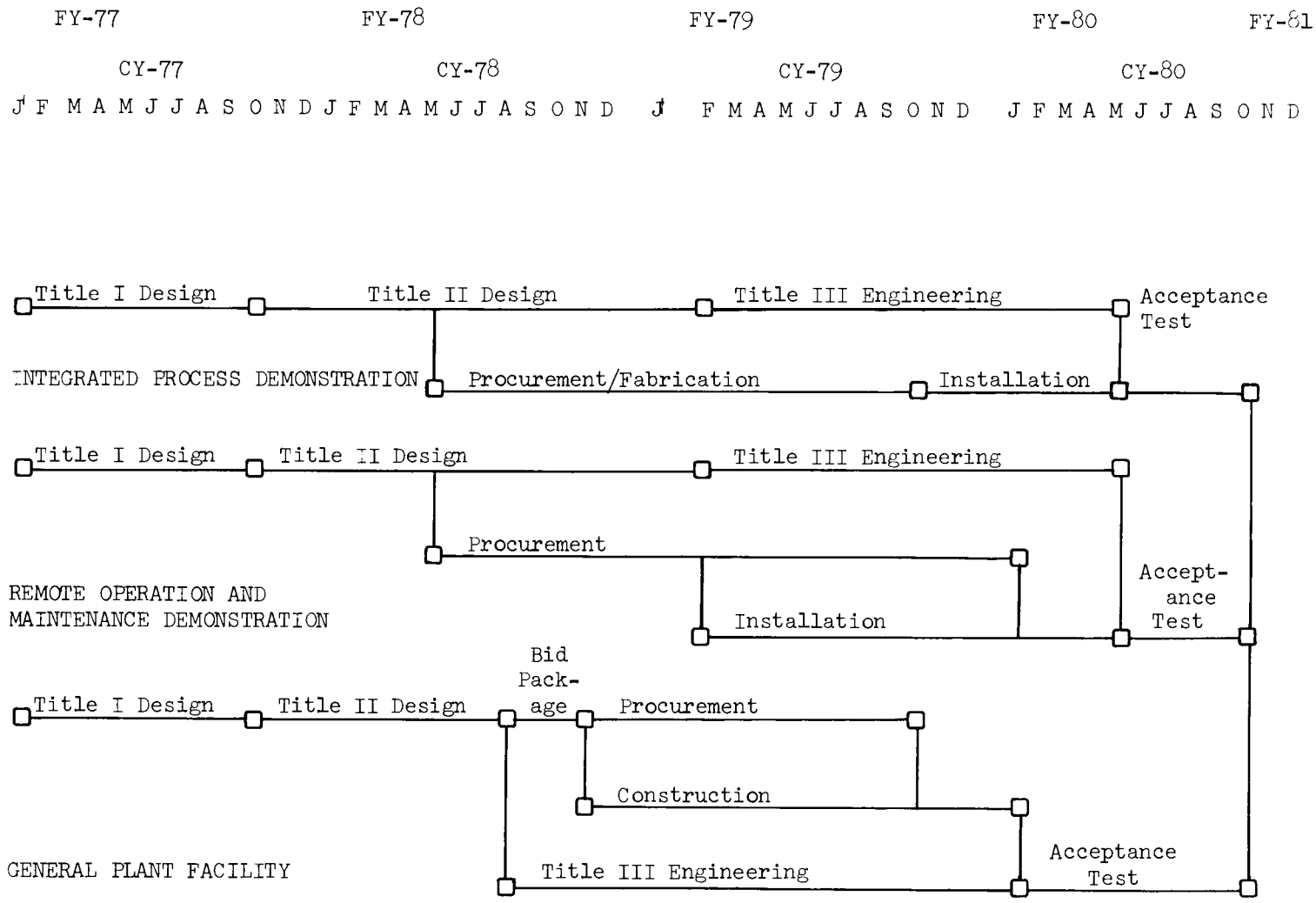

Fig. 6.1. LMFBR Integrated Prototype Equipment Test (IPET) facility design and construction schedule.

The financial schedule for the IPET facility (Table 6.3) reflects the most recent Schedule 44 funding request and timetable.

Table 6.1. Engineering estimate for IPET

Task	Man-hours		
	Title 1	Title II	Title III
Instrumentation (UCC-ND Engineering)	6,000	7,950	
I&C engineering	2,500	5,585	
Civil and architectural	1,540	1,900	
Piping and mechanical design	235	550	
Site engineering	233	48	
Environmental control (HVAC[a])	288	530	
Process design	9,500	25,250	
Electrical	4,440	3,740	
Development engineering	3,500	9,000	
Project management	2,500	3,000	
Planning, scheduling, cost estimating	500	750	
Engineering analysis	1,500	500	
Total man-hours	32,735	58,803	
Cost	$544,800	$985,000	$970,200
Total engineering cost	$2,500,000		

[a]Heating, ventilation, and air conditioning.

6.1 LMFBR Facility Engineering

The UCC-ND Engineering design of the initial phase of the vessel off-gas system was completed. The procurement and installation of equipment is in progress. Items to be installed during the initial phase include filter housing, a stack, and control equipment. A second phase calls for the installation of off-gas collection ducting, with provisions to add an off-gas scrubber in the future.

Approval was received to purchase water demineralization equipment and services from an outside vendor; the request for bids has been submitted. This method of obtaining demineralized water was found to

Table 6.2. IPET work breakdown structure (4000)[a]

General plant facility (4100)		IPD[b] facility (4200)		ROMD[c] facility (4300)		Operations support (4400)		General project support (4500)	
*4110	Land improvements	*4210	Engineering support systems	*4310	Engineering support systems	*4410	Manuals	*4510	Project management
*4120	Other structures	4211	Electrical	4311	Electrical	4411	Operator training	*4520	Special reports
4121	Cooling tower	4212	Process equipment layouts	4312	Fabrication and inspection	4412	Operating	4521	Quality assurance
*4130	Building additions	4213	Process utilities	*4320	Cell arrangements	4413	Safety	4522	Title I
4131	Diesel generator	*4220	Computer	4321	Mechanical cell	4414	Maintenance and repair	4523	Environmental assessment
4132	Transmitter room	4221	Data and control requirements	4322	Process cell	*4420	Procedures	4524	Safety analysis
4133	Chemical makeup	4222	Interface and site preparation	4323	Maintenance cell			4525	Design criteria document
4134	Storage	4223	Computer hardware	*4330	Transfer systems			4526	Project reporting requirements
*4140	Building modifications	4224	Computer software	*4340	Manipulator system				
4141	ROMD	*4230	Mechanical head end	4341	Crane				
4142	Office expansion	4231	Disassembly	4342	Electromechanical manipulator				
*4150	Utilities	4232	Shear	4343	Master slave				
4151	Sprinkler system	4233	Voloxidizer	*4350	Viewing				
4152	Cooling water, steam and condensate	4234	Dissolver	4351	TV				
4153	HVAC[d]	4235	Clarifier	4352	Optics				
4154	Instrumentation	*4240	Solvent extraction	4353	Lighting				
4155	Electrical	4241	Fuel adjustment	*4360	Simulated shielding				
		4242	First cycle solvent extraction	4361	Structural				
		4243	UO_3 production	4362	Windows				
		4244	High-level organic treatment	4363	Penetrations				
		*4250	Vessel off-gas	*4370	Cell configurations				
		4251	NO_x scrubber						
		4252	$Mg(NO_3)_2$ acid concentrate						
		4253	Iodox						
		*4260	Solid and liquid waste						
		4261	Metallic waste disposal						
		4262	Acid receiving and recycling						
		4263	Liquid waste disposal						
		*4270	Chemical makeup						
		4271	Chemical makeup						
		4272	Synthetic fluid production						
		*4280	Process instrumentation						
		4281	Process and instrument diagrams						
		4282	Loop diagrams						
		4283	Main panels						
		4284	Transmitter racks						
		4285	Control room						

[a]Major tasks are indicated with an asterisk.

[b]Integrated process demonstration.

[c]Remote operation and maintenance demonstration.

[d]Heating, ventilation, and air conditioning.

be the most economical of those studied. Since the water-softening equipment is returned to the vendor for regeneration, no liquid-waste effluents are produced onsite.

Table 6.3. IPET construction project financial schedule (dollars)

Fiscal year	Authorizations	Appropriations	Obligations	Costs
1977	600,000	600,000	600,000	600,000
1978	3,000,000	3,000,000	3,000,000	3,000,000
1979	12,400,000	12,400,000	12,400,000	12,400,000
1980	0	0	0	4,000,000
1981	0	0	0	400,000

General Plant Project (GPP) funding for electrical power supply equipment has been authorized, and procurement of Phase I is in progress. A lump-sum bid for construction work is being requested. If no bidders reply, a cost plus fixed fee contract will be sought. This project will provide 1500 kVA of electrical power for the LMFBR fuel reprocessing experimental program at the site. A second 1500-kVA addition is planned for FY 1978 to meet the expanded power requirements at that time.

The former Experimental Gas-Cooled Reactor control room in Building 7601 is being renovated to provide 24 offices to meet the immediate needs of program personnel. The completion of this GPP-funded project is expected by July 1977.

UCC-ND Engineering has completed the design for the refurbishment of and modification to the existing waste-collection system. ERDA approval is expected soon for this $88,000 GPP-funded project. When completed, the waste-collection system comprised of tanks, connecting lines, pumps, and a load-out station will provide means for the orderly management of process-waste disposal at the 7600 site.

REFERENCE FOR SECTION 6

1. Staffs of the UCC-ND Engineering Division and the LMFBR Fuel Reprocessing Program, *Conceptual Design Report for Integrated Prototype Equipment Test Facility*, Project No. 78-ORNL-13, X-OE-18 (September 1976).

ORNL/TM-5879
Dist. Category UC-79c

INTERNAL DISTRIBUTION

1. J. T. Bell
2. M. Bender
3. M. R. Bennett
4. R. E. Blanco
5. J. O. Blomeke
6. W. D. Bond
7. B. F. Bottenfield
8. N. C. Bradley
9. R. E. Brooksbank
10. K. B. Brown
11-20. W. D. Burch
21. J. M. Chandler
22. W. E. Clark
23. M. E. Clifton
24. L. T. Corbin
25. R. M. Counce
26. D. J. Crouse
27. B. F. Crump
28. F. L. Culler
29. B. C. Duggins
30. D. E. Dunning
31. J. H. Evans
32. M. J. Feldman
33. D. E. Ferguson
34. L. M. Ferris
35. J. H. Goode
36. N. R. Grant
37. W. S. Groenier
38. D. C. Hampson
39. B. A. Hannaford
40. W. O. Harms
41. J. N. Herndon
42. W. D. Holland
43. D. E. Horner
44. A. R. Irvine
45. P. R. Kasten
46. A. D. Kelmers
47. J. Q. Kirkman
48. J. A. Klein
49. C. E. Lamb
50. B. E. Lewis
51. A. L. Lotts
52. J. C. Mailen
53. A. P. Malinauskas
54. L. Maya
55. L. E. McNeese
56. R. P. Milford
57. J. G. Morgan
58. J. M. Morrison
59. J. P. Nichols
60. E. L. Nicholson
61. E. D. North
62. J. H. Pashley
63. F. L. Peishel
64. H. Postma
65. R. H. Rainey
66. W. F. Schaffer, Jr.
67. C. D. Scott
68. J. D. Sease
69. T. Shapiro
70. B. B. Spencer
71. R. G. Stacy
72. M. J. Stephenson
73. W. G. Stockdale
74. O. K. Tallent
75. D. B. Trauger
76. W. E. Unger
77. V. C. A. Vaughen
78. B. L. Vondra
79. C. D. Watson
80. B. S. Weil
81. T. D. Welch
82. M. E. Whatley
83. J. R. White
84. R. G. Wymer
85. O. O. Yarbro
86. S. Beard (consultant)
87. L. Burris, Jr. (consultant)
88. A. B. Carson (consultant)
89. E. L. Gaden, Jr. (consultant)
90. C. H. Ice (consultant)
91. W. H. Lewis (consultant)
92. R. B. Richards (consultant)
93. A. Schneider (consultant)
94. M. J. Szulinski (consultant)
95. J. S. Theilacker (consultant)
96. A. K. Williams (consultant)
97-98. Central Research Library
99. ORNL — Y-12 Technical Library
Document Reference Section
100-101. Laboratory Records
102. Laboratory Records, ORNL RC
103. ORNL Patent Office
104. Nuclear Safety Information Center

☆ U.S. GOVERNMENT PRINTING OFFICE: 1977-748-189/48

EXTERNAL DISTRIBUTION

105. Director, Reactor Division, ERDA-ORO
106-107. Director, Division of Nuclear Fuel Cycle and Production, ERDA, Washington, D.C. 20014
108-109. Director, Division of Reactor Research and Development, ERDA, Washington, D.C. 20014
110. Research and Technical Support Division, ERDA-ORO
111-362. Given distribution as shown in TID-4500 under UC-79c — Fuel Recycle category (Applied)